Molecular interactions between ethylene and gibberellic acid pathways in plants

Dissertation

zur Erlangung des Doktorgrades der
Mathematisch-Naturwissenschaftlichen Fakultät
der Christian-Albrechts-Universität
zu Kiel

vorgelegt von

Guillaume Rzewuski

Kiel

2004

Referentin: **Prof. Dr. M. Sauter**
Korreferentin: Prof. Dr. K. Krupinska
Tag der mündlichen Prüfung: 07.06.04
Zum Druck genehmigt: 07.06.04

Erklärung:

Hiermit erkläre ich, dass ich die vorliegende Arbeit selbständig angefertigt habe und keine anderen als die angegebenen Quellen und Hilfsmittel benutzt habe.
Die Dissertation wurde bisher an keiner anderen Hochschule oder Universität vorgelegt.

Kiel, April 2004 Guillaume Rzewuski

Teile der vorliegenden Arbeit sind veröffentlicht

Rzewuski, G. and Sauter, M. (2002). The novel rice (*Oryza sativa* L.) gene OsSbf1 encodes a putative member of the Na+/bile acid symporter family. *J. Exp. Bot.* **53**:1991-1993.

Index pages

1. Introduction.

1.1. Flooding is a threat for plant survival.

Plants are sessile organisms whose survival relies on continuous adaptation to environmental stimuli and internal cues. Flooding is a severe threat for survival of terrestrial plants because it impedes gas diffusion, limiting oxygen supply and leading to anaerobiosis of submerged plant parts or tissues. Low oxygen supply impedes mitochondrial respiration, since dioxygen is the final electron acceptor in the respiration chain. To support glycolysis and generation of ATP in the absence of mitochondrial respiration, the glycolytic cosubstrate NAD^+ must be regenerated through an alternative route. Therefore, under hypoxia, metabolism is switched from oxidative to fermentative. End products of fermentation in plants are ethanol and lactate. Accumulation of lactate leads to acidification of the cytoplasm, which is detrimental to the cell. However, a mechanism avoiding acidosis referred to as "pH-stat" (Roberts *et al*., 1984; 1985) involves the inhibition of lactate dehydrogenase at acidic pH and favours the formation of ethanol, a neutral fermentation end product.

Depending on their ability to withstand periods of oxygen deficit, plants species are classified as flood-sensitive, flood-tolerant or wetland. Flood-sensitive plants such as *Pisum sativum* or *Lycopersicon esculentum* exhibit an injury response to anoxia and generally can not survive more than 24 hours without oxygen, mainly because of cytoplasmic acidosis. Flood-tolerant plants can withstand anoxia for longer periods. In *Zea mays*, the pH-stat mechanism of inhibition of lactate dehydrogenase permits stabilisation of the cytoplasmic pH for three to five days. Eventually the cytoplasm acidifies as a consequence of lactate accumulation or proton leakage from the vacuole, and cells die. Wetland plant species such as *Oryza sativa* display metabolic features that allow survival for extended periods of hypoxia. A mechanism of stabilisation of the cytoplasmic pH that does not involve lactic acid fermentation in rice efficiently prevents acidosis of the cytoplasm (Menegus *et al*., 1991). Moreover, mobilisation of starch reserves to produce energy for the maintenance of basal rates of metabolism under low oxygen concentrations has been cited as a major determinant of flooding tolerance in rice (Setter *et al*., 1997; Dennis *et al*., 2000). In addition to altered cellular metabolism in response to low oxygen supply, wetland plant species possess diverse anatomical and morphological features that permit survival in semi-aquatic environments. For instance, plants such as rice constitutively form aerenchyma, which are continuous gas columns formed in cortical tissues. Flooding further promotes aerenchyma formation, thereby

facilitating O_2 transport from aerated leaves to flooded organs. In addition, flooding promotes adventitious root growth from the nodes of rice stems. Adventitious roots facilitate mineral and water absorption from the surrounding water, and anchor the plants to the soil when flooding waters have recessed. But the most striking adaptation of semi-aquatic plants is flooding-avoidance. In rice, extremely well adapted cultivars are grouped under the terms "deepwater" or "floating" rice. They display rapid internode elongation in response to submergence, so that part of their foliage is always kept above the rising water levels, thus enabling access to atmospheric oxygen. Such rice cultivars can withstand four to five months of flooding and eventually reach postflood lengths of up to several meters. Several deepwater rice varieties are grown in Southeast Asia, where monsoon rains periodically flood rice fields and cause severe grain losses. Contrary to their excellent adaptation to semi-aquatic environments, deepwater rice cultivars tend to have low yields and poor culinary qualities in comparison with other lowland rice cultivars. Therefore, growing interest attempts to combine high grain yield and culinary qualities with flooding tolerance. The identification of a major quantitative trait-locus (QTL) linked to flooding tolerance in rice was a first step in understanding how certain rice cultivars can withstand prolonged periods of submergence (Toojinda *et al*., 2003). However, the genes responsible for flooding tolerance in this QTL remain to be identified.

1.2. Submergence-induced internode elongation is a suitable system to study hormone signalling.

Beyond its agricultural importance, deepwater rice is a plant model well suited for studying growth regulation. The uppermost growing internode is composed of three anatomically distinct tissues organised basipetaly. In a 5 mm-long zone located just above the second node, the intercalary meristem (IM) is a rib meristem that provides the internode with new cells. Cells elongate while displaced towards the cell elongation zone (EZ), to reach a mature size of about 150 µm in rapidly growing internodes and 50 µm in uninduced stems (Sauter and Kende, 1992). Formation of secondary walls and lignin deposition eventually occur in the cell differentiation zone (DZ) located above the EZ up to the first node. The physiological as well as the cellular basis of submergence-induced internodal elongation are well documented (Kende *et al*., 1998).

Submergence-induced internode elongation is mediated by the interplay between three phytohormones, ethylene, abscisic acid and gibberellin. Gas diffuses 10.000 times slower in

water than in air (Jackson, 1985). As a consequence, ethylene, which is synthesised throughout development is physically entrapped in submerged tissues. In addition to ethylene entrapment, lower partial pressures in oxygen caused by submergence promote ethylene synthesis (Métraux and Kende, 1983) which results in accumulation of ethylene. In growing internodes of deepwater rice the partial pressure of ethylene was shown to increase as early as 1 hour after beginning of submergence (Raskin and Kende, 1984). The first committed step of ethylene biosynthesis is the conversion of S-adenosylmethionine to 1-aminocyclopropane-1-carboxylic acid (ACC) by ACC synthase (ACS, EC 4.4.14). In addition to ACC, ACS produces in the same reaction 5'-methylthioadenosine (MTA) which is then converted to methionine by the so-called "Yang cycle" or MTA recycling pathway. This pathway recycles the methylthio-moiety of MTA to methionine which can then be activated to S-adenosylmethionine and used in another round of ethylene production. The MTA recycling pathway therefore allows high rates of ethylene synthesis without diminishing the supply of S-adenosylmethionine (Miyazaki and Yang, 1987). Expression of *OS-ACS5* encoding the isoform 5 of ACC synthase from rice is induced within 1 hour of submergence, suggesting that this gene plays a fundamental role in the early submergence-induced internodal ACC production (Van Der Straeten *et al*., 2001). Induction of *OS-ACS5* expression is consistent with the previous observation that ACS activity is stimulated and reaches highest levels in growing internodes of submerged plants within 2 hours (Cohen and Kende, 1987). Ethylene is synthesised from ACC by the ACC oxidase (ACO, EC 1.14.17.4) in a non rate-limiting step.

Subsequent to the increase in ethylene content, the balance between levels of the growth-promoting hormone gibberellin (GA) and the growth-inhibiting hormone abscisic acid (ABA) is drastically altered. After 3 hours of partial submergence, the level of ABA drops to one quarter of that measured before submergence (Hoffmann-Benning and Kende, 1992). Because responsiveness to GA is a function of ABA content, decrease in ABA levels increases responsiveness to GA. After 4 hours a four-fold increase in GA_1, a bioactive gibberellin in rice, is observed. Higher amounts of GA, as well as higher GA-responsiveness result in increased growth rates of the youngest internode (Figure 1). Submergence-induced petiole elongation of the dicotyledonous *Rumex palustris* involves as well ethylene, ABA and GA, which interact through a signalling cascade that resembles that observed in submerged deepwater rice (Voesenek *et al*., 2003).

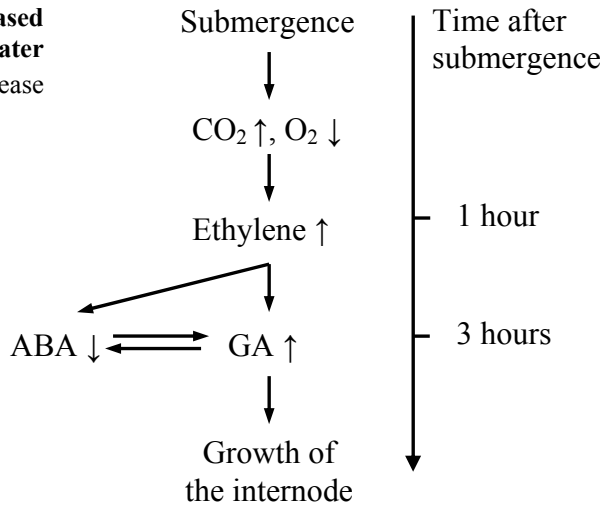

Figure 1: Hormonal changes leading to increased growth of the youngest internode in deepwater rice. ABA, abscisic acid; GA, gibberellin; ↑, increase in concentration; ↓, decrease in concentration.

Two mechanisms through which GA exerts a growth-promoting effect in deepwater rice have been so far proposed. The first mechanism includes modifications of the plasticity of the cell wall. In excised stem sections of deepwater rice which contain the growth-responsive internode, GA induces expression of *OS-EXP2* and *OS-EXP4* coding for α-expansins (Cho and Kende, 1997a-b) and of 5 genes encoding β-expansins (Lee and Kende, 2001). α- and β-expansins are cell wall loosening enzymes that are thought to break the hydrogen bonds between hemicellulose and cellulose (McQueen-Mason and Cosgrove, 1994). In growth-responsive internodes cell elongation is facilitated by GA-induced expansins which modify the plastic properties of the cell wall. GA also modifies the direction of cellulose microfibril (CMF) deposition in the outer epidermis of the growing internode. The CMFs, consisting of (1→4)-β-glucan, are deposited in a transverse direction in the intercalary meristem, while in the cell elongation zone of uninduced stems CMFs are deposited in an oblique direction. Elongation is facilitated when CMFs are oriented transversely. In submerged deepwater rice plants or in GA-treated stem sections, CMFs remain transversely oriented in the elongation zone, enabling cells to elongate faster and to a greater extent (Sauter *et al*., 1993).

The second mechanism which explains growth-promoting effects of GA resides in the enhancement of the cell division rate by GA. In the intercalary meristem of submerged deepwater rice, the time required for one round of cell division is reduced to 7 hours from 24 hours needed in air-grown plants (Métraux and Kende, 1984). Lorbiecke and Sauter (1998, 1999), found that GA activates cells which are in the G1 phase to enter the S phase at an enhanced rate.

In one report, it was described that auxin has a synergistic effect on internodal elongation of excised deepwater rice stem sections when combined with gibberellin (Azuma *et al*., 1990). In Arabidopsis roots, auxin was shown to promote root growth by potentiating the gibberellin response (Fu and Harberd, 2003). Whether auxin assists in regulating internodal growth in deepwater rice remains unclear.

Brassinosteroids are steroid-derived plant hormones that induce a broad spectrum of responses that include an increased rate of stem elongation, bending of the grass lamina joint (Wada *et al*., 1981), reorientation of cellulose microfibrils and enhanced ethylene production. The most biologically active brassinosteroid is brassinolide, a C28-steroid widely distributed throughout the plant kingdom. The rice mutant d61, originally identified through its dwarf phenotype, is less sensitive to exogenously-applied brassinolide because it carries a mutated putative brassinosteroid receptor gene (Yamamuro *et al*., 2000). In d61, the intercalary meristem develops but cells in the elongation zone fail to elongate indicating a role for brassinosteroids in internode elongation. An involvement of brassinosteroids in submergence-induced internodal elongation in deepwater rice has however not been studied yet.

1.3. Ethylene signalling.

Identification of components of the ethylene signalling pathway has relied mainly upon molecular and genetic analysis of mutants showing an altered response to ethylene. A typical phenotype obtained by submitting etiolated seedlings to ethylene gas is the triple response phenotype which is characterised by limited hypocotyl and root elongation, increased radial swelling of the hypocotyl and exaggerated curvature of the apical hook. Arabidopsis mutants affected in components of ethylene signalling can be classified into three categories, constitutive triple-response mutants (CTR), ethylene-insensitive mutants (EIN) and tissue-specific ethylene-insensitive mutants (Guo and Ecker, 2004).

Molecular analysis of ethylene-insensitive mutants allowed for instance the identification of ethylene receptors. In Arabidopsis, five receptors were identified, which show a high degree of functional overlap (Alonso and Ecker, 2001). Ethylene receptors are related to the bacterial two-component sensors. Mutations in *CTR1* result in a constitutive triple-response phenotype. (Kieber *et al*., 1993). CTR1 is able to physically interact with the ethylene receptors ETR1 and ERS (Clark *et al*., 1998) and was shown to be a Raf-like Ser/Thr protein kinase that is part of a MAP kinase cascade that mediates ethylene signalling (Ouaked *et al*., 2003). Mutation in *EIN3* causes ethylene insensitivity which is epistatic to *CTR1*, implying that *EIN3* acts downstream of *CTR1*. EIN3 is a putative transcription factor that acts

at the end of the ethylene transduction pathway (Chao *et al*., 1997). It is able to *trans*-activate expression of the *ERF1* gene (Solano *et al*., 1998) that encodes an Ethylene-Response-Element-Binding-Protein (EREBP). Overexpression of *ERF1* in Arabidopsis resulted in the activation of ethylene response genes and subsequently in a variety of phenotypes typically obtained through ethylene treatment such as the triple-response phenotype. EIN3-like transcription factors have been characterised from other plant species. At least five tobacco *EIN3-like* (*NtEIL*), three tomato *EIL* (*LeEIL*) and two Mung Bean *EIL* (*VR-EIL*) genes have been identified, and some of these genes encode proteins with biological function and DNA-binding capacity identical to EIN3. The finding of EIN3 orthologues from other plant species supported the idea that nuclear events induced by ethylene signal transduction rely on similar mechanisms, and that physiological responses to ethylene in plants are regulated mainly at the transcriptional level (Bleecker and Kende, 2000).

Most recent advances in research on ethylene signal transduction showed that levels of EIN3 protein are regulated by ethylene, through two F-box proteins that target EIN3 to the proteasome degradation pathway. These F-box proteins, EBF1 and EBF2, are components of the $SCF^{EBF1/EBF2}$ E3 ubiquitin-ligase complexes (Potuschak *et al*, 2003; Guo and Ecker, 2003).

1.4. Gibberellin synthesis and signalling.

Gibberellins constitute a group of tetracyclic diterpenes for which 126 members have been identified so far. Biologically active GAs are best known for their influence on seed germination, leaf expansion, stem elongation, flower and trichome initiation and flower and fruit development. Gibberellins are synthesised from geranylgeranyl diphosphate produced mainly through the plastidial methylerythritol phosphate pathway (Kasahara *et al*., 2002). Geranylgeranyl diphosphate is converted to bioactive gibberellins through the activity of terpene cyclases, P450 monooxygenases and 2-oxoglutarate-dependent dioxygenases (Hedden and Kamiya, 1997). Among the latter class of enzymes, GA20-oxidase and GA3β-hydroxylase catalyse the last steps of the synthesis of GA_4, the major gibberellin in Arabidopsis shoots (Talon *et al*., 1990). The genes encoding these enzymes were shown to be subjected to negative feedback regulation by the action of gibberellin itself (Hedden and Kamiya, 1997).

To date, no candidate GA-receptor has been characterised, and how plant cells sense GA remains unknown. On the other hand, downstream GA signalling events are better understood. Molecular and genetic approaches led to the identification of two classes of GA-response mutants based on their vegetative phenotype and response to GA. The first group is

composed of GA-insensitive dwarf mutants which resemble mutants that are deficient in GA biosynthesis in that they are stunted, have dark-green leaves and a delayed flowering time, but which cannot be rescued by GA application, unlike GA-auxotrophs. Gain-of-function mutations in the genes encoding the Arabidopsis DELLA proteins growth repressors *GAI*, *RGA*, *RGL1* or *RGL2* produce such dwarf plants (Gomi and Matsuoka, 2003). Due to their nuclear-localisation, DELLA-proteins are thought to be transcriptional regulators. Application of GA results in disappearance of RGA from the nucleus (Dill *et al*., 2001; Silverstone *et al*, 2001). The current model for GA action is that growth is promoted by a GA signal that relieves plants of DELLA-mediated growth-restraint (Harberd, 2003). Most recent findings in rice indicate that, through an unknown protein kinase, GA induces phosphorylation of the DELLA protein SLR1. Phosphorylation is a prerequisite for polyubiquitination of SLR1 by the SCF^{GID2} E3 ligase complex. DELLA proteins harbouring polyubiquitin chains are degraded by the 26S proteasome and relieve restraint on plant growth (Fu *et al*., 2002; Sasaki *et al*., 2003).

The second group of GA-response mutations appears to confer a GA-independent phenotype, in that mutants show slender, elongated stems and are early-flowering. The Arabidopsis loss-of-function *spindly* (*SPY*) mutant is able to germinate on medium containing paclobutrazol, an inhibitor of gibberellin synthesis which blocks germination of wild-type Arabidopsis seeds (Jacobsen and Olszewski, 1993). The *SPY* gene encodes a putative *O*-linked *N*-acetyl-glucosamine transferase which is thought to glycosylate and thereby to modulate the activity of DELLA proteins (Jacobsen *et al*., 1996).

1.5. Emerging common regulatory mechanisms.

The plant hormones ethylene and gibberellin are involved in different, yet non-exclusive developmental processes. The signal transduction of these hormones leads to EIN3 for ethylene and the DELLA proteins for gibberellin which are nuclear proteins responsible for the induction or the repression of ethylene and gibberellin responsive genes, respectively. Recent findings indicate that levels of the transcriptional regulators EIN3 and SLR1, a DELLA protein from rice, are regulated through proteasome-mediated degradation. Each of these transcription factors is a specific target of SCF-E3 ubiquitin-ligase (SKP1-CULLIN-F-box) complexes whose specificity is determined by the F-box protein component. For instance the F-box protein GID2 specifies ubiquitination of the DELLA protein SLR1 by the SCF^{GID2} E3 ubiquitin-ligase complex (Sasaki *et al*., 2003), while the DELLA protein RGA from Arabidopsis is specifically ubiquitinated by the SCF^{SLY1} complex (McGinnis *et al*., 2003).

EIN3 was recently shown to be regulated in the same way by the $SCF^{EBF1/EBF2}$ E3 ubiquitin-ligase complex (Potuschak *et al*, 2003; Guo and Ecker, 2003).

Several AUX/IAA transcription factors involved in auxin signalling were shown to be regulated as well through SCF^{TIR1}-mediated ubiquitination and subsequent proteasome degradation (Kepinski and Leyser, 2002). These findings indicate that regulation of SCF and modification of specificity by an interchanging F-box protein may constitute a cross point of interactions between hormone signalling pathways.

1.6. Interactions between ethylene and gibberellin signalling.

Germinating seedlings produce ethylene when the soil prevents their growth. Ethylene triggers the so-called "triple response" phenotype characterised by decreased hypocotyl and root growth and by the formation of an apical hook. The apical hook is a transient structure that is caused by asymmetric growth of the inner and outer sides of the hypocotyl. It is believed to protect the shoot apical meristem from mechanical damage when seedlings break through the soil. Ethylene and gibberellin interact during apical hook formation and maintenance. Ethylene was shown to induce nuclear accumulation of RGA, a DELLA protein growth repressor which opposes effects of GA (Vriezen *et al*., 2004). If stabilisation of DELLA proteins by ethylene is a widespread regulation mechanism, this finding partly explains why ethylene generally acts as a repressor of growth (Achard *et al*., 2004). During apical hook formation ethylene-mediated stabilisation of DELLA proteins is thought to result in a decrease of GA content such that the negative feedback exerted by GA on GA biosynthesis is alleviated. Consequently, local increases in GA content activate growth on the upper side of the hypocotyl which produces a pronounced curvature of the hypocotyl defined as "apical hook". Differential growth seems also to be the result of differential GA-sensitivity on the upper and on the lower sides of the hypocotyl (Vriezen *et al*., 2004).

In growing internodes of partially submerged deepwater rice, ethylene shows growth-promoting effects by drastically increasing pools of bioactive gibberellins (Hoffmann-Benning and Kende, 1992). Therefore, it is possible that interactions between ethylene and gibberellin in rice internodes are similar to these observed during apical hook formation and maintenance in Arabidopsis.

1.7. Plant development and regulation of hormone levels.

How the developmental stage of a cell or tissue influences hormone action has until recently seldom been questioned in hormone signalling. Nevertheless current research tends to prove that several factors, first identified for their involvement in cell fate determination or cell differentiation, influence hormone synthesis. Among these, KNOX homeodomain proteins and MADS-box proteins have attracted much attention because they define plant architecture during the vegetative and the reproductive phases, respectively.

KNOX proteins, encoded by *KNOTTED1-LIKE* homeobox genes, are transcription factors that preferentially accumulate in indeterminate cells around the shoot apical meristem (SAM), but not in determinate lateral organs such as leaves (Jackson *et al*., 1994; Nishimura *et al*., 1999). KNOX proteins are considered to play a role in the maintenance of the indeterminate meristematic identity of the cells that constitute the SAM (Reiser *et al*., 2000). The KNOX protein NTH15 from tobacco was recently shown to bind to the promoter sequence of the GA biosynthetic 20-oxidase gene *Ntc12* (Sakamoto *et al*., 2001), involved in the oxidation steps leading to the formation of the bioactive gibberellin GA_1 (Hedden and Kamiya, 1997). Induction of NTH15 through a steroid-inducible system revealed that NTH15 suppressed expression of the *Ntc12* gene, with a rapid decrease in levels of bioactive gibberellin as a result (Sakamoto *et al*., 2001). In Arabidopsis, one of the functions of the KNOX protein SHOOTMERISTEMLESS (STM) is to prevent transcription of the GA-biosynthesis gene *AtGA20ox-1* in the SAM. Diverse lines of evidence suggest that repression of GA biosynthesis by KNOX homeodomain proteins promotes meristematic activity (Hay *et al*., 2002). In rice, loss-of-function of the homeobox KNOX factor OSH15 results in dwarf plants with abnormal internode development and morphogenesis. Since these mutants harbour primary defects in cell division in the uppermost internode, OSH15 appears to play a role in maintaining meristematic activity in the intercalary meristem (Sato *et al*., 1999). Whether OSH15 regulates hormone levels in rice internodes is not known.

MADS-box proteins are best known from the ABC model of flower development. This model assumes that the identity of the four floral whorls (sepals, petals, stamens and carpels) is determined in flower primordia by three concentrically organised fields of MADS-box gene activity. Recently, the ABC(DE) model of flower development added the “D” function that specifies ovule identity and the “E” function that represents non-MADS-box cofactors required for the identity of the three inner whorls (Theissen and Saedler, 2001). MADS-box proteins are involved as well in growth during vegetative development. For instance, activation of axilary meristem development was observed in potato after suppression

of the vegetative MADS-box gene *POTM1* (Rosin *et al*., 2003), while ectopic expression of the potato *STMADS16* gene in tobacco resulted in altered architecture of the inflorescence with increased branching and internode length (García-Maroto *et al*., 2000). Expression studies in Arabidopsis pinpointed a role for MADS-box proteins in root development (Burgeff *et al*., 2002). Recent work reported on the effects of overexpression of a C-terminally truncated OsMADS14 protein in rice. Truncation in the C-terminal transcriptional activation domain resulted in a dominant negative mutation accompanied by phenotypic alterations such as internode elongation at the seedling stage and an increased number of internodes during vegetative development, that were throught to be the result of alterations in the expression of GA metabolism genes. Plants overexpressing OsMADS14 displayed higher levels of the GA biosynthetic genes *GA20Ox1* and *GA20Ox2* transcripts than wild type plants, while transcript levels of *GA2Ox1*, a gene that inactivates bioactive gibberellin, and transcript levels of the negative regulators of GA signalling *OsSPY* and *SLR1* were reduced. It was hypothesised that OsMADS14 is a negative regulator of internode elongation that represses expression of GA biosynthetic genes and induces negative regulators of GA signalling (Jeong *et al*., 2003).

1.8. Aim of the work presented: Ethylene to gibberellin signalling in deepwater rice.

Hormone-linked physiological events leading to enhanced internodal elongation during submergence have been extensively studied in deepwater rice. However, little is known about the signalling pathway converting the ethylene signal into increased GA levels and responsiveness.

The aim of this study was to identify and characterise genes involved in the ethylene to gibberellin signalling pathway in deepwater rice. Since physiological responses to ethylene are mediated by the activation of ethylene-responsive genes, we proposed the hypothesis that in deepwater rice, ethylene induces transcription of genes that take part in increasing rates of GA biosynthesis or in increasing responsiveness to GA.

The first question to resolve concerned the way in which to trigger higher levels of ethylene in the growth-responsive internode. Through low oxygen concentration and limited gas diffusion, submergence induces synthesis and accumulation of ethylene. On the other hand, hypoxic conditions occurring in submerged tissues were not desired because of the induction of hypoxy-related genes that could mask detection of ethylene to gibberellin signalling genes. In order to avoid hypoxia excised stem sections were directly provided with

the ethylene precursor ACC under normoxic conditions. Kinetics and dose-response of ACC-induced internodal growth were determined so that time-points between perception of ethylene and ethylene-induced growth were defined.

In order to isolate ACC-induced (*aci*) genes in stem sections prior to growth induction, a PCR-based subtractive hybridisation was performed. *Aci* genes that were induced by submergence, by ACC or by ethylene, but not by gibberellic acid GA_3 were assigned a putative function in ethylene to gibberellin signalling. Further characterisation of candidate genes was performed using rice and Arabidopsis as plant models for functional studies.

2. Material and methods.

2.1. Material.

2.1.1. Plant material.

Deepwater rice seeds, *Oryza sativa* L. cv. Pin Gaew 56 were originally provided by the International Rice Research Institute (IRRI, Los Bañjos, Philippines). T-DNA insertion lines and wild-type seeds from the *Arabidopsis thaliana* ecotype Columbia 0 were obtained from GABI-KAT (Max-Planck Institute, Köln, Germany).

2.1.2. Rice λgt11 cDNA library.

A rice cDNA library was kindly provided by Dr. H. Kende and Dr. E. Van der Knaap (MSU-DOE, Plant Research Laboratory, Michigan State University, USA). It was prepared from intercalary meristem of stem sections treated for ½, 2 ½ and 6 ½ hours with GA_3. cDNAs synthesised with oligo-dT and random hexamers were size fractionated and after ligation of adapters were cloned at the EcoRI site of the LacZ gene in λgt11. Size fractionation resulted in a library enriched in cDNAs larger than 1.5 kb that was used to isolate several cDNAs in this study.

2.1.3. Chemicals, enzymes and kits.

All chemicals that were used in "p.a." or "molecular biology" grade, and enzymes as well as kits for molecular biology were provided by Amersham Biosciences (Freiburg, Germany), Applied Biosystems (Weiterstadt, Germany), Duchefa (Haarlem, The Netherlands), Dynal (Hamburg, Germany), Eurogentec (Seraing, Belgium), Invitrogen (Karlsruhe, Germany), MBI (St.Leon-Rot, Germany), Promega (Mannheim, Germany), Qiagen (Hilden, Germany), Roche (Mannheim, Germany), Roth (Karlsruhe, Germany), Sigma (Taufkirchen, Germany) or Stratagene (Heidelberg, Germany). Double distilled water, obtained from a Milli-Q Water system (Millipore, Bedford, USA) was used to prepare all solutions, and is referred to as "water" or H_2O.

2.1.4. Molecular markers.

To estimate both sizes and quantities of DNA fragments after agarose gel electrophoresis, an aliquot of Smart Ladder (Eurogentec, Seraing, Belgium) was loaded on each gel. For Southern blot analysis using the DIG labelling and detection kit (Roche, Mannheim, Germany), the DNA molecular weight marker Dig VII was used. When needed, an RNA molecular marker ranging from 0.24 to 9.5 kb from Invitrogen (Karlsruhe, Germany) was run together with the samples during RNA gel electrophoresis. After transfer the position of the bands was marked with a pencil on the membranes after a brief staining in methyl blue.

2.1.5. Vectors and bacterial strains.

Cloning was performed using chemically-made competent *Escherichia coli* DH5α cells, prepared according to Inoue *et al*. (1990). The *E. coli* host strain used to propagate the λgt11 rice cDNA library was LE392.

Arabidopsis transformation was performed with the *Agrobacterium tumefaciens* strain GV3101::pMP90RK (Koncz and Shell, 1986). It harbours one chromosomal marker gene conferring resistance to rifampicin, and two Ti plasmid marker genes providing resistance to kanamycin and gentamicin. The vectors used in this study are given in Table 1.

Table 1: Vectors used in this study.

Vector	Source / Company
pGEMT-Easy	Promega (Mannheim, Germany).
pCR® 2.1-TOPO	Invitrogen (Karlsruhe, Germany).
pTOPO-ENTRY	Invitrogen (Karlsruhe, Germany).
pBSIISK$^-$	Stratagene (Heidelberg, Germany).
pB2WG7	Flanders Interuniversity Institute for Biotechnology, Gent, Belgium.
pPZP312	Dr. C. Fankhauser, Département de biologie moléculaire, Université de Genève, Switzerland.
pGUS-SB	Dr. M. Gahrtz, Insitut für Allgemeine Botanik, Hamburg, Germany.
pUhGFPC3-N	BD Biosciences (Heidelberg, Germany).

2.1.6. Primers.

Primers were obtained from Roth (Karlsruhe, Germany) or Sigma-ARK (Darmstadt, Germany). SUB25 and KS22 were phosphorylated at the 5'-end and KS18-biotin was biotinylated at the 5'-end. All primers are listed in Table 2.

Table 2: Primers used in this study.

Name	Sequence (5'→ 3')
T7	TAATACGACTCACTATAGGG
M13-reverse	GGAAACAGCTATGACCATG
Ataci3-1F1	TCAGCTCCTTTGTGGTCATT
Ataci3-1R1	GAATCATGTCTCAGCGTCTTAG
Ataci3-1F2	GCTTATGCAATCGATCATCCTG
Ataci3-1R2	GGACATAGACAGCGATATCT
Ataci3-1R3	TAAGCCACTGTCCAGGATGA
Ataci3-1R3	TAAGCCACTGTCCAGGATGA
o8409	ATATTGACCATCATACTCATTGC
03144	GTGGATTGATGTGATATCTCC
o9525	CCACACGTGGATCGATCCGTCG
o19706	GAACCCTAATTCCCTTATCTGGG
At5g6p-Xba	TCTAGAGTTGGATGCATTCGACCATG
At5g6p-Bam	GGATCCGTCTCAGAATGACCACAAAG
Ataci3-WG.F	CCTTTGTGGTCATTCTGAGAC
Ataci3-WG.R	CACCTATATATACACACACTCT
Ataci3-GFP F	GGGCTGCAGATGGGATTTGGAGTA
Ataci3-GFP R	CATCTGCAGTTTGGCAGCTTCTCT
SUB21	CTCTTGCTTGAATTCGGACTA
SUB25	**P**-TAGTCCGAATTCAAGCAAGAGCACA
KS18	CGGTATCGATAAGCTTGA
KS18-biotin	biotin-CGGTATCGATAAGCTTGA
KS22	**P**-TCAAGCTTATCGATACCGC

2.2. Methods.

2.2.1. Plant growth conditions.

2.2.1.1. Rice growth conditions.

Rice seeds were germinated on a layer of wet Whatman paper in the dark at 26°C for three days. Germinated seeds were transferred to 1.7-L pots containing a mixture of 1/5 sand, 1/5 vermiculite and 3/5 humus. Seedlings were grown for two weeks under a plastic cover to provide high humidity. They were watered with distilled water to keep salt concentrations low. After two weeks, a nutrient solution was provided, consisting of 0.1% (v/v) Wuxal Top N 12-4-6 (12% N, 4% P_2O_5, 6% K_2O plus trace elements, Aglukon, Düsseldorf, Germany). The plants were grown in a greenhouse in a 14-hour light period (200 μEinstein·m^{-2}·s^{-1}) at 27°C and a 10-hour dark period at 19°C, with an overall humidity of 70% (Sauter, 1997).

2.2.1.2. Partial submergence of deepwater rice plants.

In a 600-L tank filled with tap water at about 25°C, 10 to 12 week-old rice plants were partially submerged so that the leaf tips remained above the water. Incubations were made under continuous light at 27°C (Lorbiecke and Sauter, 1998).

2.2.1.3. Ethylene treatment of deepwater rice plants.

Seeds of deepwater rice were sent to Ghent, Belgium, and plants were grown there for 8 weeks under the conditions described above. Intact plants were subjected to ethylene treatment at 1 ppm in a gas-tight chamber under a controlled gas flow to keep atmospheric gas composition constant during the whole experiment. Since plant samples had to be taken every hour, the ethylene flow was adjusted in real-time in order to reach the 1 ppm of ethylene as fast as possible after the door of the chamber was opened. Partial pressure of ethylene in the chamber was monitored by gas chromatography (HP G1520A, Hewlett Packard, Brussels, Belgium). The experiment was performed in collaboration with Drs. Vriezen and Van der Straeten (Department of Molecular Genetics, Ghent University, Belgium).

2.2.1.4. Hormone treatment of stem sections.

Twenty cm-long stem sections, cut 2 cm below the second node (counting from the top) and comprising the first internode were incubated in 30 mL of hormone solutions in 150 mL beakers without flooding the node. For the indicated times, sections were kept in Plexiglas cylinders to maintain a water-saturated atmosphere. Growth of the internodes was measured with a ruler. As a control stem sections incubated in the same volume of water were used.

2.2.1.5. Collection of rice tissue for isolation of total RNA.

After the indicated incubation times, either the intercalary meristem, the elongation zone, the differentiation zone or a 1-cm segment comprising the intercalary meristem and part of the elongation zone were collected from the youngest elongating internode. For each RNA extraction, samples from at least 3 internodes were pooled in order to average biological variations.

2.2.1.6. Growth of *Arabidopsis thaliana*.

To obtain synchronous germination imbibed Arabidopsis seeds were stratified at 4°C in the dark for 48 hours and then transferred to a growth chamber under long day conditions with 16 hours of light (100 μEinstein·m^{-2}·s^{-1}) and 8 hours of dark at 22°C and 18°C, respectively.
Unless stated otherwise, Arabidopsis seeds were sown on a 1:1 sand-humus mixture that was frozen at –80°C for a few hours prior to use to kill insect larvae. Plants were watered regularly with tap water. When seedlings were grown on nutrient media, sterile conditions had to be observed. Seeds were surface-sterilised for 15 minutes in 1 mL of 0.5% (w/v) sodium hypochloride. After a brief centrifugation, seeds were resuspended in autoclaved water. This washing step was repeated five times. Using a sterile brush, seeds were laid out on square plates containing 30 mL of half-strength Murashige and Skoog (1962) medium (Duchefa, Haarlem, The Netherlands), 0.9% (w/v) agarose and 1.5% (w/v) sucrose. In this study, this basic medium is referred to as MS-agarose. When needed, the appropriate hormone was added to the cooled but still liquid medium before the plates were poured. After stratification the plates were placed either in complete darkness at 22°C or in a growth chamber in a 16-hour light period (100 μEinstein·m^{-2}·s^{-1}) at 22°C and a 8-hour dark period at 18°C.

2.2.2. Molecular biology techniques.

2.2.2.1. Small and medium scale preparation of plasmid DNA.

Plasmid DNA mini preparations essentially followed the alkaline lysis method developed by Birnboim and Doly (1979). For medium scale preparations, HiSpeed Midiprep kits were used (Qiagen, Hilden, Germany).

2.2.2.2. Polymerase chain reaction (PCR).

All PCRs were performed either in a Uno Thermoblock (Biometra, Goettingen, Germany) or in a PTC-200 thermal cycler (MJ Research, Biozym Diagnostik GmbH, Oldendorf, Germany). Unless stated otherwise, general conditions to amplify DNA were used as follows:
1: Initial denaturation at 94°C, for 2 or 3 minutes.
2: Denaturation in each round of amplification at 94°C for 30 to 50 seconds.
3: Primer annealing was performed at 5°C below the lowest annealing temperature calculated for the two primers used, for 30 to 50 seconds.
4: Elongation at 72°C, for 1 minute per 1 kb of fragment to be amplified.
Steps 2, 3 and 4 were repeated between 30 and 35 times.
5: A final elongation step was performed at 72°C for 5 minutes.

2.2.2.3. Cloning of PCR products.

Products obtained from amplification with a non-editing Taq (*Thermophilus aquaticus*) DNA polymerase were subcloned in vectors harbouring 3'-dT protruding termini, in a non-directional manner, according to the instructions provided by the suppliers. The vectors used were either pCR® 2.1-TOPO (Invitrogen, Karlsruhe, Germany) or pGEMT-Easy (Promega, Mannheim, Germany).

2.2.2.4. Screening of a rice λgt11 cDNA library.

A λgt11 cDNA library from rice was screened in order to isolate full-length cDNAs of ACC-induced genes that were identified through subtractive hybridisation.

Primary screening.

In order to propagate the phage library, a single colony from the suppressive host strain LE392 was inoculated in 50 mL of liquid LB medium with 0.2% (w/v) maltose and 10 mM $MgSO_4$ and grown overnight at 30°C. The culture was spun down for 10 minutes at 3.000 g and the cell pellet was resuspended in 10 mM $MgSO_4$ such that the cell suspension had an optical density of 0.8 at a wavelength of 600 nm. Six hundred µL of bacteria were combined with 50.000 pfu from the λgt11 library and incubated at 37°C for 15 minutes. The infected bacteria were then mixed with 6.5 mL of prewarmed NZCYM-Top-agar (Sigma, Taufkirchen, Germany) and the mixture was spread on large (15 cm in diameter) NZCYM-agar plates. After 4 to 6 hours at 37°C, the plates were incubated overnight at 4°C.

Plaques were lifted twice on circular Hybond N nylon membranes (Amersham Biosciences, Freiburg, Germany) carefully marked for orientation to enable identification of positive plaques later on. Each membrane was air-dried, and successively put for 5 minutes on Whatman papers soaked first with a denaturing solution (0.5 N NaOH, 1.5 M NaCl), and secondly soaked with a neutralisation solution (1.5 M NaCl, 0.5 M Tris-HCl at pH 7.5 and 1 mM EDTA). Lastly, the membranes were put for 10 minutes on filter paper soaked with 2X SSC. Denatured DNA was covalently bound to the membranes using a UV crosslinker (Stratagene, Heidelberg, Germany). Detection of positive plaques with DIG-labelled probes was performed as described in section 2.2.2.7.

Secondary screening and isolation of single plaques.

Regions of agar containing the identified positive plaques were excised with a pipette tip, put into 150 µL of SM buffer (Sambrook *et al*., 1989) and covered with a drop of chloroform. To isolate single plaques, dilutions of the recovered phages were used to infect the host strain again. On small Petri dishes (9 cm in diameter) the whole screening procedure was repeated until single positive plaques were identified.

Phage DNA preparation and excision of the cDNA.

Phage DNA was prepared as described by Lee and Clark (1997). Plaques were excised and incubated in 1 mL of SM medium (Sambrook *et al*, 1989) for 3 hours at 37°C under shaking at 225 rpm. One hundred µL of the resulting phage suspension was mixed with 500 µL of bacteria and incubated for 20 minutes at 37°C. Infected bacteria were inoculated in 50 mL of liquid LB medium with 0.3% (v/v) glycerol and 10 mM $MgSO_4$ and shaken at 260 rpm overnight at 37°C.

After lysis had occurred, 500 µL of chloroform was added to the culture. This mixture was shaken for another 30 minutes at 37°C. Cell debris was collected through centrifugation for 15 minutes at 4.000 g at 4°C. To the supernatant, 2.8 g of NaCl and 5 g of PEG_{8000} were added and dissolved. Phages were precipitated for one hour on ice and collected by centrifugation for 15 minutes at 4.000 g and 4°C. The pellet was resuspended in 1 mL of SM buffer, and subsequently treated with 20 µg DNase I and 50 µg RNase A for 30 minutes at 37°C. After centrifugation for 5 minutes at 2.000 g the phage suspension was incubated in 0.5 % (w/v) SDS, 10 mM ETDA and 50 $\mu g \cdot mL^{-1}$ proteinase K for 30 minutes at 37°C.
DNA was extracted once with phenol/chloroform 1/1 (v/v). The aqueous phase was washed with chloroform/isoamyl alcohol 24/1 (v/v) and phage DNA was precipitated in 0.3 M ammonium acetate with 2.5 volumes of ethanol. After 10 minutes centrifugation at 10.000 g, the pellet was washed with 70% ethanol, dried and resuspended in 300 µL of water.
Twenty-five µg of each phage DNA preparation was digested with EcoRI and the restriction products were visualised on an agarose gel. For each screening, the largest cDNAs were excised and eluted from the gels (GFX Gel Band Elution kit, Amersham Biosciences, Freiburg, Germany). For later use and analysis, cDNAs were subcloned into pBluescript II SK^- at the EcoRI site.

2.2.2.5. DNA sequencing.

The DNA sequencing method used was based on the termination of chain extension developed by Sanger *et al*. (1977). Reactions were carried out with the "ABI PRISM™ Dye Terminator Cycle Kit with AmpliTaq® DNA polymerase, FS" (Applied Biosystems, Weiterstadt, Germany) in a thermal cycler. Products were sent to a centralised sequencing facility at the University of Hamburg (Department of Cell Biology, UKE, Hamburg, Germany).

2.2.2.6. Extraction of genomic DNA from *Arabidopsis thaliana*.

For analysis of Arabidopsis T-DNA insertion lines by PCR, a rapid DNA isolation method was used as described by Weigel and Glazebrook (2002). A small piece of leaf was cut and ground with a micropestle in a 1.5 mL microcentrifuge tube containing 400 µL of extraction buffer (200 mM Tris-HCl at pH 7.5, 250 mM NaCl, 25 mM EDTA and 0.5 % (w/v) SDS). Debris was spun down for 5 minutes at 13.000 g and 300 µL of the supernatant were

transferred to another tube. DNA was collected after precipitation with 300 µL isopropanol by centrifuging for 5 minutes at 13.000 g. The pellet was rinsed with 70% ethanol, dried and resuspended in 100 µL TE at pH 8.0 (10 mM Tris-HCl at pH 8.0, 1 mM EDTA). One µL of DNA was used per 25 µL of PCR reaction.

For Southern blot analysis, Arabidopsis genomic DNA was needed in higher quantities and in purer grade. To achieve this, an extraction with cetyltrimethylammonium bromide (CTAB) was performed. Approximately 2 g of leaves were ground in liquid nitrogen. The resulting powder was mixed in 25 mL CTAB buffer (140 mM sorbitol, 220 mM Tris-HCl at pH 8.0, 22 mM EDTA, 800 mM NaCl, 1% (w/v) N-laurylsarcosine and 0.8% (w/v) CTAB). The mixture was incubated at 65°C for 20 minutes. Then 10 mL of chloroform was added and the tubes were shaken on a rotating inverter at room temperature for 20 minutes. Phases were resolved by centrifugation at 3.000 g for 10 minutes and DNA was precipitated from the aqueous phase by addition of 17 mL of isopropanol and incubation on ice for 10 minutes. The precipitate was collected by centrifugation at 3.000 g for 10 minutes and was resuspended in 4 mL TE. Short nucleic acids were selectively precipitated by addition of 4 mL 4 M lithium acetate, incubation on ice for 20 minutes followed by centrifugation. After an ethanol sodium acetate precipitation, the genomic DNA pellet was resuspended in 0.9 mL TE and 0.1 mL 3 M sodium acetate. The DNA was extracted successively with phenol, phenol/chloroform 1/1 (v/v) and chloroform. DNA was precipitated with ethanol, recovered by centrifugation and resuspended in TE at pH 8.0

2.2.2.7. Southern blot analysis.

Digestion of genomic DNA.

Ten µg of genomic DNA extracted from Arabidopsis leaves was digested in a total volume of 100 µL with 2 units of restriction enzyme per µg DNA. After 2 hours incubation at 37°C, another unit of enzyme per µg DNA was added and the reaction was continued for an additional 3 hours. The digested DNA was precipitated with sodium acetate and ethanol and the pellet obtained by centrifugation was resuspended in 30 µL of water.

DNA gel electrophoresis.

DNA samples were generally combined with 1/10 of loading dye (50% (v/v) glycerol, 0.005% (w/v) bromophenol blue) and run on a 1% (w/v) agarose gel in TBE or TAE (Sambrook *et al*., 1989).

Transfer of DNA.

Before transfer, DNA was depurinated by short incubation of the gel in 250 mM HCl, then denaturated in 0.5 N NaOH, 1.5 M NaCl, and the gel was re-equilibrated in 0.5 M Tris-HCl at pH 7.5 and 3 M NaCl. DNA was transferred by capillary action to a positively charged nylon membrane (Hybond N^+, Amersham Biosciences, Freiburg, Germany) in a 10X SSC solution (Sambrook *et al*., 1989). DNA was covalently bound to the membrane by crosslinking under UV light (Stratagene, Heidelberg, Germany).

Labelling of DNA probes with digoxigenin.

Non-radioactive labelling of DNA probes that were used in Southern blot analysis as well as in plaque screening was performed with the DIG system (Roche, Mannheim, Germany). cDNA probes were labelled either by PCR or by random-primed cDNA synthesis, during which reactions alkali-labile digoxigenin-dUTP was incorporated into the nascent strands.

DNA hybridisation.

Nylon membranes were prehybridised for 3 hours at 65 °C in approximately 1 mL of prehybridisation solution (5X SSC, 0.1% (w/v) N-Laurylsarcosine, 0.02% (w/v) SDS and 1% (w/v) blocking reagent (Roche, Mannheim, Germany) per 10 cm^2 of membrane. Before hybridisation, digoxigenin-labelled DNA probes were heat-denaturated for 10 minutes at 95°C, and 5 ng of probe were added per 1 mL of prehybridisation solution. Washing steps were carried out at high stringency, to avoid cross-hybridisation of the probe. Membranes were first washed twice at room temperature for 5 minutes with large volumes of 2X SSC, 0.1% (w/v) SDS, then twice at 68°C for 20 minutes in 0.2X SSC, 0.1 % (w/v) SDS. Hybridised probes were detected with an anti-digoxigenin antibody coupled to a horseradish alkaline phosphatase. After addition of the chemiluminescent substrate CSPD® (Roche, Mannheim, Germany), X-ray film (Hyperfilm™ MP, Amersham Biosciences, Freiburg, Germany) was exposed to record signals from the membrane carrying the hybridised probe and bound antibody.

2.2.2.8. Extraction of total RNA from plant tissues (Puissant and Houdeline, 1990).

Immediately after collection, plant tissues were frozen in liquid nitrogen and kept at –80°C until needed. Tissues were ground with a mortar and pestle in liquid nitrogen until a fine powder was obtained. Approximately 100 mg of powder was transferred to a 1.5 mL microcentrifuge tube. One mL of Trizol reagent (Invitrogen, Karlsruhe, Germany) was added to the tissue powder. Samples were homogenised until the powder was thawed and were left standing at room temperature for 5 minutes. Two hundred µL of chloroform/isoamyl alcohol 24/1 (v/v) were added and the tubes were shaken vigorously. After 3 minutes incubation at room temperature, phases were separated by centrifugation at 4°C and 12.000 g for 15 minutes. RNA was precipitated from the aqueous phase by addition of 500 µL of isopropanol and centrifugation at 12.000 g for 10 minutes. The pellet was briefly rinsed with 500 µL of 4 M LiCl and resuspended in 500 µL TE at pH 8.0. Residual polysaccharides were washed out with 500 µL of chloroform/isoamyl alcohol 24/1 (v/v) and RNA was precipitated by addition of 66 µL 3 M sodium acetate at pH 5.0 and 500 µL isopropanol. After recovery of the RNA by centrifugation for 10 minutes at 12.000 g, the pellet was slightly dried and resuspended in 50 µL water. An incubation at 55°C led to complete dissolution of the RNA.

2.2.2.9. Isolation of mRNA.

Polyadenylated transcripts were isolated from around 300 µg of total RNA by binding to polystyrene-latex particles coated with $dC_{10}T_{30}$ oligonucleotides, according to the suppliers instructions (Oligotex mRNA midi kit, Qiagen, Hilden, Germany).

2.2.2.10. Preparation of cDNA libraries from rice and *Arabidopsis thaliana*.

Twenty cm-long rice stem sections comprising the youngest internode were incubated for 0 minutes, 40 minutes or 90 minutes in 30 mL of 10 mM ACC. One-cm portions of the internode that contained the intercalary meristem and part of the elongation zone were collected and used for extraction of total RNA. mRNA was isolated from 300 µg total RNA per sample with the Oligotex mRNA midi kit (Qiagen, Hilden, Germany). Three rice cDNA

libraries were prepared from 5 µg mRNA, in accordance with the instructions supplied by the manufacturer (TimeSaver cDNA synthesis kit, Amersham Biosciences, Freiburg, Germany), using dT_{12-18} oligonucleotides as primers for reverse transcription. The cDNAs obtained in a final volume of 100 µL were digested completely with 2 restriction enzymes, Rsa I and Alu I, which both cut in a blunt end manner in the middle of the tetranucleotide recognition sites AGCT and GTAC, producing short cDNAs. The three libraries composed of short cDNAs were used for subtractive hybridisation. They were called "L0" (Library 0), "L40" and "L90" for simplification.

An *Arabidopsis thaliana* cDNA library was made from mRNA isolated from stems, roots and leaves harvested at different developmental stages, as well as from silliques and flowers. cDNAs were synthesised using dT_{12-18} oligonucleotides. The library was exploited for isolation of partial or full-length cDNAs by PCR.

2.2.2.11. Northern blot analysis.

RNA gel electrophoresis.

RNA samples were prepared in the following way: 15 to 20 µg samples of RNAs were precipitated overnight at –80°C with 0.4 M NaCl and ethanol. After centrifugation, the supernatant was discarded and the pellet was dried briefly. RNA was resuspended in 20 µL of RNA-loading buffer (50% (v/v) deionised formamide, 5% (v/v) formaldehyde, 1X MOPS, 0.005% (w/v) bromophenol blue), heat-denaturated at 55°C for 10 minutes and chilled on ice. RNA samples were separated under denaturing conditions in formaldehyde-agarose gels (1% (w/v) agarose, 6% (v/v) formaldehyde, 1X MOPS) using 1X MOPS as a running buffer.

RNA Transfer.

RNA was transferred by capillary forces to a nylon membrane (Hybond N^+, Amersham Biosciences, Freiburg, Germany) with 10X SSC (Sambrook *et al*., 1989). After crosslinking of RNA, membranes were briefly rinsed in 2X SSC buffer.

Labelling of cDNA probes with α-[^{32}P]-dCTP.

Using the Ready-To-Go dCTP labelling kit (Amersham Biosciences, Freiburg, Germany), α-[^{32}P]-dCTP (3000 Ci/mmol) was incorporated into the probes by random prime labelling. Each labelling reaction was conducted at 37°C for at least 2 hours. Non-incorporated α-[^{32}P]-dCTP was removed by allowing the reaction to flow through an SHR-300 column (Amersham

Biosciences, Freiburg, Germany). Twenty-five to 30 ng of heat-denaturated cDNA and 30 to 50 µCi of α-[^{32}P]-dCTP were used per reaction.

Detection of radioactively labelled probes.

Membranes were blocked in prehybridisation solution (10% (w/v) dextran sulphate, 1% (w/v) SDS, 1 M NaCl and 100 µg·mL^{-1} fish sperm DNA) for 3 hours at 68°C, after which the heat-denaturated radioactively labelled probe was added. Hybridisation was carried out overnight at 68°C. The membranes were rinsed briefly in 1X SSC, then successively washed at high stringency once in 1X SSC for 15 minutes at 68°C and once in 0.1% (w/v) SDS, 1X SSC for 15 minutes at 68°C. Hybridised probes were detected by exposure of an X-ray film (Hyperfilm^{TM} MP, Amersham Biosciences, Freiburg, Germany) to the membranes in autoradiography cassettes coated with intensifying screens (8 times), at –80°C.

2.2.2.12. Subtractive hybridisation.

The aim of the subtractive hybridisation was to isolate cDNAs corresponding to genes, the expression of which was induced in rice stem sections after ACC treatment. The methodology, taken from Wang and Brown (1991) and Buchanan-Wollaston and Ainsworth (1997) was used as adapted by Lorbiecke (1998). Of the three rice cDNA libraries, L40 and L90 (2.2.2.10) were used as "target" populations of cDNAs from which a "driver" population (L0) was subtracted.

Ligation of adapters to the cDNAs.

Adapters were ligated to the blunt-end cDNAs in order to allow amplification by PCR and cloning. Adapters were created by annealing two pairs of oligonucleotides. To the "target"-cDNA populations SUB21-SUB25 adapters were ligated. The adapters were made by hybridisation of the oligonucleotides SUB21 and SUB25 which are complementary to each other. Primer SUB25 was phosphorylated at the 5'-end to allow ligation to the blunt-ended cDNAs. The constituted double-stranded adapter contained an EcoRI restriction site as shown below to facilitate cloning of the cDNAs into pBluescript II SK^{-}.

```
SUB21     5'-     CTCTTGCTTGAATTCGGACTA   -3'
SUB25     3'-ACACGAGAACGAACTTAAGCCTGAT-P-5'
```

To the "driver"-cDNA population the adapter KS18-KS22 was ligated. It was obtained as described previously by annealing of the complementary oligonucleotides KS18 and KS22.

KS18	5'- CGGTATCGATAAGCTTGA -3'
KS22	3'-ACACGCCATAGCTATTCGAACT-**P**-5'

Ligation products were separated by electrophoresis on 1.3 % (w/v) low melting-point agarose gel (Type VII, Sigma, Taufkirchen, Germany). The adapters were excised from the gel and the gel was run with inverted polarities to concentrate the cDNAs in narrow bands.

Amplification of cDNA libraries by PCR.

Five µL of molten agarose containing cDNAs was used for each of the twenty PCR reactions needed to amplify the libraries. These PCR reactions, in a total volume of 100 µL 1X PCR buffer (0.2 mM dNTPs, 1.5 mM $MgCl_2$, 0.5 µM primer, 2.5 units of Taq polymerase; Invitrogen, Karlsruhe, Germany), were made with "driver"-cDNAs using KS18 primer biotinylated at the 5'-end, and using non biotinylated SUB21 primer with "target"-cDNAs. The following program was used for amplification (Figure 2).

Figure 2: Program for amplification of cDNA libraries

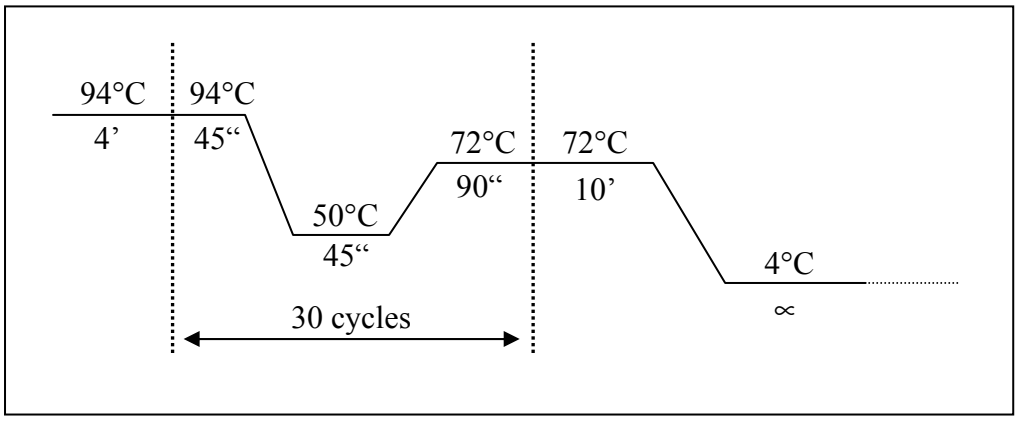

cDNAs amplified in the 20 reactions were combined in one tube, extracted with phenol/chloroform 24/1 (v/v) and phenol, and precipitated from the aqueous phase with 0.1 volumes of 4 M NaCl and 2.5 volumes of ethanol, overnight at –20°C. cDNAs were recovered by a centrifugation at 11.000 g for 30 minutes, were washed with 70% ethanol and resuspended in water.

Subtractive hybridisations.

Five µg of "driver"-cDNAs were combined with 0.5 µg of "target"-cDNAs, precipitated overnight and resuspended in 10 µL of HE buffer (10 mM Hepes at pH 7.3, 1 mM EDTA). cDNAs were denaturated for 3 minutes at 100°C, chilled on ice and added to 10 µL of 2X hybridisation buffer (1.5 M NaCl, 50 mM Hepes at pH 7.3, 0.2% (w/v) SDS). After addition of a drop of mineral oil, cDNAs were denaturated again for 3 minutes at 100°C and incubated at 65°C for 20 hours in a thermal cycler. After hybridisation, 80 µL of water were added, the mineral oil was discarded and 100 µL of 2X binding buffer (10 mM Tris-HCl at pH 7.5, 2 M NaCl, 1 mM EDTA) were added. Biotinylated cDNAs were removed from the solution by binding to 100 µL corresponding to 2 mg of Dynabeads M-280 Streptavidin (Dynal, Hamburg, Germany) in a 1.5 mL microcentrifuge tube. Binding occurred under constant shaking for 30 minutes at room temperature. Then the paramagnetic beads were attracted to the side of the tube with a magnet and the solution containing non-biotinylated cDNAs (fraction SUB1) was carefully removed from the tube. Two-and-a-half µg of "driver"-cDNAs were combined with the subtracted "target"-cDNAs and the hybridisation procedure was repeated as described earlier except that hybridisation was performed for 2 hours only. After another subtraction, 1 µL of the SUB2 "target"-cDNA population was amplified by PCR with the SUB21 primer, using the conditions described above (Figure 2).

One half µg of the resulting PCR products (SUB2-PCR) were mixed with 10 µg of the "driver"-cDNAs and further subtractive hybridisations were carried out as explained above. This way, fractions SUB3 and SUB4 were obtained and the process was repeated a third time to produce the SUB5 and SUB6 populations of cDNAs.

The whole procedure was carried out twice to produce two subtractive libraries, L40 versus L0 (called later on L40-0) and L90 versus L0 (L90-0) which were enriched in cDNAs corresponding to genes induced after 40 minutes or 90 minutes of treatment with ACC, respectively.

2.2.3. Molecular genetic methods.

2.2.3.1. Construction of an *Ataci3-1* promoter-GUS fusion plasmid.

A 1.2 kb fragment of putative promoter sequence, beginning with the start codon of *Ataci3-1* was amplified by PCR using genomic DNA from *Arabidopsis thaliana* as a template. The primers used were At5g6p-Xba and At5g6p-Bam (Table 2) containing either an XbaI or a BamHI restriction site which allowed excision of the promoter from the subcloning vector

pGEMT-Easy and its directional cloning into pGUS-SB in front of the *uidA* gene encoding β-glucuronidase. The whole cassette comprising the promoter, the *uidA* gene and a nopaline synthase (nos) terminator was excised at the XbaI and SpeI sites and cloned into pPZP312 at the XbaI restriction site.

2.2.3.2. Construction of an *Ataci3-1* overexpression plasmid.

Cloning was based on the Gateway system (Invitrogen, Karlsruhe, Germany). *Ataci3-1* was amplified by a proofreading Taq polymerase (Invitrogen, Karlsruhe, Germany) from the subcloning vector pGEMT-Easy (Promega, Mannheim, Germany) with the gene-specific primers Ataci3-WG.F and Ataci3-WG.R (Table 2). The antisense primer Ataci3-WG.R contained a mismatching tail (5'-CACC) that allowed directional cloning of the cDNA into pENTR/D-TOPO, a so-called "Entry" vector, by "flap ligation" with topoisomerase I (Cheng and Shuman, 2000).

The destination vector, pB2WG7, was actually designed to receive cDNAs in antisense orientation (the recombination sites for bacteriophage λ *att*R1 and *att*R2 were inverted in comparison to the pB2GW7 vector designed for overexpression). However, the pB2WG7 vector contained all the elements needed for overexpression, that is to say a cloning site located between a strong constitutive promoter and a terminator (both derived from the cauliflower mosaic virus 35S). The *Ataci3-1* cDNA was therefore cloned into the "Entry" vector in antisense orientation such that the recombination event between "Entry" and "Destination" vector produced a sense orientation of the cDNA. This construct was used for overexpression of *Ataci3-1* in *Arabidopsis thaliana*.

2.2.3.3. Direct DNA transfer into *Agrobacterium tumefaciens.*

A single Agrobacterium colony was picked, inoculated in 2 mL of YEP medium at pH 7.0 (10 $g.L^{-1}$ yeast extract, 10 $g.L^{-1}$ peptone, 5 $g.L^{-1}$ NaCl) and grown overnight at 28°C with gentle shaking. This preculture was used to inoculate 50 mL of the same medium. Bacteria were grown until an OD_{600} of about 0.5 was reached. Cells were spun down for 5 minutes at 3.000 g and resuspended in 10 mL of 150 mM NaCl. Bacteria were spun down again and resuspended in 1 mL of ice-cold 20 mM $CaCl_2$. Two hundred µL of bacteria were combined with 1 µg of binary plasmid DNA and were incubated on ice for 30 minutes. Cells were frozen for 1 minute in liquid nitrogen and were then allowed to thaw in a water bath at 37°C.

After addition of 1 mL YEP medium, cells were shaken at 180 rpm and 28°C for 4 hours. To reduce the volume of cells for plating, they were spun down briefly and resuspended in 100 µL of YEP medium. Finally, cells were plated on YEP-agar (YEP, 1.5% agar (w/v)) plates containing the appropriate antibiotics and incubated at 28°C until growth of transformed colonies.

2.2.3.4. *Agrobacterium tumefaciens*-mediated transformation of Arabidopsis.

Agrobacterium colonies resistant to gentamicin, kanamycin, rifampicin and spectinomycin were picked, inoculated in 5 mL YEP medium containing the four antibiotics and grown at 28°C overnight. The preculture was used to inoculate 500 mL of YEP medium containing the antibiotics, omitting rifampicin. *Agrobacterium* cells were grown overnight at 28°C with gentle shaking. After addition of 15 g of sucrose and 150 µL of Silwet L-77 (Lehle Seeds, Round Rock, Texas, USA), stems of two week-old *Arabidopsis* plants were dipped in the culture for 1 minute and placed in a growth chamber, first under cover for 2 days to promote *Agrobacterium* growth, then under normal conditions to allow seed set.
The progeny (generation T_0) was sown on square trays of soil and after 5 days was sprayed every second day with a solution of 200 µM BASTA (AgrEvo, Berlin, Germany) dissolved in water. After a few days, plants resistant to BASTA were easily identifiable because they were green amongst yellow dying non-resistant plants. Resistant plants were transferred to individual pots. Subsequent analysis was performed on T_1 seedlings from ten independent transformants.

2.2.3.5. Histochemichal localisation of promoter activity by whole mount GUS staining.

T_1 *Arabidopsis* plants were grown either in soil or on MS-agarose plates containing different hormones (see section 2.2.1.6). Tissues were harvested and stored on ice in 1.5 mL microcentrifuge tubes filled with 90% acetone, until all samples were ready. They were incubated at room temperature for 20 minutes and were then washed on ice with 1 mL staining buffer (0.2% (w/v) Triton-X100, 50 mM sodium-phosphate buffer at pH 7.2, 2 mM $K_4[Fe(CN)_6]$, 2 mM $K_3[Fe(CN)_6]$). The staining buffer was replaced by a staining solution containing the chromogenic substrate X-Gluc (staining buffer plus 5-bromo-4-chloro-3-

indolyl β-D-glucuronide at a final concentration of 2 mM), which was vacuum-infiltrated into the tissues for 20 minutes. To reveal the staining, samples were incubated overnight at 37°C. Tissues were subjected to an increasing ethanol series (20%, 35% and 50% ethanol at room temperature for 30 minutes each) and fixed in FAA solution (50% ethanol, 5% formaldehyde and 10% acetic acid) for at least 30 minutes. For tissues with high chlorophyll content, treatment with another ethanol series, 70%, 80%, 90% and 95% was performed for 30 minutes each. Tissues were cleared overnight in 100% ethanol at 4°C and then partially rehydrated in a decreasing ethanol series (90%, 80% and 70%). Pictures of seedlings and tissues in 70% ethanol were taken through a binocular microscope (Olympus SZX9, maximum magnification 100 times, Hamburg, Germany) of through a brightfield microscope (Leitz Orthoplan, Wetzlar, Germany) with a Nikon Coolpix 4500 (Nikon, Düsseldorf, Germany) digital camera.

2.2.3.6. Cryosections of Arabidopsis tissues.

Arabidopsis tissues fixed in FAA were embedded in Leica Jung tissue freezing medium (Leica Mikrosysteme Vertrieb GmbH, Bensheim, Germany), then quickly frozen and kept at –20°C for a short period. Frozen samples were mounted on a cryo-microtome (Leica Jung Frigocut 2800E) and 20 to 30 µm-thick sections were made. Following analysis and photographs were made using a Leica DC300F digital camera mounted on a Leica DMLS microscope (Leica Mikrosysteme Vertrieb GmbH, Bensheim, Germany).

2.2.3.7. Construction of an *Ataci3-1-gfp fusion* plasmid.

PstI restriction sites were inserted at both ends of the *Ataci3-1* cDNA by PCR, using a proofreading Taq polymerase and the primers Ataci3-GFP F and Ataci3-GFP R (Table 2). Cloning of the amplified cDNA into the Pst I site of pUhGFPC3-N resulted in a hybrid gene with a conserved open reading frame, encoding an AtACI3-1-GFP fusion protein with GFP being fused to the carboxyl terminus of AtACI3-1.

2.2.3.8. Ballistic transformation of epidermal onion cells.

Five µg of plasmid were combined with 2 mg gold particles in a total volume of 50 µL of water. Binding of DNA to the gold particles was triggered by the addition of 50 µL of 2.5 M

$CaCl_2$ and 20 µL of 0.1 M spermidin. After 20 minutes incubation at room temperature, gold particles were spun down at 2.300 g for 1 minute. The pellet was resuspended and washed twice with 70% ethanol and finally resuspended in 50 µL absolute ethanol. For each assay, 10 µL of the gold suspension were spread on a macrocarrier and particles were shot at 1350 psi (Biorad PDS-1000/He biolistic Particle delivery system, München, Germany) on onion epidermis strips stretched on MS-agarose plates.

2.2.3.9. Subcellular localisation of the ATACI3-1-GFP fusion protein in epidermal onion cells.

After an overnight incubation at 26°C in the dark, bombarded onion epidermis strips were placed between a microscope slide and a coverslip in liquid MS medium. Using a confocal-laser scanning microscope (CLSM, TCS SP, Leica Mikrosysteme Vertrieb GmbH, Bensheim, Germany), samples were excited with an excitation beam with a wavelength of 488 nm provided by an Ar/He/Ne laser and the signal emitted between 510 and 550 nm was recorded and attributed a green colour. Bright field pictures of the same cells were taken and were digitally overlaid with the fluorescent green signal.

2.2.4. Database searches and sequence analysis.

Database searches were performed on the BLAST servers from the National Center of Biotechnology Information, USA (http://www.ncbi.nlm.nih.gov/BLAST/) and the Genomenet Bioinformatics Center based at Kyoto University, Japan (http://blast.genome.ad.jp).
Additional information about genomic sequences, ESTs and available mutants was obtained through The Arabidopsis Information Resource (TAIR, http://www.arabidopsis.org), The Institute for Genomic Research (TIGR, http://www.tigr.org/tdb/e2k1/osa1) and the Nottingham Arabidopsis Stock Centre (NASC, http://www.nasc.nott.ac.uk) web sites.
Alignments of DNA and protein sequences, as well as calculations of hydrophobicity profiles were made using the BioEdit 5.0.9 software (Hall, 1999).

3. Results.

Previous work showed that growth induction in the youngest internode of partially submerged deepwater rice plants is triggered by ethylene (Kende *et al*., 1998). Submergence induces synthesis and accumulation of ethylene within 1 hour, through altered gas composition and limited gas diffusion, (Raskin and Kende, 1984). Ethylene subsequently causes a decrease in ABA level, an increase of gibberellin GA_1 concentration, and an increase in responsiveness to gibberellin, with enhanced internodal elongation as a result (Hoffmann-Benning and Kende, 1992). Alterations in ethylene, ABA and gibberellin levels after submergence were measured in a 1-cm portion at the base of the youngest growth-responsive internode that encompasses the intercalary meristem and part of the elongation zone. If interactions occur during submergence between ethylene and gibberellin, signalling components are expected to be localised in this portion of the internode. It was therefore used in this study to identify genes involved in signalling between ethylene and gibberellin. However since submergence is not only a signal for growth induction but also for induction of hypoxia-related genes it was chosen to provide the ethylene signal without imposing hypoxic conditions. Excised rice stem sections were treated with ACC, to avoid induction of hypoxic genes which could mask expression of ethylene to gibberellin signalling genes.

First, a time course analysis of growth induction by ACC was performed. Based on the results obtained, a subtractive hybridisation was performed at appropriate time points in order to isolate genes that were induced by ACC prior to growth induction. Genes that were induced by submergence, by ACC or by ethylene, but not by gibberellic acid GA_3 were assigned a putative function in ethylene to gibberellin signalling.

3.1. Isolation of genes induced by ACC in rice stem sections.

3.1.1. Induction of internodal growth by ACC.

ACC is converted to ethylene by ACC oxidase (ACO, EC 1.14.17.4) in the second committed step of the ethylene biosynthesis pathway. In most tissues, ACO activity is not limiting to ethylene synthesis. Rice stem sections were treated with ACC at different concentrations in order to determine optimal conditions for growth induction.

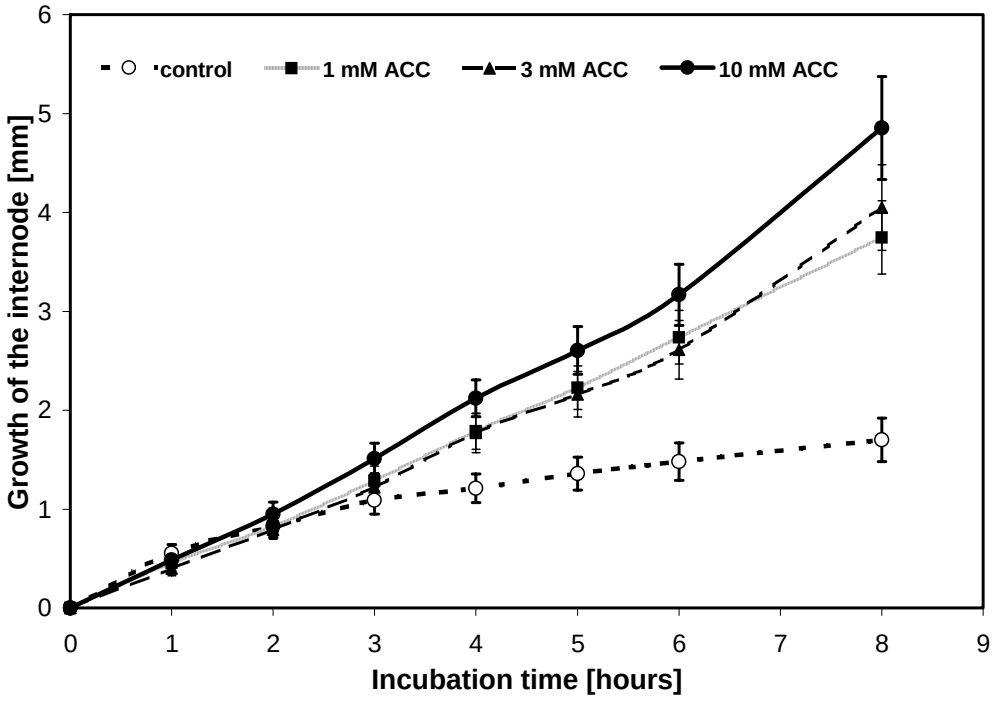

Figure 3: Growth of internodes incubated with 1 mM, 3 mM, 10 mM ACC or without ACC. Results are averages of internodal growth measured from 18 to 21 stem sections in two independent experiments. Error bars represent standard deviation.

In comparison to control sections, increased growth was observed with 1 mM, 3 mM and 10 mM ACC (Figure 3). The highest growth rate was achieved with 10 mM ACC, indicating that the growth response was dose-dependent. Internodes of sections incubated with 10 mM ACC elongated close to 4 times more than sections incubated without ACC. Use of ACC concentrations higher than 10 mM did not result in higher growth rates (data not shown), indicating that either the growth response or ACC uptake and conversion to ethylene by ACC oxidase were saturated. The lag phase of ACC-induced growth was between 2 and 3 hours with 10 mM ACC and between 3 and 4 hours with 1 mM and 3 mM ACC. Based on these results, we chose to use 10 mM ACC for all subsequent experiments to reduce the lag phase to less than 3 hours and in order to induce a maximum growth-response.

Since ethylene to gibberellin signalling occurs prior to growth of the internode, isolation of genes involved in this signalling pathway was attempted at 40 minutes and at 90 minutes of treatment with 10 mM ACC. Two time points were chosen to achieve better coverage of the signal transduction events.

3.1.2. Isolation of ACC-induced genes by subtractive hybridisation.

The subtractive cDNA library L40-0 was obtained by subtracting cDNAs from untreated tissue from cDNAs from tissue treated with 10 mM ACC for 40 minutes. The subtractive cDNA library L90-0 was obtained by subtracting cDNAs from untreated tissue from cDNAs from tissue treated with 10 mM ACC for 90 minutes. From the two subtractive cDNA libraries L40-0 and L90-0, cDNAs were cloned into the EcoRI site of pBluescript II SK$^-$. Bacterial clones obtained after transformation were randomly picked, plasmid DNA was extracted and inserts were sequenced using the T7 primer (Table 2). Analysis of the sequences allowed identification of twelve different cDNAs. These were termed aci for ACC-induced (Table 3).

Clone	Length (bp)	Isolated from L40-0	Isolated from L90-0
aci1	285	0	1
aci2	261	7	5
aci3	280	1	1
aci3'	226	4	7
aci4	238	7	0
aci5	338	9	0
aci6	388	2	0
aci7	192	1	0
aci8	437	1	0
aci9	380	1	0
aci10	214	0	2
aci11	183	0	1
		Σ 33	**Σ 17**

Table 3: A*ci* clones isolated by subtractive hybridisation.

The cDNAs *aci3'* and *aci3* sequences were partially identical. While the ends of both cDNAs aligned to 100%, an additional fragment of 54 bp was inserted at position 135 of *aci3'*. Since this particular clone was found twice in two different subtractive libraries, it was concluded that *aci3* did not result from an amplification or cloning artefact.

Both libraries were redundant for several cDNA species: *aci2*, *aci3*/*aci3'*, *aci4* and aci5 were found between 5 and 9 times in the L40-0 library, whereas *aci*2 and *aci3'*

represented most of the clones found in the L90-0 library (Table 3). Because of the redundancy of the libraries further sequencing was not performed.

Due to progress made in collecting and annotating rice full-length cDNAs in the course of this work, in particular after publication of 28.000 cDNA clones from the Rice Full-length cDNA Consortium (Kikuchi *et al*., 2003), it was recently possible to assign to each *aci* clone a corresponding full-length cDNA. However, this was not the case at the beginning of this work. Thus full-length cDNA sequences that were obtained by screening of a rice λgt11 cDNA library are highlighted as part of the present work.

3.1.3. Expression of *aci* genes in ACC-treated stem sections.

To validate differential expression of the *aci* genes identified by subtractive hybridisation, Northern blot analysis was performed. For identification of differentially expressed genes, excised stem sections were used as for growth experiments. In order to exclude the possibility that the effects found resulted from handling of the internodes such as cutting or mechanical stimuli, controls were incubated without ACC for 0 or 90 minutes. In addition, incubation with ACC for 180 minutes was included to see if ACC induction of gene expression was a short-term effect or if it extended over a longer period of time. Two groups of genes could thus be distinguished: genes for which transcript levels changed in parallel in treated and untreated stem sections and genes for which elevated transcript levels were detected with ACC treatment.

Transcript levels of *aci1*, *aci2*, *aci6*, *aci9* and *aci11* were weakly and transiently induced after 90 minutes of treatment with ACC (Figure 4). Levels of these transcripts were also slightly induced after 90 minutes in controls, indicating that these genes might be wound-regulated. Since no data were obtained for 180 minutes in controls it was not possible to say if the transient gene expression observed with ACC was a specific effect. Sequence analysis did not point to a role for these genes in signalling. Therefore, with the exception of *aci6*, genes with similar expression in control and ACC-treated tissues were not characterised further. A brief description of the *aci* genes of this category and homologies to related genes are given. Sequences of homologous cDNAs and conceptual translation products are found in the appendix (Chapter 7).

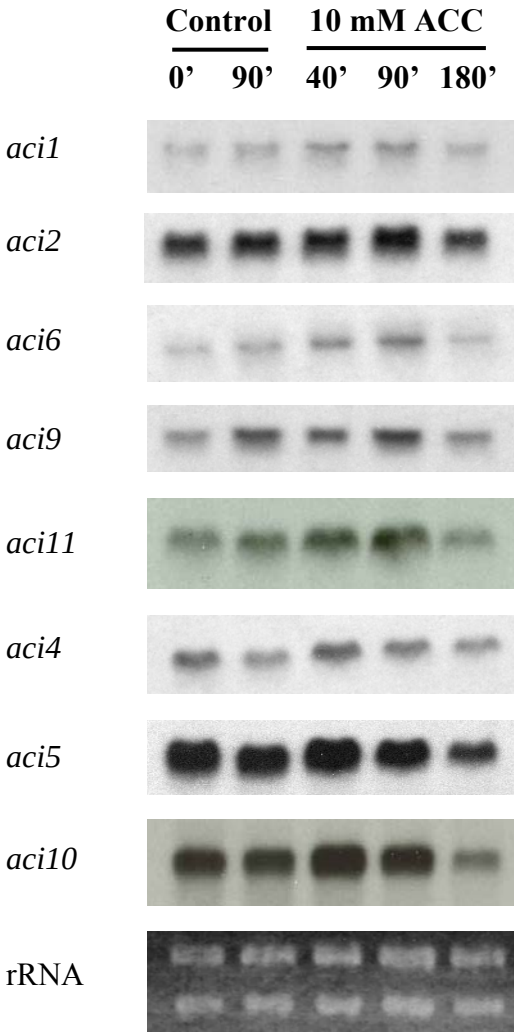

Figure 4: Expression of *aci* genes not specifically regulated by ACC.
Stem sections were incubated with 10 mM ACC for 40 minutes, 90 minutes or for 180 minutes. Control sections were incubated without ACC for 0 minutes or for 90 minutes. Filters containing 20 µg of RNA per lane were successively hybridised with different ^{32}P-labelled probes. EtBr-stained rRNA shows equal loading of the gel.

Aci1 showed identity to a cDNA registered in the database under the accession number AK121440 (Appendix 7.1.). This cDNA encodes a protein of 344 amino acids (accession number P0481E08) which showed high homology with 8 other proteins from rice. Identity between P0481E08 protein and the rice homologues ranged from 49% to 56%. In Arabidopsis, 7 proteins with significant homology to P0481E08 were found. None of these were assigned a function.

Aci2 was identical to a cDNA published in the database. The homologous cDNA AK099201 encodes an open reading frame of 927 nucleotides corresponding to a protein of 309 amino acids (Appendix 7.2.). Homology searches clearly identified this protein as ascorbate peroxidase (APX, EC 1.11.1.11). It was 86% identical with a thylakoid-bound APX from tobacco (accession number BAA78552.1). However, homology in the same range was found as well with stromal forms of the enzyme, leaving a doubt on the exact localisation of the protein derived from AK099201. Ascorbate peroxidases participate in detoxification of intracellular H_2O_2, using ascorbate as reductant (Smirnoff, 1996).

A cDNA corresponding to *aci6* was found in the database under the accession number AK104932. It encodes a protein of 408 amino acids that was renamed OsSBF1 (Appendix 7.6.). OsSBF1 shared 73% identical and 84% similar amino acids with a protein from Arabidopsis, termed accordingly AtSBF1. A full-length cDNA of *Atsbf1* was isolated by PCR from an Arabidopsis cDNA library and deposited in the Genebank database under the accession number AF498303. In a domain search, both rice and Arabidopsis proteins were recognised as members of the sodium/bile acid family of cotransporters previously identified in non-plant organisms, hence the names OsSBF1 and AtSBF1 were chosen. Members of this family of integral transmembrane proteins are found in archaea, bacteria and eukaryotes. Figure 5 gives an alignment between OsSBF1, AtSBF1 and three sequences from representative sodium-dependant cotransporters from different organisms.

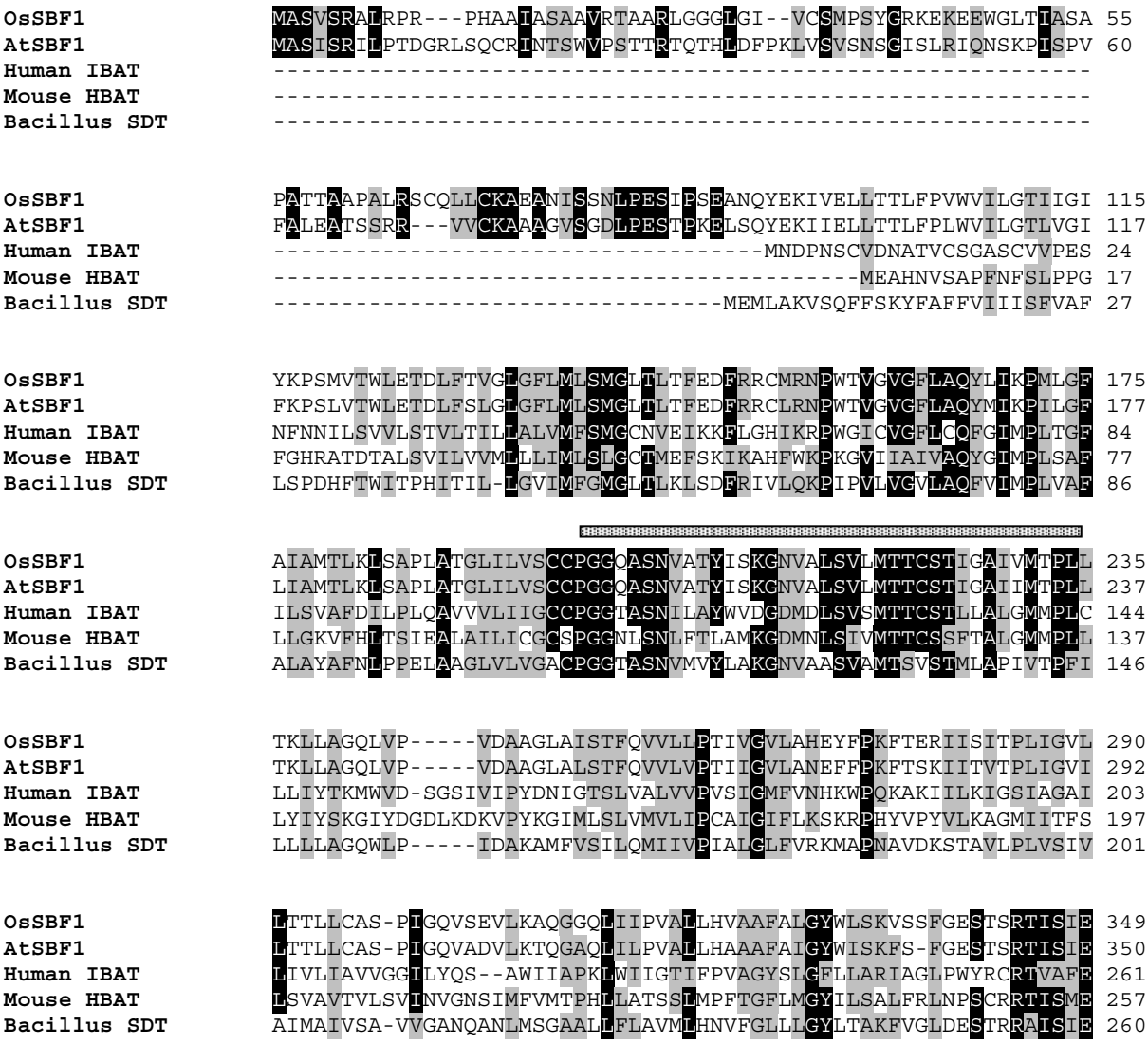

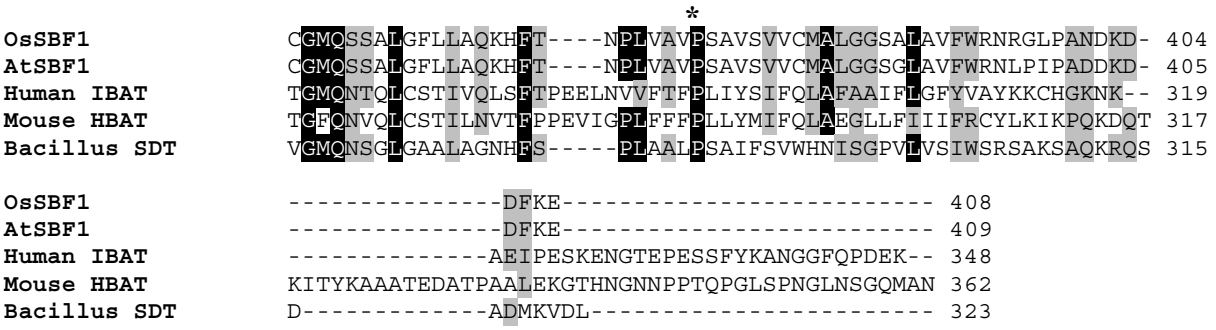

Figure 5: Sequence alignment of sodium-bile acid symporter-like proteins. Sequences are from rice (OsSBF1), Arabidopsis (AtSBF1), human (IBAT, for ileal bile acid transporter; accession number I38655), mouse (HBAT, for hepatic bile acid transporter; accession number BAA19846.1) and *Bacillus halodurans* (SDT, for sodium-dependent transporter; accession number NP_241724.1). The dotted bar indicates the signature domain for SBF proteins. The asterisk points out a proline residue that was shown to be essential for bile acid transport.

Mammalian ileal sodium-dependent bile acid transporters were shown to be involved in reabsorption of bile acids from the intestinal duct in a part of the intestine called ileum Transmembrane proteins are necessary to mediate transport of bile acids through the plasma membrane of intestinal epithelial cells because bile acids are polar hydrophobic compounds (Hallén *et al*., 1999). OsSBF1 showed 56% similarity with the human ileal bile acid transporter (IBAT; accession number I38655). Not only the primary sequence was conserved between OsSBF1 and human IBAT (Figure 5). Hydrophobicity plot analysis (Kyte and Doolittle, 1982) showed a similar distribution of predicted transmembrane alpha-helices in OsSBF1 compared to the human IBAT (Figure 6). This suggested that secondary structure was also preserved. Furthermore, an amino acid shown to be essential for bile acid transport (Wong *et al*., 1995), Pro^{290}, was conserved in plant SBF proteins (Figure 5). These findings strongly supported the idea that plant SBF proteins were functionally related to mammalian sodium-dependent bile acid transporters. However, bile acids have not been shown to occur in plants. In plants, sulphonated brassinosteroids are the only cholesterol-derived compounds that are structurally related to bile acids. In *Brassica napus*, *O*-sulphonation of brassinosteroids by a steroid sulphotransferase results in inactivation of the hormone (Rouleau et at., 1999). It was therefore hypothesised that OsSBF1 plays a role in transport of sulphonated brassinosteroids. Results obtained on OsSBF1 have been published (Rzewuski and Sauter, 2002).

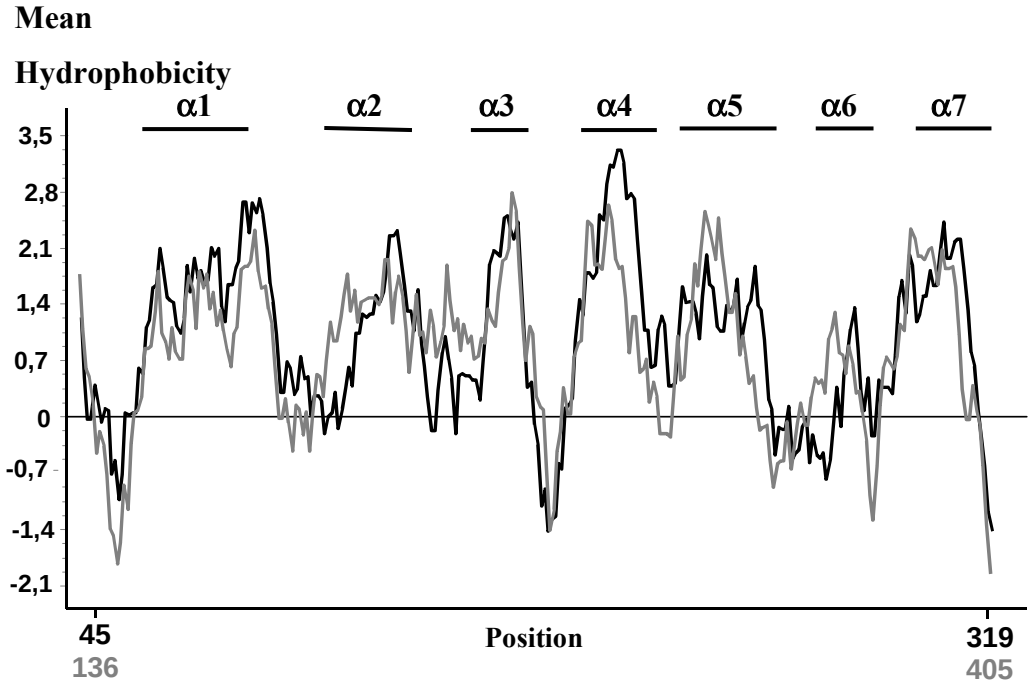

Figure 6: Hydrophobicity plots of the human IBAT (black line) and OsSBF1 (grey line). Black bars indicate alpha helices 1 to 7 in the human ileal sodium-bile acid transporter. Beginning and end positions of the portions of analysed sequences is given below the graph, in black for the human protein and in grey for the rice protein. Hydrophobicity mean profiles were calculated with a scanning window of 11 residues.

Aci9 was identical to a cDNA published under the accession number AK120851 (Appendix 7.9.). This cDNA codes for a protein of 584 amino acids that shared 58% identical amino acids with the copine protein BONZAI 1 from *Arabidopsis thaliana* (Hua *et al*., 2001). Copines constitute a recently characterised class of ubiquitous proteins, for which homologues were found in plants, animals and protozoa (Creutz *et al*., 1998). Human copines were shown to recruit intracellular target proteins to phospholipid bilayers in a calcium-dependent manner, resulting in a modification of enzymatic activity of the target proteins (Tomsig *et al*., 2003). Copines are therefore believed to be involved in calcium signalling. In plants, a role in vesicle trafficking was evoked (Hua *et al*., 2001).

A full-length cDNA corresponding to *aci11* was published under the accession number AY320036. *Aci11* covers 22 nucleotides of the 5'-UTR and 160 nucleotides of the coding sequence of AY320036 (Appendix 7.11.). This cDNA was previously shown by Sami-Subbu *et al*. (2001) to encode a protein of 986 amino acids that was termed Rp120. Rp120 is a cytoskeleton-associated RNA-binding protein involved in sorting prolamin RNA in rice endosperm. Until now, the gene was not shown to be expressed in tissues other than endosperm.

Expression of *aci4*, *aci5* and *aci10* appeared weakly induced after 40 minutes of ACC treatment and declined thereafter (Figure 4). After 90 minutes transcript levels were reduced not only in ACC-treated stem sections but also in control sections indicating that changes in gene expression were not caused by ACC treatment but rather by excision of stem sections. Expression of these genes was therefore not analysed further.

The cDNA sequence of *aci4* was identical to the coding sequence of a calcium-dependent lipid-binding like protein (CLB1), published under the accession number AK060230 (Appendix 7.4.). The rice protein CLB1 shared 65% identical and 84% similar amino acids with the CLB1 protein from tomato that was characterised by Kiyosue and Ryan (1997). Its function there was however not understood.

Aci5 showed sequence identity with a cDNA deposited under the accession number AK064893, at positions 504 to 840 (Appendix 7.5.). The open reading frame found in the full-length cDNA encoded a protein of 609 amino acids and was likely to be a phosphoglucomutase (EC 5.4.2.2). It shared 82% identical and 90% similar residues with the *Arabidopsis* plastidic phosphoglucomutase PGM (Periappuram *et al.*, 2000). Phosphoglucomutases catalyse the reversible conversion reaction between glucose-1-phosphate and glucose-6-phosphate.

The nucleotide sequence of *aci10* was identical to positions 1055 and 1267 of the cDNA AK067183. AK067183 encodes a protein of 986 amino acids (Appendix 7.10.). It was identified by homology searches as aconitate hydratase, or aconitase (EC 4.2.1.3), a pivotal enzyme of the citric acid cycle.

Genes which were specifically induced by ACC were of particular interest, since selection of candidate genes for the ethylene to gibberellin pathway was primarily based on inducibility by ethylene.

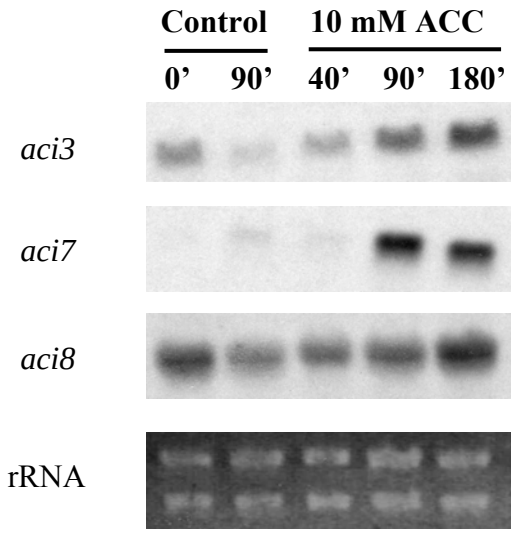

Figure 7: Expression of *aci* genes which were specifically regulated by ACC.
Filters carrying 20 µg RNA per lane (Figure 4) were successively hybridised with different ^{32}P-labelled probes. rRNA was stained with EtBr to show equality of RNA loading.

Signals detected in Northern blot analysis with probes for *aci3*, *aci7* or *aci8* showed that all corresponding genes had a basal expression level (Figure 7) prior to control treatment at 0 minutes. This was also true in the case of *aci7* where a signal was observed after longer exposure on X-ray film (data not shown).

Aci8 transcripts decreased in control tissue after 90 minutes. With ACC, a transient decrease at 40 minutes was followed by recovery of transcript levels at later time points (Figure 7). A similar expression pattern was observed for *aci3* with a transient decline at 40 minutes and a subsequent increase at 90 minutes and 180 minutes of ACC treatment. At 90 minutes, transcript amounts in ACC-treated sections were higher than in untreated sections (Figure 7). Expression of *aci7* showed highest induction in gene expression after 90 minutes of ACC-treatment, while expression in untreated sections was little or not altered (Figure 7). Among all *aci* genes, *aci7* was most strongly induced by ACC.

3.2. Characterisation of the ACC-induced genes.

3.2.1. Characterisation of *aci*8.

A full-length cDNA corresponding to *aci8* was isolated from a rice λgt11 cDNA library using the *aci8* cDNA obtained through subtractive hybridisation as a probe. The cDNA was excised from bacteriophage DNA and subcloned into pBluescript II SK$^-$. The ends of the insert were sequenced using the vector-specific primers T7 and M13-reverse. Analysis of the sequences revealed that the ends of the isolated cDNA were identical to a cDNA registered under the accession number AK099686. A protein of 845 amino acids, later named OsACI8, was deduced from the longest open reading-frame. The partial *aci8* cDNA isolated through subtractive hybridisation covered 178 nucleotides of the sequence encoding the C-terminus of the protein and 259 nucleotides of the 3'-untranslated region (Appendix 7.8.).

The OsACI8 protein was 33% identical to a protein from Arabidopsis encoded by the gene At4g24690 (Figure 8). The rice protein also possessed homology with protein sequences deduced from cDNAs of two other plant species. One partial cDNA from pineapple was published under the accession number AY098509 (Neuteboom *et al*., 2002). The deduced protein sequence of 309 amino acids aligned with the C-terminus of OsACI8, at position 502 up to the end of the sequence (Figure 8). Alignment revealed 52% identity between the rice and the pineapple protein. Expression of the pineapple gene was described to be enhanced in

fruits, as compared to expression in roots or in aerial parts of the plant (Neuteboom *et al*., 2002). A cDNA isolated from maize was published under the accession number AY108354. It is 2108 bp long and encodes a protein of 575 amino acids. The protein sequence aligned with that of OSACI8 from position 277 to the end of the sequence with a few gaps (Figure 8). Homology between rice and maize proteins was higher than between rice and pineapple proteins, with 60% and 52% identity respectively, showing better conservation between proteins from monocotyledonous plants.

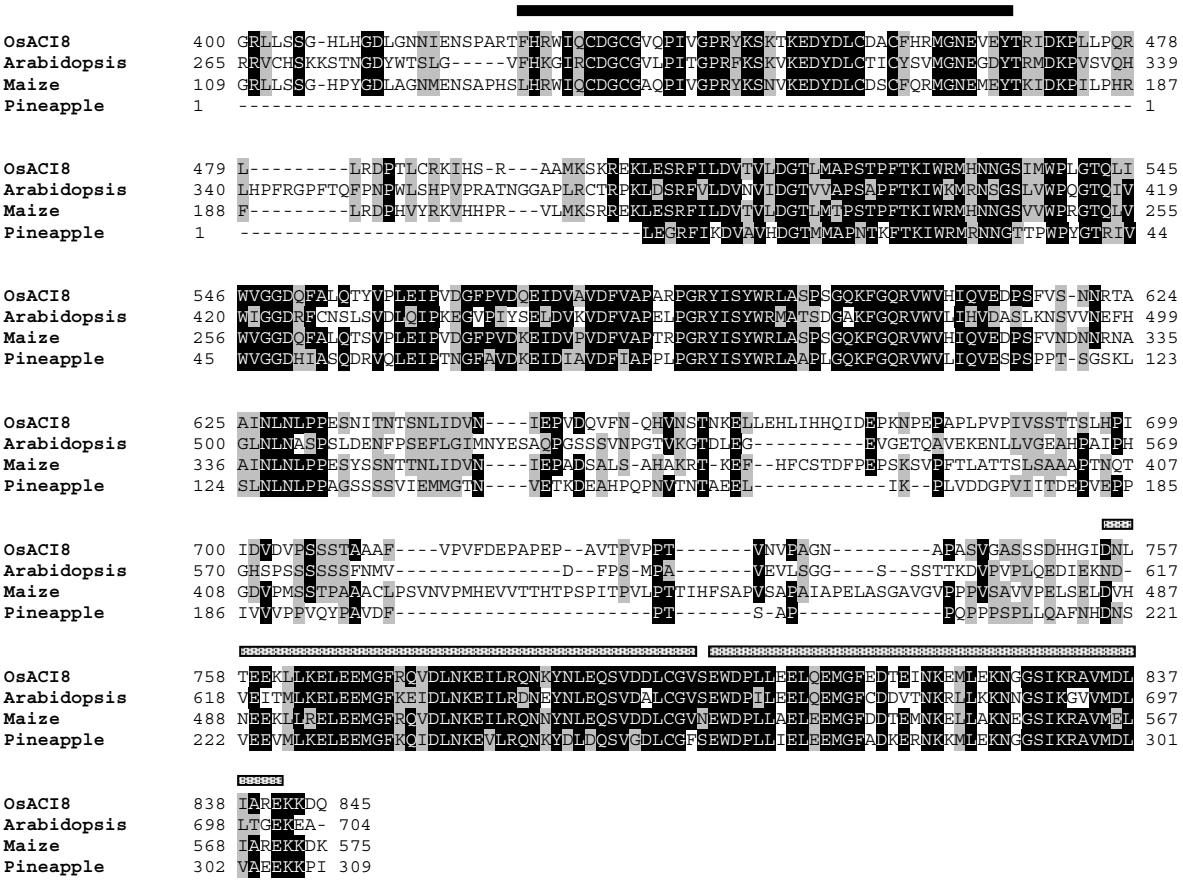

Figure 8: Alignment of the predicted protein sequence of OSACI8 (accession number AK099686) with homologues from Arabidopsis (accession number At4g24690), maize (accession number AY108354) and pineapple (accession number AY098509). Extended N-terminal sequences from rice and Arabidopsis-proteins (399 and 264 amino acids, respectively) were omitted from the alignment. The black bar indicates location of a putative ZZ domain. Dotted bars indicate locations of two consecutive putative UBA domains.

Proteins homologous to OsACI8 had no assigned function. However, searches for functional domains at the PFAM server (http://www.sanger.ac.uk) in the OSACI8 sequence revealed the presence of two putative ubiquitin-associated domains (UBA domains) and one putative ZZ-domain. In OsACI8 homologues, two UBA domains were also predicted to occur within the well-conserved C-termini of the proteins. Due to the fact that the cDNA from

pineapple was truncated, a ZZ domain was found in Arabidopsis and maize proteins only (Figure 8).

The UBA domain is a small domain composed of three alpha helices. It was found in several proteins connected to the ubiquitin and ubiquitination pathway (Hofmann and Bucher, 1996). Multiubiquitin chains were shown to bind to the UBA domain (Wilkinson *et al*., 2001). The ZZ domain is a zinc-finger domain initially identified in dystrophin and found later on in numerous proteins (Pontig *et al*., 1996). It is believed to be involved in protein-protein interactions. The simultaneous presence of two UBA domains and one ZZ domain in OsACI8 and its homologues (Figure 8) suggested a possible role for OsACI8 in regulation of protein degradation through the proteasome pathway.

In rice, the protein most closely related to OsACI8 was a putative protein (accession number 5414.t00003) that showed 40% identical and 61% functionally similar amino acids with OsACI8. It was predicted to contain a ZZ domain but no UBA domain (data not shown), indicating that OsACI8 and 5414.t00003 protein had a distinct function. Since no other homologues were found in Arabidopsis, it was postulated that *Osaci8* and its Arabidopsis counterpart At4g24690 were single-copy genes.

3.2.2. Regulation of O*saci8* gene expression.

Intact rice plants were partially submerged. Expression of *Osaci8* was analysed in the 1-cm basal part of growing internodes after different duration of submergence treatment (Figure 9). In non-submerged plants at 0 hours and in plants submerged for 1 hour, levels of *Osaci8* transcript were similar. Transcript levels decreased after 2 hours and after 4 hours of submergence. Lowest *Osaci8* RNA content was observed after 10 hours of treatment. *Osaci8* expression gradually recovered after 14 hours, 18 hours and 24 hours of submergence.

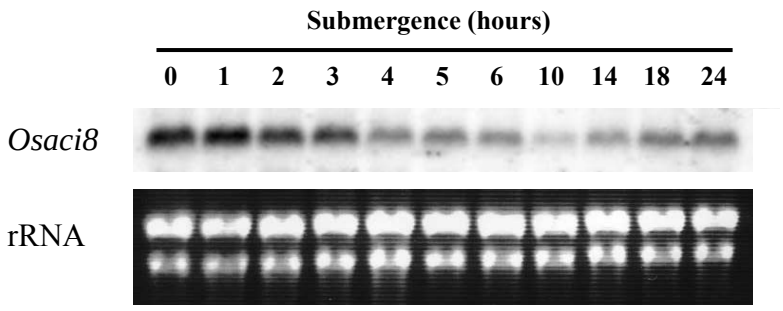

Figure 9: Expression of *Osaci8* in a 1-cm part of the youngest internode encompassing the meristem and part of the elongation zone isolated from intact plants partially submerged for the times indicated. Twenty µg RNA were loaded per lane. EtBr-stained rRNA is shown as a loading control.

Expression of *Osaci8* was further studied in the intercalary meristem, the elongation zone and in the differentiation zone of the youngest internode of deepwater rice plants submitted to partial submergence. Expression patterns in the three zones (Figure 10) differed from the expression pattern observed in 1-cm portions (Figure 9). Tissue-specific analysis revealed a transient increase preceding decline of mRNA to below control levels. In the intercalary meristem, transcripts accumulated transiently after 2 hours of submergence. After 4 hours of submergence transcript levels of *Osaci8* were back to the level measured at 0 hours. Subsequently, levels declined further. After 6 hours of submergence expression was lower than in control plants at 0 hours. In the elongation zone, *Osaci8* expression transiently increased at 4 hours. In the differentiation zone, elevated levels of transcript were detected between 2 hours and 6 hours of submergence. Overall induction of *Osaci8* gene expression was highest in the differentiation zone.

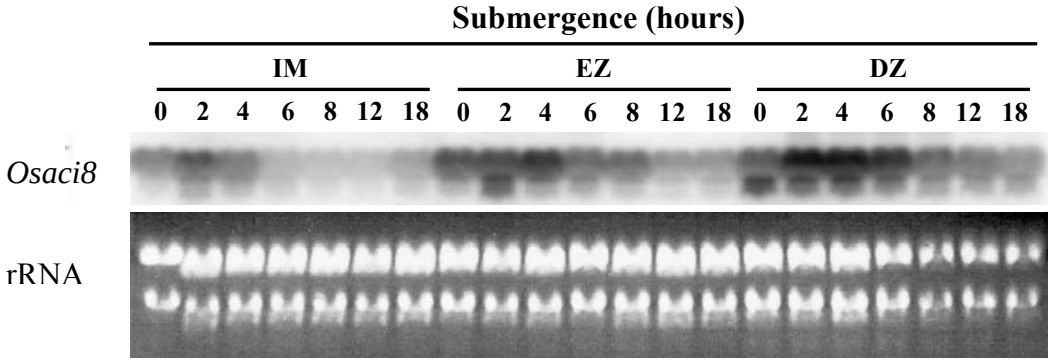

Figure 10: Expression of *Osaci8* in the intercalary meristem (IM), the elongation zone (EZ) and in the differentiation zone (DZ) of the youngest growth-responding internodes of partially submerged plants. Twenty-five µg RNA was loaded per lane. Control tissues were taken from nonsubmerged plants at 0 hours. Loading of the gel is shown through EtBr staining of rRNA.

To further investigate the distribution of *Osaci8* transcripts in rice stems, *Osaci8* expression was examined in various stem tissues collected from air-grown plants. In the first node (counting from the top, Figure 11B), in the intercalary meristem, the elongation zone and in the differentiation zone of the first internode *Osaci8* transcript levels were similar (Figure 11A). In the second node which is located just below the intercalary meristem, expression was higher than in all other tissues. *Osaci8* expression was also higher in the third node but to a lesser extent than in the second node. Altogether, these results indicated a tissue-specific regulation of *Osaci8* expression, with higher levels in nodes.

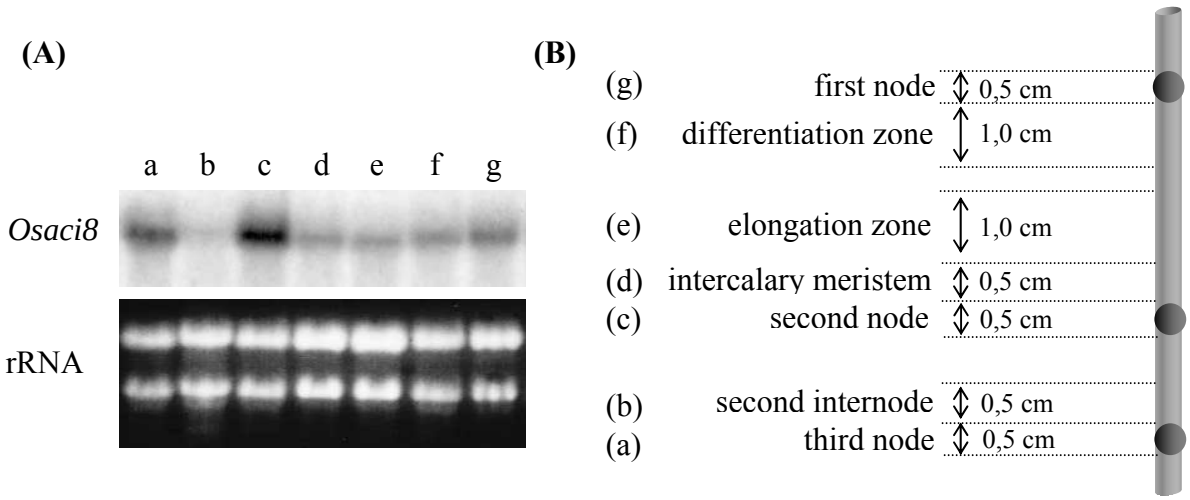

Figure 11: (A) Northern blot analysis of *Osaci8* expression in various tissues from stems of air-grown rice plants. Twenty µg RNA were loaded per lane. (a) third node, (b) second internode, (c) second node, (d) intercalary meristem, (e) elongation zone, (f) differentiation zone, (g) first node. EtBr-stained rRNA shows gel loading.
(B) Schematic representation of a rice stem. Leaves inserted at the nodes are not shown. Nodes and internodes were numbered counting from the top. Tissues were collected as indicated.

Ethephon (2-chloroethylphosphonic acid), an ethylene-releasing compound, was used as a chemical precursor of ethylene gas to treat excised stem sections. Expression of *Osaci8* in the 1-cm basal part of growing internodes was compared in stem sections treated with 150 µM ethephon and in control sections incubated without ethephon (Figure 12). No major differences were observed between stem sections incubated with and without ethephon. This experiment showed that ethylene had no effect on *Osaci8* expression. Moreover, ethephon treatment did not reproduce induction of expression observed previously with ACC after 180 minutes of treatment (Figure 7). Taken together, these data showed that unlike what was concluded initially, *Osaci8* was not regulated by ethylene. Hence, further characterisation of *Osaci8* was not attempted.

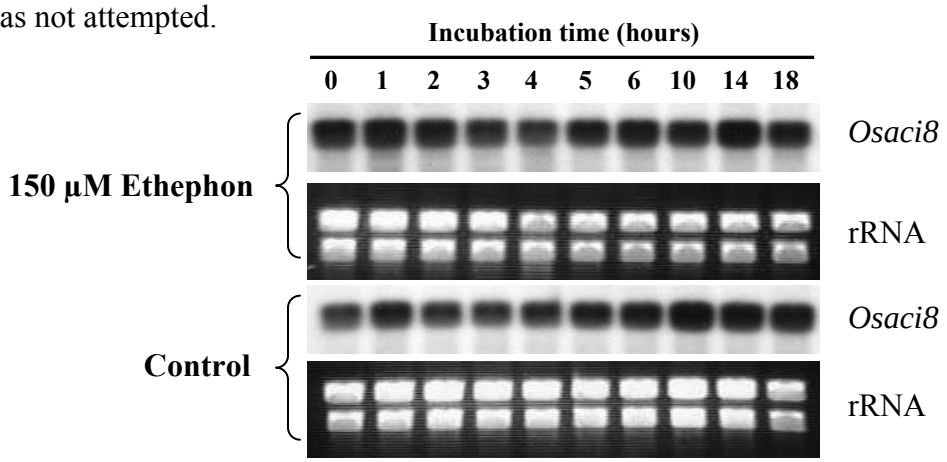

Figure 12: Expression of *Osaci8* analysed in stem sections incubated with 150 µM ethephon and in control stem sections incubated without ethephon. Twenty µg RNA were loaded per lane. Ethephon-treated sections and control sections were incubated for the times indicated. EtBr-stained ribosomal RNA provides a control for gel loading.

3.2.3 Characterisation of *aci7*.

Aci7 was identical to the coding sequence of the cDNA published in the database under the accession number AF050200 (Appendix 7.7.) and coding for the rice submergence-induced protein 2 (SIP2). Interestingly, AF050200 had been isolated through subtractive hybridisation in a screening aimed to identify genes involved in adventitious roots growth in deepwater rice (Lorbiecke, 1998). It was shown that *SIP2* was induced after submergence not only in adventitious roots but also in the youngest growing internode, predominantly in the intercalary meristem and in the elongation zone. Moreover, induction of *sip2* expression was induced in excised stem sections through ethephon treatment, indicating that submergence enhanced-expression of *SIP2* was probably due to ethylene signalling (Lorbiecke, 1998). However, the function of SIP2 was not described.

In the present study, another piece of evidence was obtained, which suggested that *SIP2* (corresponding to *aci7*) expression was driven by ethylene. Expression of the gene was highly enhanced in excised stem sections treated for 90 minutes with 10 mM ACC (Figure 7).

Search for homologous proteins and conserved domains identified SIP2 as a member of the acireductone dioxygenase family ARD/ARD' (Figure 13), which are characterised by a metal binding centre and a double-stranded beta helix domain involved in carbohydrate binding and representing the signature domain of the cupin superfamily of proteins (Dunwell *et al*., 2004). Four proteins with close homology to SIP2 were found in rice and in Arabidopsis (data not shown). SIP2 was therefore renamed OsARD1. An alignment of 4 representative members of the ARD/ARD' family from rice, human, yeast and bacteria is given in Figure 13. The metal binding centre $EHxH(x)_nH$, where x represents any amino acid, was conserved in all ARD/ARD' sequences (Figure 13). In *Klebsiella oxytoca,* the two acireductone dioxygenase enzymes ARD and ARD' share the same amino acid sequence, but bind different metal ions. ARD binds Ni^{2+}, whereas ARD' binds Fe^{2+} (Dai *et al*., 1999). Indicative of the function of the carbohydrate binding domain found in ARD/ARD' proteins (Figure 13), the two enzymes share the same ribose-derived substrate, 1,2-dihydroxy-3-keto-5-(methylthio)pentene, but yield different products. ARD' yields the alpha-keto precursor of methionine and formate, thus forming part of the ubiquitous methylthioadenosine (MTA) recycling pathway that converts MTA to methionine. This pathway is responsible for the tight control of the concentration of MTA which is a powerful inhibitor of polyamine biosynthesis and transmethylation reactions. ARD yields methylthiopropionate, carbon monoxide and formate, and thus prevents conversion of MTA to methionine (Dai *et al*., 1999, 2001).

Whether or not plant homologous ARD enzymes also possess two biochemical properties remains to be clarified. To that end, *in vitro* enzyme assays are currently carried out.

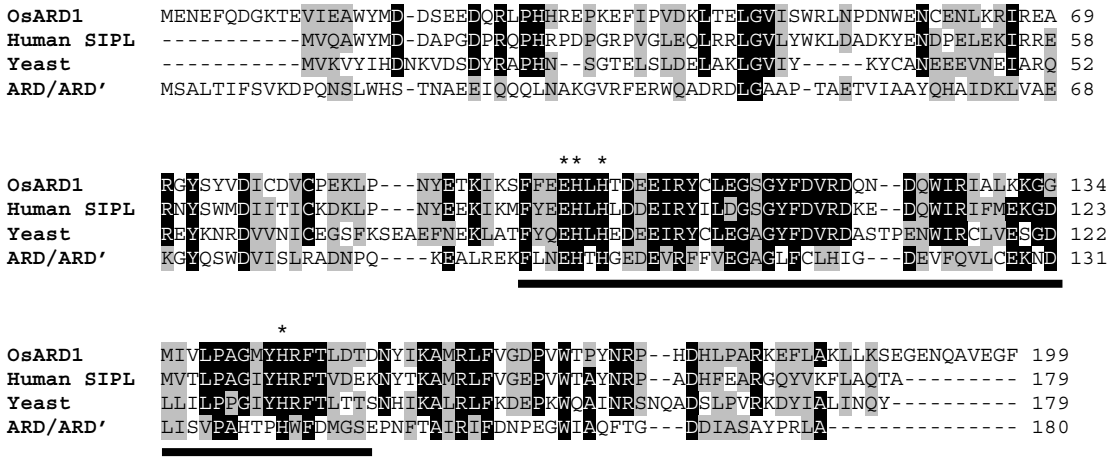

Figure 13: Alignment of 4 representative members of the acireductone family of dioxygenases from rice (OsARD1; accession number AF050200) , human (SIPL for submergence-induced protein-like; accession number AAH01467), Saccharomyces cerevisiae (yeast unknown protein; accession number CAA88525) and *Klebsiella oxytoca* (ARD/ARD'; accession number A59159). Amino acid residues are numbered on the right. Identical residues are shaded in black and residues with similar chemical properties are shaded in grey. Amino acids involved in the metal binding centre are identified by asterisks. The carbohydrate binding domain is underlined by a black bar.

In plants, the MTA recycling pathway has been characterised at the biochemical level. This metabolic route functions in recycling the methylthio-moiety of MTA, a by-product of ethylene synthesis, into S-adenosylmethionine, which serves as substrate for ACC synthase in the first committed step of ethylene synthesis. The MTA recycling pathway therefore allows high rates of ethylene synthesis without diminishing the supply of S-adenosylmethionine (Miyazaki and Yang, 1987). If *Osard1* encodes an enzyme involved in the MTA recycling pathway, ethylene regulation of *OsARD1* constitutes the first report of an activation of the MTA cycle through ethylene-mediated induction of gene expression. Since homology and domain searches pointed to a putative function for OsARD1 in the MTA recycling pathway which is related to ethylene biosynthesis rather than ethylene to gibberellin signalling, this gene was not further characterised in the frame of this work.

3.2.4. Characterisation of *aci3*.

3.2.4.1. Sequence analysis.

Using the cDNA *aci3'* obtained through subtractive hybridisation as a probe, a full-length cDNA of *aci3'* was isolated from a rice λgt11 cDNA library. After excision from the bacteriophage DNA, the cDNA was cloned into pBluescript II SK⁻ at the EcoRI site. Ends of the cDNA were first sequenced using the primers T7 and M13-reverse (Table 2) that anneal to regions of pBluescript flanking both sides of the insert. Further sequencing of the insert was performed through "primer walking". Resulting sequences were aligned and assembled into one cDNA sequence of 1888 bp. The longest ORF encoded a protein of 605 amino acids (Appendix 7.3.). The gene corresponding to the full-length cDNA was termed *Osaci3-1*. *Osaci3-1* is located on chromosome 3 and was later published as part of a BAC clone (accession number AC103891). *Osaci3-1* belongs to a gene family with 11 members in rice and related sequences in Arabidopsis also exist as gene family with 11 members.

As mentioned in section 3.1.2 (Table 3), cDNA sequences of *aci3* and *aci3'* were identical, except for a 54 bp insertion found in *aci3* (Figure 14).

```
aci3'  GAATCTCAGAGGTGCAGTGCAGGCTTGCAGCGGAGTTGTTCACTTGTAGGCTCCTTCCTT 60
aci3   GAATCTCAGAGGTGCAGTGCAGGCTTGCAGCGGAGTTGTTCACTTGTAGGCTCCTTCCTT 60

aci3'  AACCTGCTCAATGTATCATAGCCGCTCCAAGAG---------------------------- 93
aci3   AACCTGCTCAATGTATCATAGCCGCTCCAAGAGATAGGATCAGTTCTTGGCTAATGCCTA 120

aci3'  ----------------------------CGACTCTGTTAGAATGCTCAGAATGGATGGCAC 126
aci3   ATGATCTTGACGAATTTGCATCGGCAGCGACTCTGTTAGAATGCTCAGAATGGATGGCAC 180

aci3'  GGATTTGTCTTCCCCAAGGTGCAATGTTCAGCATCTACAGAATGCCGAAGAACTGAAGGA 186
aci3   GGATTTGTCTTCCCCAAGGTGCAATGTTCAGCATCTACAGAATGCCGAAGAACTGAAGGA 240

aci3'  TCAGAATAGCACCAATAAGAGGCTGCCCCGGACTACAGAG                     226
aci3   TCAGAATAGCACCAATAAGAGGCTGCCCCGGACTACAGAG                     280
```

Figure 14: Alignment of the nucleotide sequences of the cDNAs *aci*3 and *aci*3'. Nucleotides are numbered on the right. The sequence shaded in grey corresponds to an additional fragment found in *aci3*.

It was concluded that *aci3* was neither a cloning nor an amplification artefact because it was identified in two independently obtained subtractive libraries, L40-0 and L90-0 (Table 3). Analysis of the genomic sequence revealed that *aci3* and *aci3'* were both derived from *Osaci3-1*. Sequences of *aci3* and *aci3'* both aligned to 100% with the genomic DNA sequence (Figure 15). The first identical region revealed by alignment of *aci3* or *aci3'* with genomic

DNA was arbitrarily termed first exon. It was not excluded that the actual 5' leader sequence of the *Osaci3-1* transcript could be longer than in the cloned full-length cDNA. Since the additional fragment contained in *aci3* was contiguous to the second exon (Figure 15, grey-shaded sequence), it was not clear if the fragment was part of the first intron or if it belonged to the second exon. Splicing of intron sequences requires interaction between a set of ribonucleoproteins with conserved sequences from the precursor RNA (Padgett *et al*., 1986). In most introns, the conserved sequences are a GU dinucleotide at the 5' splice donor site and an AG dinucleotide at the 3' splice acceptor site. AG dinucleotides typically found at the 3' splice site of introns were present at both the 3'-end of the intron sequence preceding the additional fragment found in *aci3* and at the 3'-end of the additional fragment itself. It therefore appeared that *aci3* and *aci3'* cDNAs were derived from a single transcript that was alternatively spliced. When spliced out, the additional fragment found in *aci3* produced a messenger RNA corresponding to *aci3'*.

```
 99901 caaagattag agaggaggag cccttcttga gctcagaggt gcagtgcagg cttgcagcgg
 99961 agttgttcac ttgtaggctc cttccttaac ctgctcaatg tatcatagcc gctccaagag
100021 gtgagaagct tgtagctttg gttacagcac cctggttggg gttgcaggtt gaaaataaag
100081 cttgtagctt tacttcttgt taccaagtta cagatattga tctctgacca gatgctatga
100141 ttctacatgt tttagatagg atcagttctt ggctaatgcc taatgatctt gacgaatttg
100201 catcggcagc gactctgtta gaatgctcag aatggatggc acggatttgt cttccccaag
100261 gtgcaatgtt cagcatctac aggtaatttg gtggtggtgg agataaaatg gcttgttact
100321 tattgcttca tttgttcatt ctcttgactc caagcatgtg ggtcggtgtc atttttgctg
100381 gtaaaaaatt tcacagcaga atttcccctc ctttttcccc ttaactttct gaaccatttt
100441 cttctgccca agatcagtac agaactcttg actagtgcat ttgctatgtc cctttggaat
100501 ataatctctc tttttttcag tccataaccc aaaacatctc acttttcttt ctatttttct
100561 gttcacggaa ggaatgccgaa gaactgaagg atcagaatag caccaataag aggctgcccc
100621 ggactacaga gctcccatgc tctttgatac aagaggtaag aagtagacat cgcaagtatt
100681 gcacaaagtt tccgatgttg tagcatattt gtgtgataca tggactactt taaagcgtgt
```

Figure 15: Alignment of *aci3* and *aci3'* with the rice genomic sequence. *Osaci3-1* was identified as part of the BAC clone AC103891. Location of the sequences in the BAC clone is given by the positions on the left side. Underlined sequences correspond to the deduced first three exons of *Osaci3-1*. The grey-shaded sequence corresponds to the insert found in the *aci3* cDNA. AG dinucleotides typically found at the 3' splice acceptor sites are written in bold.

The part of the second exon that was thought to be alternatively spliced in the *Osaci3-1* mRNA contained four stop codons in frame with the putative methionine codon responsible for translation start (Figure 16). Removal of the 5'-end of exon 2 resulted in elimination of the four stop codons and brought the coding sequence in frame with another putative translation start found 13 codons upstream of the translation start suggested for *aci3*.

```
aci3   47    TAG GCT CCT TCC TTA ACC TGC TCA ATG TAT CAT AGC CGC TCC AAG   91
       16     *   A   P   S   L   T   C   S   M   Y   H   S   R   S   K   30

       92    AGA TAG GAT CAG TTC TTG GCT AAT GCC TAA TGA TCT TGA CGA ATT  136
       31     R   *   D   Q   F   L   A   N   A   *   *   S   *   R   I   45

       137   TGC ATC GGC AGC GAC TCT GTT AGA ATG CTC AGA ATG GAT GGC ACG   181
       46     C   I   G   S   D   S   V   R   M   L   R   M   D   G   T   60


aci3'  47    TAG GCT CCT TCC TTA ACC TGC TCA ATG TAT CAT AGC CGC TCC AAG   91
       16     *   A   P   S   L   T   C   S   M   Y   H   S   R   S   K   30

       92    AGC GAC TCT GTT AGA ATG CTC AGA ATG GAT GGC ACG GAT TTG TCT  136
       31     S   D   S   V   R   M   L   R   M   D   G   T   D   L   S   45

       137   TCC CCA AGG TGC AAT GTT CAG CAT CTA CAG AAT GCC GAA GAA CTG   181
       46     S   P   R   C   N   V   Q   H   L   Q   N   A   E   E   L   60
```

Figure 16: Partial protein sequences deduced from *aci3* and *aci3'* cDNAs. Positions are given on the left and on the right of each sequence. The protein sequence deduced from *aci3* (top) reveals five stop codons, symbolised as asterisks. The boxed sequence corresponds to the 5' end of exon 2. A putative translation start is indicated in bold. Splicing of the 5'end of exon 2 produced *aci3'*, for which part of the deduced protein sequence is shown (bottom). Another putative translation start, represented in bold, was brought in frame with the translation start suggested for *aci3*. Underlined amino acids are conserved in AtACI3-1 and AtACI3-2, the two closest homologue from Arabidopsis. Basic amino acids are shaded in grey.

Among the 12 amino acids uncovered by differential spliced removal of the 5' end of the second exon, five were found to be conserved in the related Arabidopsis proteins AtACI3-1 and AtACI3-2. AtACI3-1 and AtACI3-2 are the two proteins from Arabidopsis with the highest homology to OsACI3-1 (Figures 17 and 18). Conservation of these residues in ACI3 proteins underlined a possible functional role of the N-termini. Alternative splicing resulted in enrichment of basic amino acids at the N-terminus of OsACI3-1 (Figure 16, grey shaded residues) that may define a degenerate bipartite nuclear localisation signal. It is possible that OsACI3-1 function or subcellular localisation is partly regulated at the posttranscriptional level through differential splicing of *Osaci3-1* precursor RNA. However, this level of regulation was not studied further. In subsequent analysis, OsACI3-1 refers to the protein that results from removal of the 5'-end of exon 2, i.e. that encoded by cDNA *aci3'*.

Homology searches in rice and Arabidopsis databases led to the identification of 11 putative proteins related to OsACI3-1 in each species. Surprisingly, searches for expressed *Osaci3-1*-related genes in EST databases or for OsACI3-1-related proteins in translated EST databases were unsuccessful, indicating tight regulation or low levels of expression of the *Osaci3*-related genes in plants. No proteins related to OsACI3 were found in animals or in bacteria, indicating that ACI3 proteins constitute a class of plant-specific proteins. In rice, 11 proteins sharing at least 15% identical amino acids with OsACI3-1 were designed as OsACI3 homologues and assigned increasing numbers with decreasing homology. In Arabidopsis, the

closest homologue to OsACI3-1 was termed accordingly AtACI3-1. Arabidopsis proteins related to AtACI3-1 were assigned increasing numbers with decreasing homology. None of the OsACI3-1 related proteins from rice or Arabidopsis had an assigned function. One previously described protein from *Antirrhinum majus* showed homology to OsACI3-1. The recently characterised MIP1 protein was 28% identical and 55% similar to OsACI3-1 (Figure 18). MIP1 was described by Causier *et al*. (2003) as a MADS-box interacting protein. MIP1 was originally isolated through yeast two-hybrid screening using the MADS-box protein PLE as a bait (Davies *et al*., 1996). Interaction between MIP1 and PLE was verified by GST pull-down experiments. Additional yeast two-hybrid experiments using MIP1 as a bait were confirmed by GST pull-down experiments and showed that MIP1 could interact as well with the MADS-box proteins FAR, DEFH72 and DEFH200 (Causier *et al*., 2003). As shown through *in situ* hybridisation, the gene encoding MIP1 was expressed in floral organs. Expression of the gene was concomitant with that of the genes coding for PLE, FAR, DEFH72 and DEFH200, supporting further the possibility of *in vivo* interactions between MIP1 with these MADS-box proteins. MIP1 was also shown to interact with proteins involved in regulation of transcription (Causier, personal communication). Moreover, MIP1 alone could activate transcription of the reporter gene used in the yeast two-hybrid experiments. Combined with the presence of a putative bipartite localisation signal in the N-terminal half of MIP1, it was hypothesised that MIP1 functions as a transcription factor (Causier *et al*., 2003).

Phylogenetic analysis of OsACI3-1-like proteins from rice, Arabidopsis and *Antirrhinum majus* showed that OsACI3-1 clustered together with AtACI3-1, AtACI3-2 and MIP1 into one group (Figure 17). This cluster correlated with the presence of a putative bipartite NLS and a leucine zipper domain in these proteins (Figure 18), underlining further that OsACI3-1, AtACI3-1, AtACI3-2 and MIP1 belonged to the same functional group. None of the other OsACI3-1 related proteins harboured such a combination of domains. However, all OsACI3-1 related sequences showed a conserved motif of 16 amino acids (Figure 18) with the consensus sequence EKLAFWINxYNAxxMH, where x represents variable amino acids. Highest homology between OsACI3-1-like proteins was found around this domain (Figure 18), indicating conservation of an essential function. However this conserved motif had no homology with proteins or domains of known function. More distantly related OsACI3 proteins were not considered further. Subsequent sequence analysis were hence performed with those homologues which clustered in the same group as OsACI3-1.

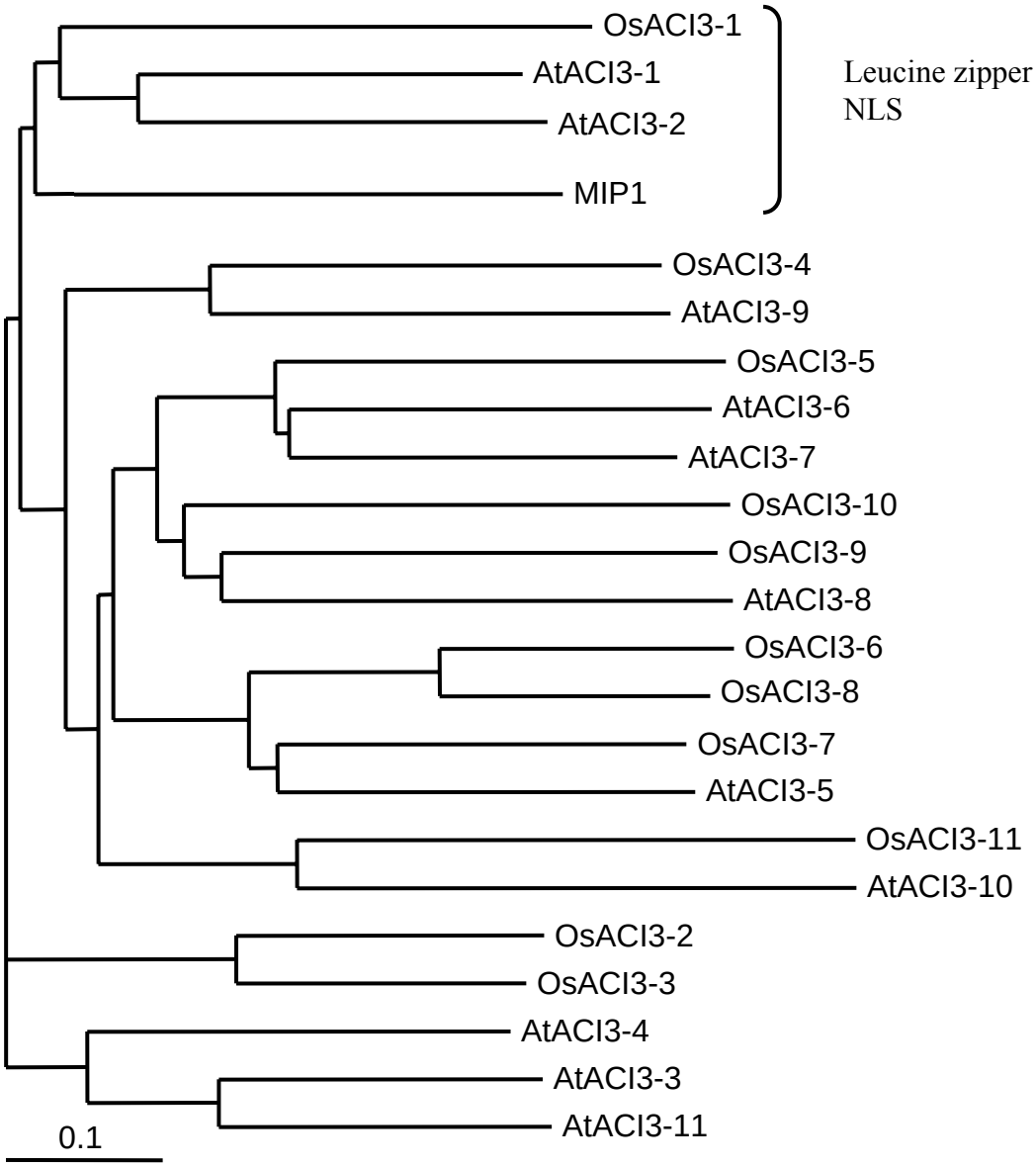

Figure 17: Phylogenetic analysis of OsACI3-1-like proteins from rice, *Arabidopsis thaliana* and *Antirrhinum majus.* The consensus tree was generated using the neighbour-joining method, based on a ClustalW alignment (http://www.ebi.ac.uk/clustalw/) and visualised with the program Treeview. The scaled bar indicates the frequency of amino acid substitutions. OsACI3-1, AtACI3-1, AtACI3-2 and MIP1 showed a common leucine zipper domain and putative NLS. Accession numbers for the rice ACI3-related proteins were 6607.t00026 (OsACI3-1), 3604.t00001 (OsACI3-2), 4867.t00014 (OsACI3-3), 2085.t00020 (OsACI3-4), 3570.t00016 (OsACI3-5), 3481.t00003 (OsACI3-6), 2507.t00013 (OsACI3-7), 3443.t00011 (OsACI3-8), 5104.t00024 (OsACI3-9), 2188.t00010 (OsACI3-10) and 2684.t00028 (OsACI3-11). Accession numbers for the genes encoding the Arabidopsis ACI3-related proteins were, from AtACI3-1 to AtACI3-11, At5g66600, At2g23700, At1g21060, At3g18900, At1g43020, At1g16750, At4g37080, At5g42690, At5g60720, At5g47380 and At1g76620, respectively. The protein sequence of MIP1 is found under the accession number AY206499.

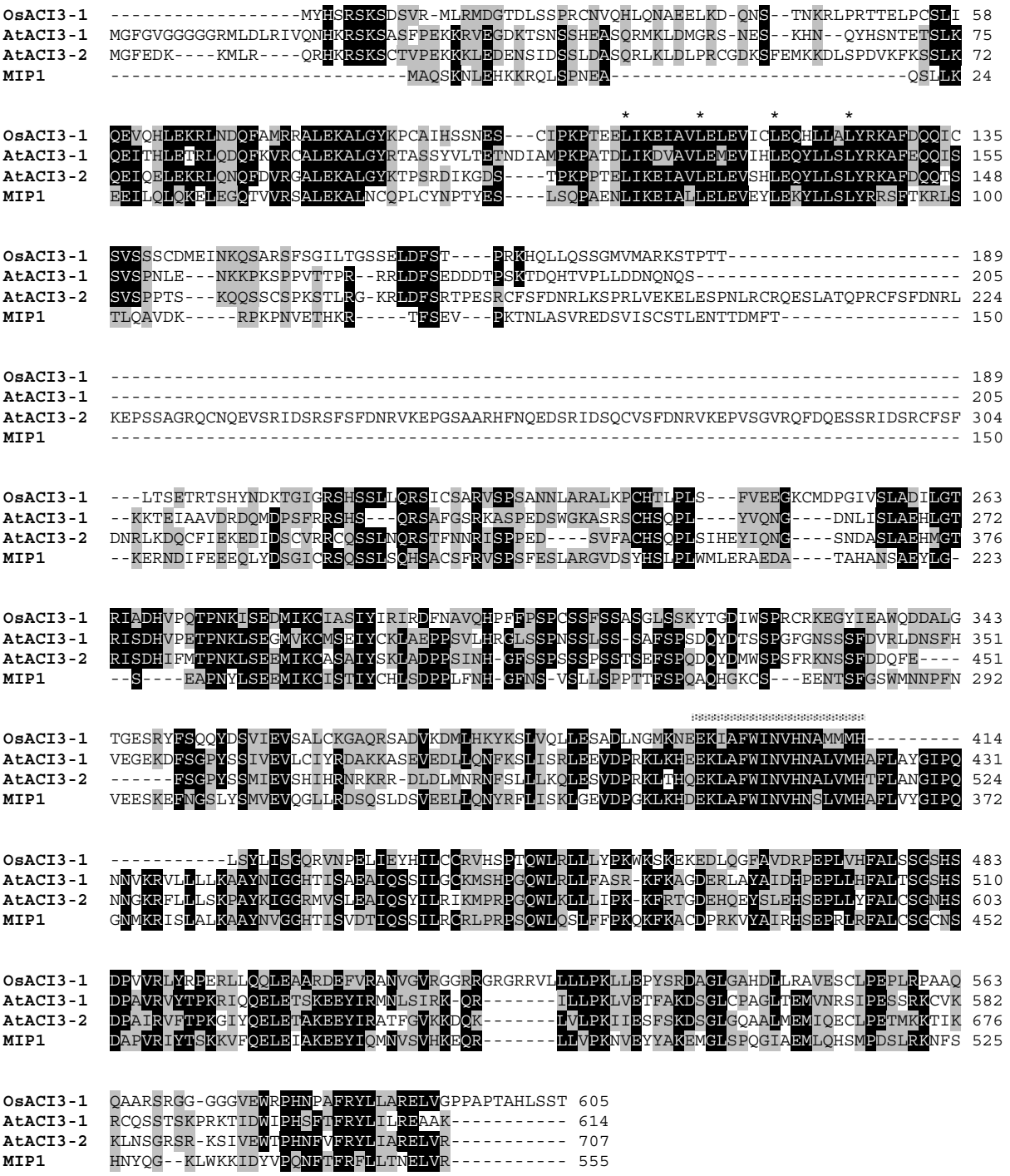

Figure 18: Alignment of OsACI3-1, AtACI3-1, AtACI3-2 and MIP1. Accession numbers are as indicated in Figure 17. Alignment was performed using ClustalW. Identical amino acids are shaded in black. Amino acids with similar chemical properties are shaded in grey. Leucine residues possibly involved in a leucine zipper domain are indicated by asterisks. The grey-dotted bar covers a region particularly well conserved in all OsACI3-1-like proteins.

The Arabidopsis proteins AtACI3-1 and AtACI3-2 are closely related with 45% identical and 63% similar amino acids. However, a stretch of about 140 amino acids was present in AtACI3-2 but was absent in AtACI3-1, MIP1 and OsACI3-1 (Figure 18). This unique sequence is composed of five highly conserved motif repeats of 19 amino acids each (Figure 19). The first and second motif are separated by 15 amino acids, whereas the second, third, fourth and fifth motif are at a distance of 8 amino acids.

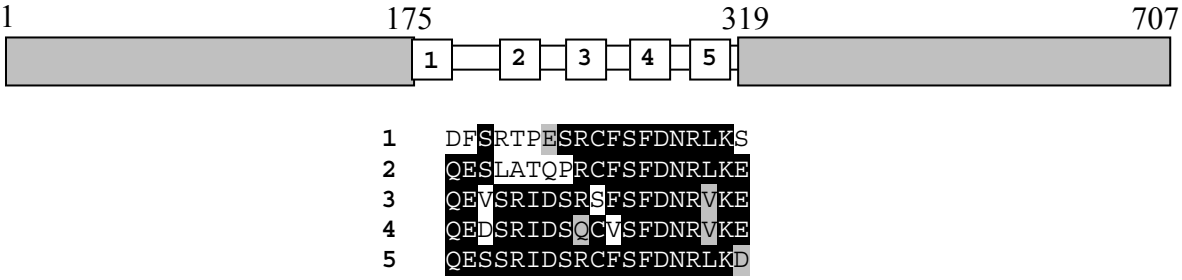

Figure 19: Schematic representation of AtACI3-2 primary structure and alignment between protein sequences of repeat motifs. N-terminal and C-terminal regions that align with homologous proteins are represented in grey. The sequence that is unique for AtACI3-2 is in white. Amino acid positions are written above the protein. Numbered boxes symbolise five repeat elements of 19 amino acids each. Sequences of the repeats, numbered on the left side, were aligned by hand. Identical amino acids are shaded in black. Amino acids with similar chemical properties are shaded in grey.

Neither the repeats nor the sequence between the repeats corresponded to known domains or motifs. The five repeats define a hydrophilic sequence rich in acidic amino acids (Figure 19). The structure prediction algorithm PSIRED (http://bioinf.cs.ucl.ac.uk/) suggested that the region forms an α-helix, at the second repeat motif. Since the repeat domain was unique to AtACI3-2 it was concluded that this protein might have a unique function in Arabidopsis. AtACI3-1 as the only other close OsACI3-1 homologue was putatively considered as functional homologue to OsACI3-1.

A putative leucine zipper domain was found in the N-terminal half of OsACI3-1, AtACI3-1, AtACI3-2 and MIP1 (Figure 18). Leucine zipper domains are defined by heptad repeats of leucine residues. They are known to be involved in protein-protein interactions (Landschulz *et al*., 1988). The region containing the leucine zipper domain was highly conserved in all four proteins (Figure 18) and was predicted to adopt a coiled coil structure, indicating conservation of protein conformation. The N-terminal half of MIP1 containing the leucine zipper domain was shown to be sufficient for binding to MADS-box proteins (Causier *et al*., 2003). The leucine zipper domain found in OsACI3-1 and AtACI3-1 may thus mediate interaction with other proteins.

3.2.4.2. Functional characterisation of ACI3 proteins from rice and Arabidopsis.

3.2.4.2.1. Subcellular localisation of AtACI3-1.

Putative bipartite nuclear localisation signals were detected in OsACI3-1, AtACI3-1, AtACI3-2 and MIP1. In plants and in eukaryotes in general, bipartite NLS are composed of two motifs of four basic amino acids separated by a few variable residues. As mentioned previously, splicing of the 5'-end of exon 2 from *Osaci3-1* transcript results in an enrichment of basic amino acids at the N-terminus of OsACI3-1. However, no motif strictly corresponding to the definition of an NLS was identified, which made the subcellular localisation of OsACI3-1 questionable (Figure 20). NLSs were found in all proteins closely related to OsACI3-1. Ten of the 26 first amino acids of AtACI3-2 are basic residues. In this basic N-terminus, a putative bipartite NLS is shown in Figure 20. In MIP1, a bipartite NLS was described as well (Causier *et al*., 2003). However, whether this NLS is able to target MIP1 to the nucleus is not known. The PSORT prediction tool (http://psort.nibb.ac.jp) predicted with 96% confidence a nuclear localisation for AtACI3-1. In addition, results from domain searches at the PFAM server (http://www.sanger.ac.uk) indicated the presence of two presumed nuclear localisation signals at both the N-terminal and the C-terminal part of the protein (Figure 20).

OsACI3-1	3- HSRSKSDSVRMLRMD -17
AtACI3-1	20- NHKRSKSASFPEKKRVEG -37
	575- SSRKCVKRCQSSTSKPRKTI -584
AtACI3-2	1- MGFEDKKMLRQRHKRSKSCTVPEKKKLE -28
MIP1	7- LEHKKRQL -14--------104- AVDKRPKPN -112

Figure 20: Putative bipartite nuclear localisation signals found in OsACI3-1, AtACI3-1, AtACI3-2 and MIP1. Possible NLSs are underlined. Basic residues are shaded in grey. Positions of the residues in the proteins are given on the sides of each sequence. AtACI3-1 has N- and C-terminal putative NLSs. The bipartite NLS described for MIP1 is interrupted by around 100 amino acids.

AtACI3-1 was identified as a putative functional homologue to OsACI3-1. In order to gain insight into the function of these proteins, the efficiency of the nuclear localisation signals found in AtACI3-1 was assessed. To test if the presumed NLSs were functional, the subcellular localisation of an AtACI3-1-GFP fusion protein was compared to that of GFP

alone after 35S-promoter driven ectopic expression in onion epidermal cells. As described in previous works (Scott *et al*., 1999; Kinkema *et al*., 2000), GFP was localised in the cytoplasm and nucleus of transformed onion cells (Figure 21). Due to its low molecular weight of 26 kD, GFP is thought to passively circulate between cytoplasm and nucleus. This is in accordance with the exclusion size of the channel of nuclear pore complexes which allows proteins of molecular weight less than 60 kD to freely diffuse in and out of the nucleus. Twenty-four hours after ballistic transformation of onion epidermis strips, the AtACI3-1-GFP fusion protein was detected in both cytoplasm and nucleus (Figure 21). The presence of AtACI3-1-GFP fusion protein in the nucleus was confirmed through optical sections at different depths in the cell using a confocal laser-scanning microscope (data not shown).

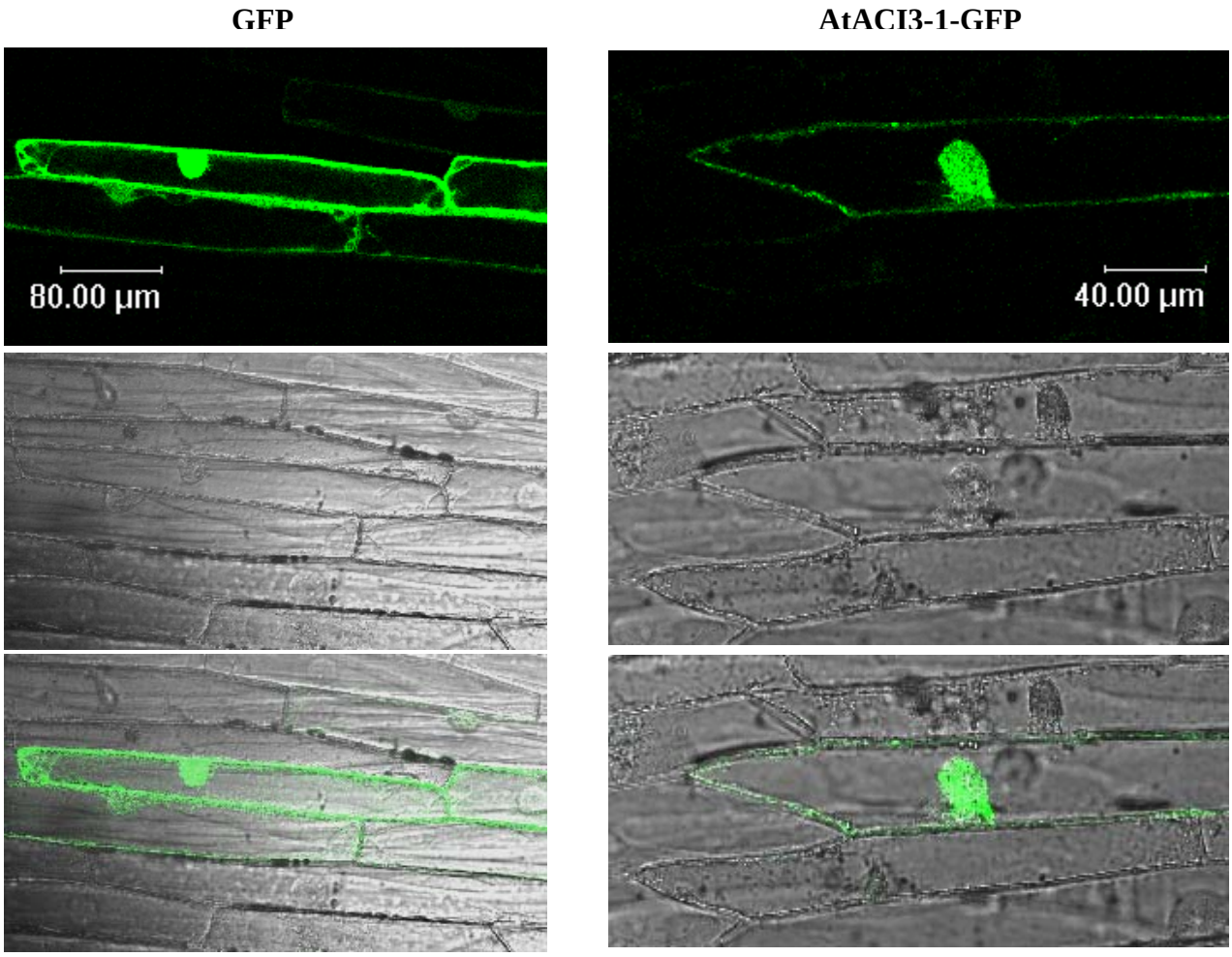

Figure 21: Subcellular localisation of GFP (left column) or AtACI3-1-GFP fusion protein (right column) in onion epidermal cells, 24 hours after transformation. Pictures were taken with a confocal-laser scanning microscope (TCS SP, Leica, Bensheim, Germany). Top: After excitation at 480 nm, the signal detected between 510 and 550 nm was attributed a green colour. Middle: Bright-field picture. Bottom: Overlay of fluorescence and bright-field images.

AtACI3-1-GFP was localised to the nucleus and to the cytoplasm after ectopic expression in onion epidermis cells. Nuclear localisation of AtACI3-1-GFP was most likely directed by an NLS present in AtACI3-1 because the predicted size of AtACI3-1-GFP is 96 kD, which well exceeds the size exclusion limit of 60 kD for passive diffusion of proteins through the nuclear pores (Raikhel, 1992).

It was noticed that, 24 hours after transformation, fluorescence generated by AtACI3-1-GFP fusion proteins was not as intense as that produced by GFP alone. Forty-eight hours after transformation, while fluorescence of GFP alone was still well detectable, AtACI3-1-GFP fusion protein displayed only a faint fluorescence (data not shown), indicating either that fusion with AtACI3-1 decreased GFP efficiency for intramolecular autoxidation, or that AtACI3-1-GFP fusion proteins were less stable than GFP alone. The prediction tool ProtParam (http://www.expasy.org) classified GFP as a stable protein on the basis of its dipeptide composition (Guruprasad *et al*., 1990), while AtACI3-1 was described as unstable. Even though no domains involved in targeting to protein degradation were found in the sequence of AtACI3-1, it cannot be excluded that AtACI3-1 directed the fusion protein AtACI3-1-GFP towards proteolytic pathways.

3.2.4.2.2. Regulation of *Osaci3-1* gene expression.

Expression of *Osaci3-1* was previously shown to be induced by 10 mM ACC in isolated stem sections of deepwater rice after 90 minutes and 180 minutes (Figure 7). To verify that ethylene was the signal that triggered induction of *Osaci3-1* expression after treatment with ACC, intact plants were treated with 1 ppm of ethylene gas, and expression of *Osaci3-1* was monitored in the 1-cm basal part of growing internodes by Northern blot analysis. *Osaci3-1* expression increased between 0 and 2 hours in the 1-cm basal part of the growing internode with ethylene treatment (Figure 22). Expression slightly declined after 3 hours but remained higher than expression in untreated plants for up to 6 hours or more. This result was clear evidence that *Osaci3-1* was regulated by ethylene. The lag phase for ethylene-regulated *Osaci3-1* gene expression was one hour or less.

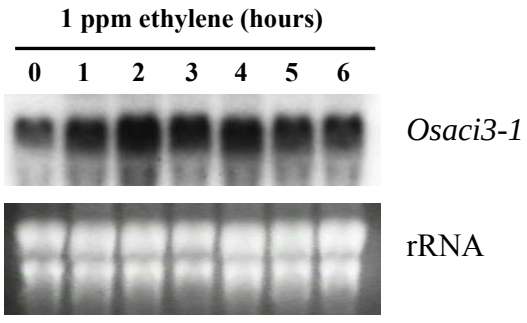

Figure 22: Time course analysis of *Osaci3-1* expression in intact plants exposed to 1 ppm ethylene. Twenty µg of total RNA extracted from the 1-cm basal part of growing internodes was loaded in each lane. Tissue from control plants was collected before onset of ethylene treatment. EtBr-stained rRNA is shown as a control for gel loading.

Ethylene was shown to accumulate within 1 hour of submergence in growing internodes of flooded deepwater rice plants (Raskin and Kende, 1984). To answer the question of whether partial submergence of rice plants resulted in *Osaci3-1* mRNA accumulation presumably due to increased endogenous ethylene levels, Northern blot analysis of *Osaci3-1* in the basal 1-cm portion of internodes collected from partially submerged intact plants was performed.

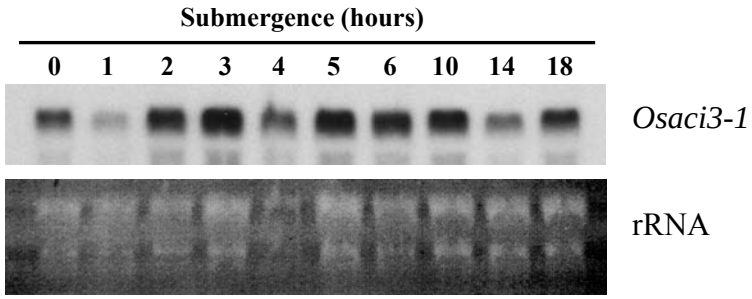

Figure 23: Time course analysis of *Osaci3-1* expression in partially submerged deepwater rice plants. Twenty µg of total RNA extracted from the 1-cm basal part of growing internodes was loaded in each lane. Tissue from control plants was collected before onset of submergence. EtBr-stained rRNA are used as a reference for loading.

Compared with non-submerged plants, *Osaci3-1* expression decreased within 1 hour of partial submergence of rice plants (Figure 23). *Osaci3-1* transcript levels recovered and exceeded control levels after 2 hours of submergence. Elevated mRNA levels were maintained up to 10 hours after onset on submergence. Expression appeared to be transiently downregulated after 14 hours and was comparable to control levels 18 hours after onset of submergence treatment. This result indicated that *Osaci3-1* is a highly regulated gene.

Induction of *Osaci3-1* expression occurred within 1 hour of treatment with 1 ppm of ethylene. In submerged plants, an increase in endogenous ethylene was observed within 1 hour of partial submergence (Raskin and Kende, 1984). Therefore induction of *Osaci3-1* expression after 2 hours of partial submergence in the same tissue in which ethylene accumulates was likely driven by increased endogenous levels of ethylene.

After detailed analysis of the time course of *Osaci3-1* gene induction, the tissue-specific regulation of gene expression was analysed. To that end, internodal tissue was separated into intercalary meristem, elongation zone and differentiation zone after partial submergence of plants. Increased *Osaci3-1* mRNA levels were observed in the intercalary meristem between 2 hours and 4 hours of submergence and in the elongation zone between 2 hours and 6 hours of submergence, whereas no induction occurred in the differentiation zone (Figure 24). In summary, after partial submergence *Osaci3-1* was expressed in growing regions which are known to produce ethylene but not in differentiated tissue and was induced within 2 hours subsequent to ethylene accumulation.

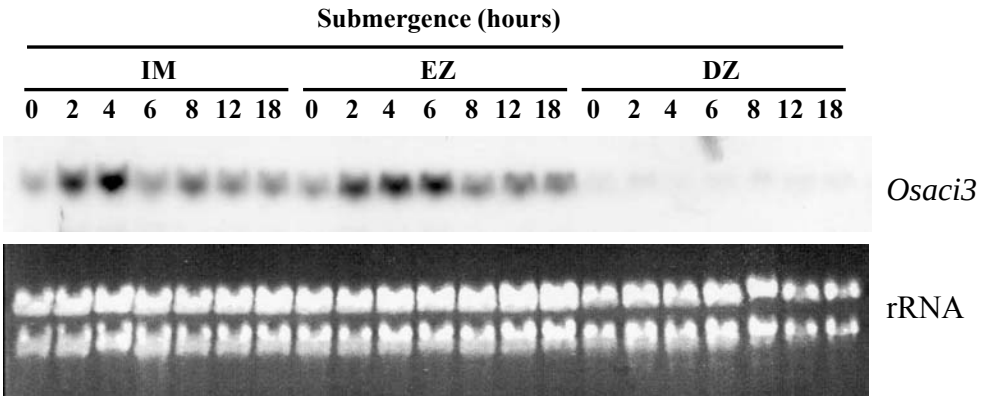

Figure 24: Spatial regulation of *Osaci3-1* expression. Total RNA was extracted from the intercalary meristem, the elongation zone and the differentiation zone of growing internodes after partial submergence of plants for the times indicated. Twenty-three µg RNA were loaded per lane. Tissues from nonsubmerged plants were harvested before onset of treatment. EtBr staining of rRNA is shown as a control for gel loading.

Tissue-specific gene expression was analysed further throughout the stem of air-grown plants and in plants which were partially submerged for 4 hours.

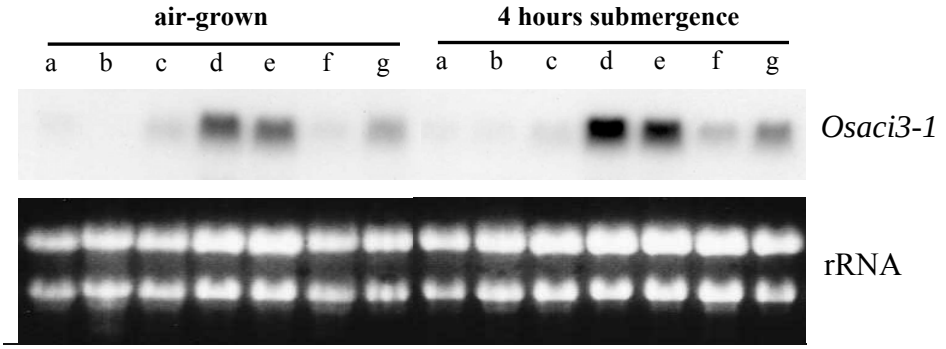

Figure 25: Tissue-specific expression of *Osaci3-1* in rice stems. Plants were air-grown or submerged for 4 hours. (a) third node, (b) second internode, (c) second node, (d, e and f) first internode, (d) intercalary meristem, (e) elongation zone, (f) differentiation zone, (g) first node. Tissues were obtained as shown in Fig. 9B. Twenty µg RNA were loaded per lane. rRNA was stained with EtBr to show gel loading.

Osaci3-1 transcripts were detected in the second node, in the intercalary meristem, the elongation zone and in the differentiation zone from the first internode and in the first node, counting from the tip (Figure 25). However, transcript levels were much higher in young tissues such as the growing internode and the first node as compared to differentiated tissues such as the third node, the second internode and the second node. As observed previously (Figure 24), expression of *Osaci3-1* was enhanced in the intercalary meristem and in the elongation zone of plants submerged for 4 hours. The slightly stronger signal observed in the differentiation zone after submergence may be due to differences in RNA loading. A basal

level of expression was detected in the youngest node of both air-grown and submerged plants. The 0.5 cm section of stem defined previously as first node (Figure 11B) contained the shoot apical meristem, which produces leaf primordia and a new node. Taken together it appeared that *Osaci3-1* was predominantly expressed in growing undifferentiated tissues.

It is known that gibberellin accumulates in growing internodes in response to submergence or in response to ethylene treatment (Hoffmann-Benning and Kende, 1992). To assess whether induction of *Osaci3-1* expression after ethylene treatment was mediated by increased gibberellin levels, expression of *Osaci3-1* was analysed in stem sections treated with 50 µM GA_3. Expression was studied specifically in the intercalary meristem and in the elongation zone. Application of GA_3 to stem sections did not alter *Osaci3-1* expression in either tissue (Figure 26) indicating that under these conditions *Osaci3-1* is specifically regulated by ethylene but not by gibberellin.

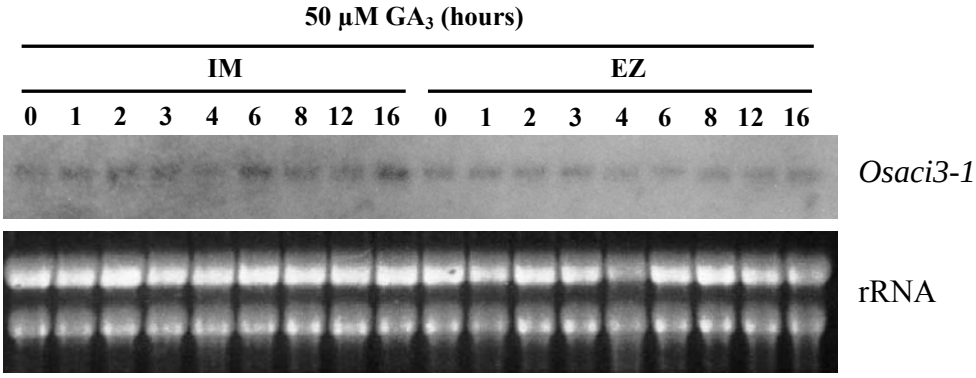

Figure 26: Time course analysis of *Osaci3-1* expression in the intercalary meristem (IM) and elongation zone (EZ) of stem sections incubated with 50 µM GA_3. Twenty-five µg total RNA were loaded in each lane. Tissues from control sections were harvested before sections were transferred to the 50 µM GA_3 solution. Gel loading is shown through EtBr-staining of rRNA.

Induction of *Osaci3-1* expression was observed in submerged plants, in ethylene-treated plants and in ACC-treated stem sections. *Osaci3-1* induction in submerged plants coincided both spatially and temporally with increased endogenous ethylene synthesis (Raskin and Kende, 1984). The highest basal levels of expression and highest induction of *Osaci3-1* expression were observed in the intercalary meristem and elongation zone of the youngest internode (Figures 24 and 25). Taken together, these data indicated that *Osaci3-1* is subject to regulation by ethylene *in planta*. Regarding the regulation of *Osaci3-1* by ethylene but not by gibberellin, *Osaci3-1* was selected as a candidate gene involved in ethylene to gibberellin signalling.

3.2.4.2.3. Spatial and temporal regulation of *Ataci3-1* gene expression.

As described previously, based on sequence homology and protein domain the Arabidopsis gene *Ataci3-1*was designated as a putative orthologue of *Osaci3-1*. To have more insight into the function of *Ataci3-1*, a first approach consisted in investigating spatial and temporal regulation of *Ataci3-1* expression through in situ localisation of GUS activity, in Arabidopsis plants transformed with an *Ataci3-1* promoter GUS-fusion construct. In a second approach, *Ataci3-1* gene inactivation by T-DNA insertion and overexpression of *Ataci3-1* in Arabidopsis were performed (sections 3.2.4.2.4. and 3.2.4.2.5.).

A fragment of 1.2 kb from the putative promoter of *Ataci3-1* was used to drive expression of a gene encoding the enzyme beta-glucuronidase (GUS) in Arabidopsis. GUS activity, revealed *in situ* through whole mount staining of Arabidopsis seedlings grown on MS-agarose plates or plants grown on soil reflected spatial and temporal regulation of *Ataci3-1* expression.

GUS staining in the cotyledons of seedlings was homogeneous one day after germination (Figure 27A) and became heterogeneous in cotyledons of 2 day-old seedlings (Figure 27B and C). At this stage, the provascular network seemed to be stained less than the surrounding mesophyll cells. At the tip of the cotyledons, a well-delimited area containing hydathodes also displayed decreased GUS activity (Figures 27B and C). In cotyledons of 3 day-old seedlings, overall GUS activity was further reduced (Figure 27D). It appeared that activity of the *Ataci3-1* promoter decreased in cotyledons first in differentiating tissues of the vasculature, then in surrounding tissues. Five days after germination, staining was not detectable anymore in cotyledons. GUS activity in hypocotyls was detected during the first two days following germination (Figure 27A).

In 7 day-old plants, high GUS activity was detected in the petiole and in the basal part of emerging leaves (Figure 27E). At later developmental stages, staining was observed along the margins of the petioles (Figure 27F). In a cross-section above the dome of the shoot apical meristem, GUS activity was obvious in the epidermis at the adaxial (upper) side of the petioles (Figure 27H). Punctuated, regularly spaced stained areas were also present at the abaxial (lower) side of older petioles (Figure 27G). Differential growth of adaxial or abaxial sides of the petiole is responsible for curvature of the leaf (Van Volkenburgh, 1999). Expression of *Ataci3-1* in the petiole was higher at the adaxial side than at the abaxial side, denoting a possible involvement of the gene in opening the angle formed between the leaf and the vertical axis of the seedling. This idea was supported by the fact that GUS activity was found in all cell layers from petioles of young leaves that still grew upright (Figure 27H).

Contrary to what was observed in cotyledons, hydathodes were the only stained areas at the apical tip of leaves (Figure 27E). Hydathodes located at developing lobes of leaves were also stained.

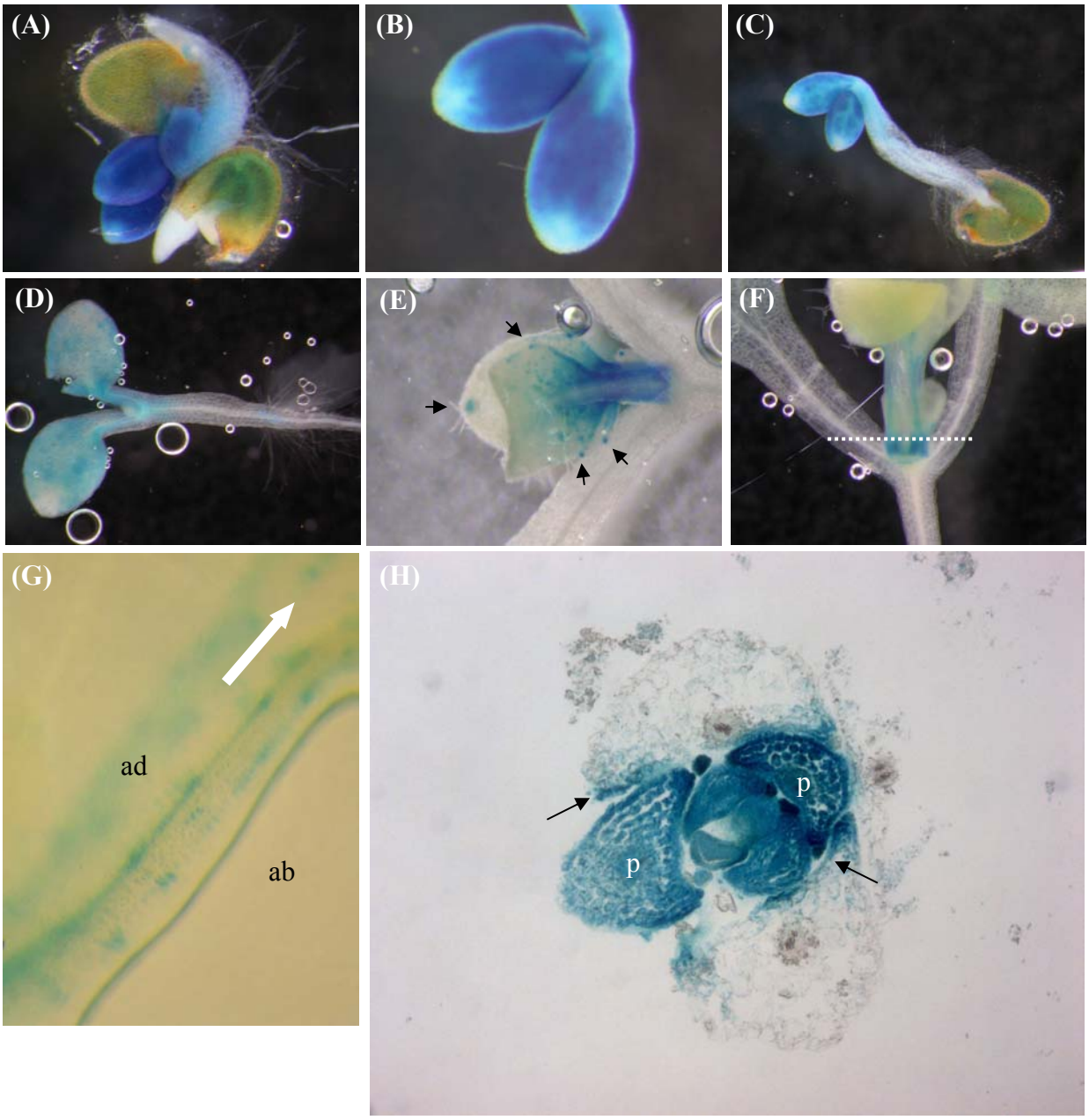

Figure 27: Histochemical staining of GUS enzymatic activity in aerial parts of seedlings grown on MS-agarose medium for 1 to 10 days. GUS activity was detected by staining with X-Gluc for 24 hours, in: (A) cotyledons and hypocotyl of germinating seeds. (B) cotyledons of 1 day-old seedling. (C) cotyledons and hypocotyl of 1 day-old seedling. (D) cotyledons of 2 day-old seedling. (E) petioles and hydathodes of the first two leaves of a 7 day-old seedling. Arrowheads indicate position of hydathodes. (F and G) margins of the petioles of the first two leaves. The adaxial (ad) and the abaxial (ab) sides of a petiole photographed from the side are shown in G. The arrow in G points towards the leaf blade. The dashed line in F gives the position of the transverse section presented in H. (H) all the cell layers of petioles (p) from young leaves were stained. The epidermis at the adaxial side of the petioles from the older true leaves is indicated with arrows.

In seedlings, the apical hook is a transient structure that is caused by asymmetric growth of the upper and lower sides of the hypocotyl region below the cotyledons. Ethylene promotes apical hook formation in etiolated seedlings by altering gibberellin sensitivity on the upper side of the hypocotyl (Vriezen *et al*., 2004). Ethylene also plays a role in maintaining the hook in a bent position during hypocotyl elongation. Five days after germination, seedlings grown with 10 µM ACC displayed different degrees of hook curvature. GUS activity was stronger at the upper side of hooks (Figures 28A, B, C and D) than at the lower side of hooks. To what extent the degree of hook bending correlates with differential *gus* expression still needs to be assessed (Figures 28B and D). Since earlier stages of apical hook formation were not investigated, it was not clear if increased expression of *Ataci3-1* on one side actually preceded differential growth of the hypocotyl.

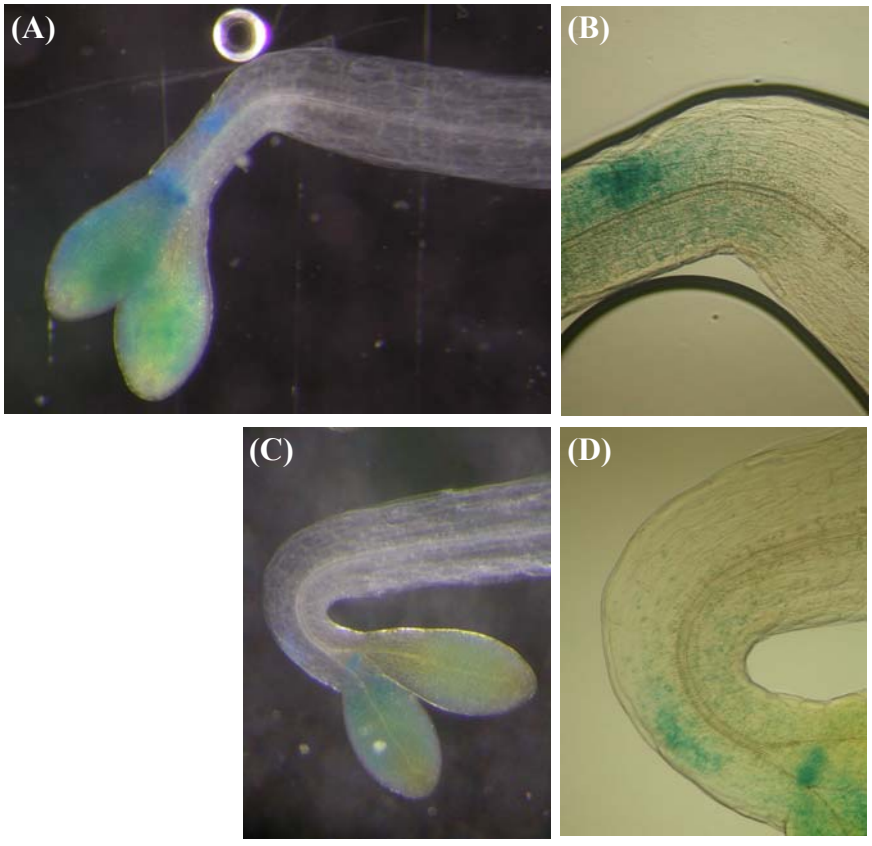

Figure 28: Histochemical localisation of GUS activity in the apical hook of 5 day-old etiolated seedlings grown in the presence of 10 µM ACC. GUS activity was detected in the upper side of the hypocotyl below the cotyledons, in seedlings displaying different hook angles. (A), the curvature of the hypocotyl describes an opened angle. (B) the same seedling observed under bright-field microscopy displays high GUS activity at the upper side of the hook. (C), the angle described by the curvature of the hypocotyl is narrower. (D), GUS staining at the upper side of the hook appears weaker under bright-field microscopy.

In Arabidopsis thaliana, the reproductive phase is characterised by the formation of a primary inflorescence, promoted by long-day conditions. Numerous secondary inflorescence stems derive from the activity of axillary meristems. In flowering 5 week-old plants, GUS activity was absent from differentiated regions of the main flower stem (data not shown), but was present in the apical part of the stem (peduncle) carrying terminal flowers (Figure 29C). Transverse sections revealed that all cell layers displayed strong GUS activity (Figure 29D). At the base of developing axillary stems (Figure 29A), GUS activity was present in cortical cells (Figure 29B). Expression of *Ataci3-1* correlated to high growth rates in the apical part of the main flower stalk and in young axillary stalks.

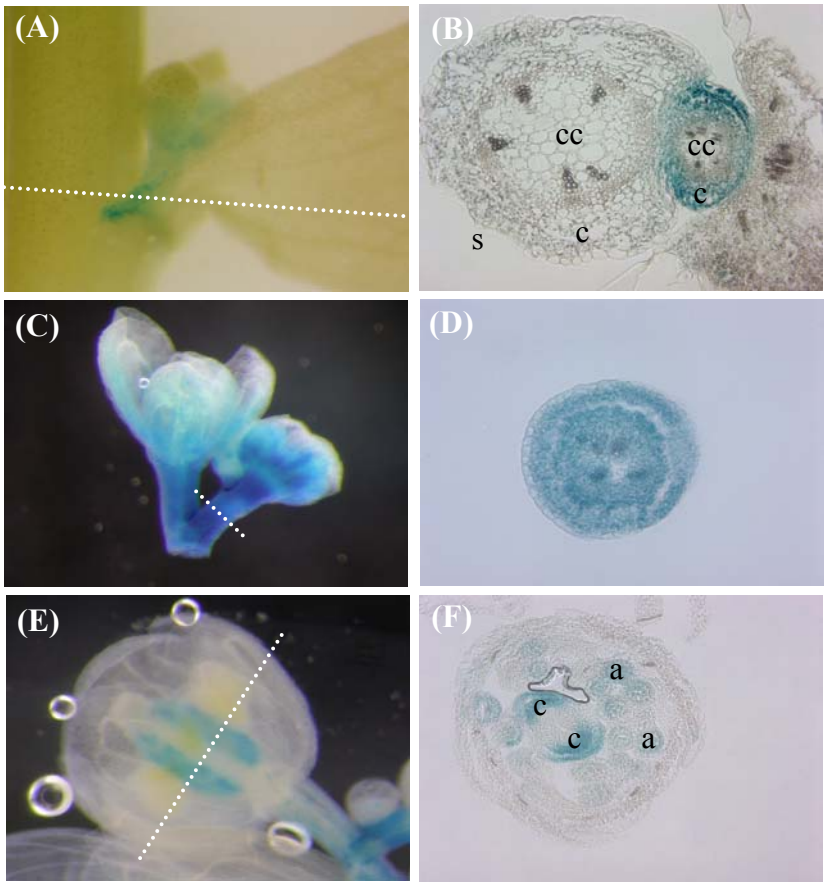

Figure 29: Histochemical detection of GUS enzymatic activity during the reproductive phase of Arabidopsis plants grown on soil. (A, C and E), whole mount staining. (B, D and F), sections along the axis represented in (A), (C) and (E), but coming from different plant material. GUS activity was detected by staining with X-Gluc for 24 hours, in: (A) axilary flower stalks. (B) cortex (c) of an axilary flower stalk along the main stem (s), while the cortex of the main stem was not stained. The central cylinder (cc) was not stained in both main and axilary stalks. (C) Terminal flower stalk and sepals. (D) All the cell layers of a peduncle are stained. (E) gynoecium. (F), anthers (a) and carpels (c).

In unfertilised flowers, sepals (Figure 29C), anthers (Figure 29F) and carpels (Figure 29E and F) displayed GUS activity. These tissues undergo rapid elongation prior to fertilisation, which suggested that expression of *Ataci3-1* in reproductive organs might also be linked to high growth rates.

In the root system, GUS activity appeared in the primary root for the first time after elongation of the root but prior to emission of secondary roots, 3 days after germination. Staining was not homogeneous along the primary root, but restricted to zones distal from the

root meristem (Figure 30A). Cross-sections in these zones localised GUS activity exclusively in the endodermis (Figure 30B), a monocellular layer that surrounds the central cylinder. Appearance of GUS activity in the endodermis preceded initiation of lateral roots from the pericycle cells located beneath the stained regions. In emerging lateral roots, enhanced GUS activity was observed at the base in a ring-like structure possibly derived from the endodermis of the primary root, while meristematic cells were not stained (Figure 30C). In one to three mm-long lateral roots (Figure 30D and E), GUS staining was confined to the base and to the tip of the root. Further microscopic investigations are needed to precisely identify in which cell types of lateral roots *Ataci3-1* is expressed.

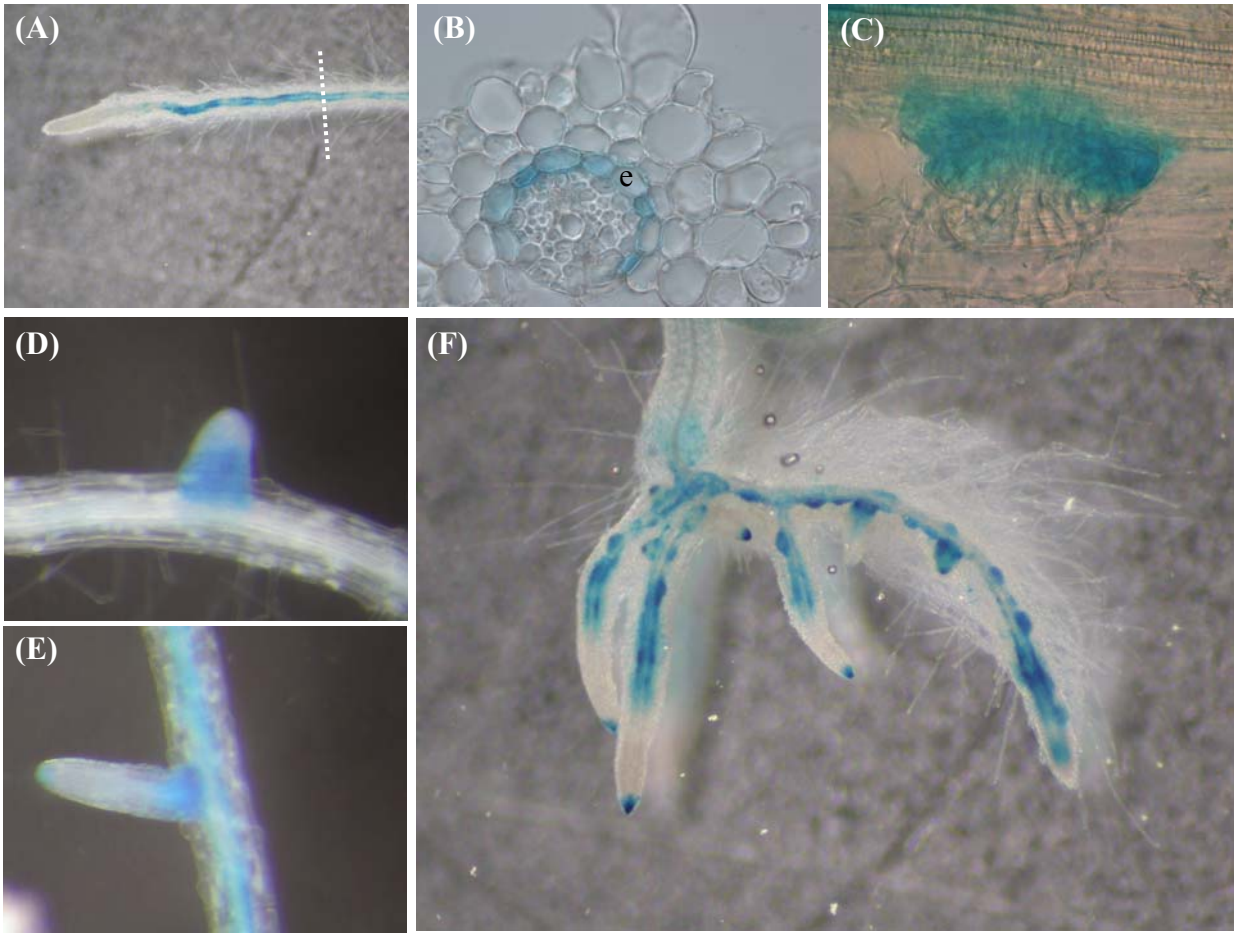

Figure 30: Histochemical detection of GUS enzymatic activity in roots of seedlings grown on MS-agarose (A to E) or on MS-agarose containing 1 µM NAA (F). GUS activity (A), in a primary root of a 3 day-old seedling. (B), in the endodermis (e). (C), at the base of an emerging lateral root. (D and E), first at the base, then at both the base and the tip of elongating lateral roots. (F), in primary and lateral roots from a 10 day-old seedling grown on MS-agarose supplemented with 1 µM NAA.

Application of auxin in the micromolar range is known to induce initiation of lateral roots in Arabidopsis. Auxin plays a central role in activating the first formative divisions of pericycle cells (Beeckman *et al*., 2001). Seedlings grown for 10 days on MS-agarose containing 1 µM

naphtalene-1-acetic acid (NAA) displayed exaggerated numbers of lateral roots. Along primary and secondary roots, numerous spots displaying high GUS activity corresponded to emerging lateral roots (Figure 30E). The elongation zone of lateral roots did not display GUS activity, but staining was present at the root tip. It was impossible to say if induction of *Ataci3-1* expression was due to NAA or due to NAA-induced lateral root initiation. GUS activity patterns in roots showed however that *Ataci3-1* expression accompanied the early stages of lateral root formation, indicating a possible function of the gene product during this process.

In rice, it was shown that *Osaci3-1* was regulated by ethylene but not by gibberellin (Figures 22 and 26). To answer to the question if expression of *Ataci3-1* was regulated by ethylene or by gibberellin, seedlings were grown in the presence or absence of 10 µM ACC or of 10 µM GA_3. After 7 days, seedlings were stained with X-Gluc for 24 hours. The presence of 10 µM ACC in MS-agarose medium resulted in stunted seedlings harbouring shorter and less ramified roots as well as smaller and curly leaves. In the same seedlings, high GUS activity was restricted to emerging leaves, whereas roots and the basal part of leaf blades displayed only faint staining (Figure 31A). In hypocotyls, cotyledons and petioles of seedlings grown with ACC, GUS activity was absent or below detection thresholds, while seedlings grown without ACC displayed staining in cotyledons and in petioles (Figure 31A). With ACC, staining in the leaf blades was located in zones of exaggerated curvature (Figure 31B). Without ACC, leaf blades were stained along the midvein, from the base up to the tip (Figure 31C).

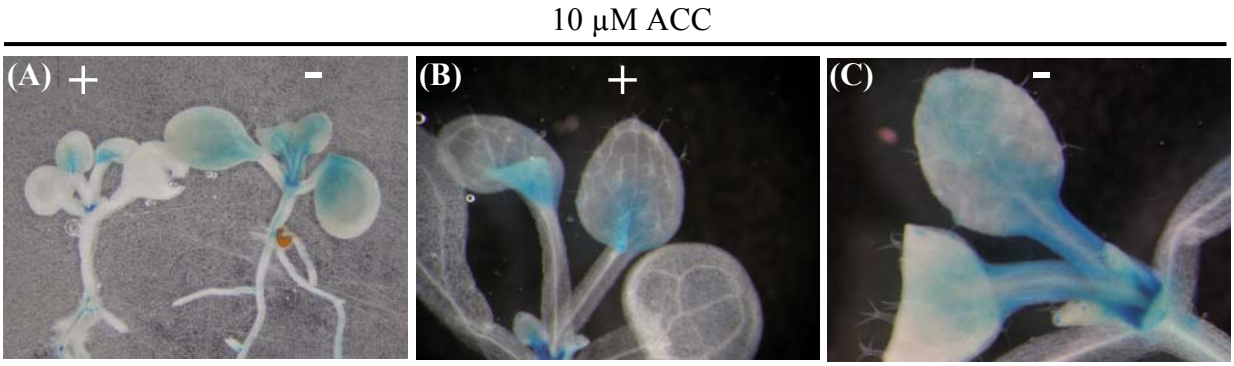

Figure 31: Histochemical localisation of GUS activity in 7 day-old seedlings grown in the presence (+) or absence (-) of 10 µM ACC. (A) GUS activity was overall reduced in shoots of ACC-treated seedlings. (B) At higher magnification, strong staining was visible in emerging leaves and slight staining was detected in true leaves only in zones of curvature. (C) At the same magnification, true leaves of seedlings grown without ACC showed GUS activity at the margins of the petioles and along the midvein in the leaf blade.

Ethylene was reported to induce leaf epinasty, that is bending downward of the leaf blade through local induction of growth (Van Volkenburgh, 1999). In ACC-treated seedlings,

restriction of *Ataci3-1* expression in the zones of curvature indicated a possible involvement of the gene in epinastic growth.

In seedlings grown for 7 days on MS-agarose containing 10 µM GA_3, GUS activity was enhanced in hypocotyls, cotyledons, petioles, and leaf blades (Figure 32A). In the same way, staining was observed all along primary and lateral roots of seedlings grown with GA_3, while staining was limited to the base and the tip of lateral roots from seedlings grown without hormone (Figure 32B). Auxin controls the growth of Arabidopsis roots through the modulation of the cellular response to gibberellin (Fu and Harberd, 2003). It appeared that the growth-promoting effect of GA_3 on both shoots and roots was accompanied by enhanced GUS activity.

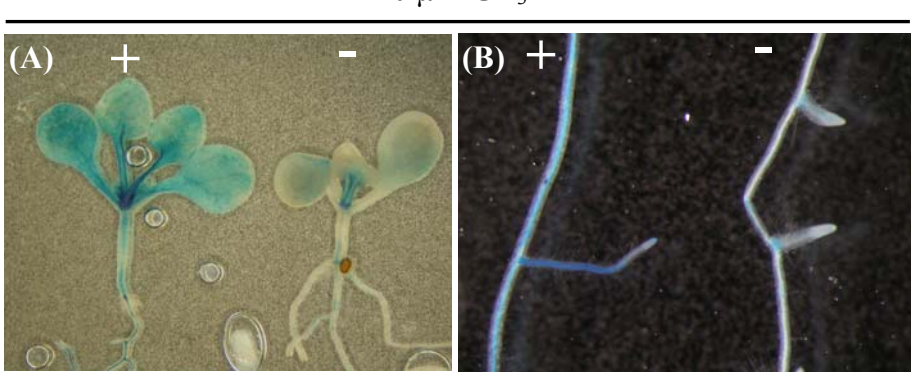

Figure 32: Histochemical localisation of GUS activity in 7 day-old seedlings grown in presence (+) or absence (-) of 10 µM GA_3. GUS activity was overall enhanced in shoots (A) and in roots (B) of GA-treated seedlings.

As compared to GUS activity in seedlings grown without hormone, overall GUS activity was reduced in seedlings grown with 10 µM ACC, while overall GUS activity was increased in seedlings grown with 10 µM GA_3. These results indicated that expression of *Ataci3-1* was repressed by ethylene and induced by gibberellin.

3.2.4.2.4. Characterisation of Arabidopsis *Ataci3-1* knock out lines.

Collections of Arabidopsis T-DNA insertion lines were screened for mutants with a disrupted *Ataci3-1* gene. Two lines were found in the GABI-KAT collection (Max Planck Institute, Köln, Germany) under the names 202E05 and 198A10 which carry a T-DNA insertion in the first intron or in the tenth exon of *Ataci3-1*, respectively (Figure 33).

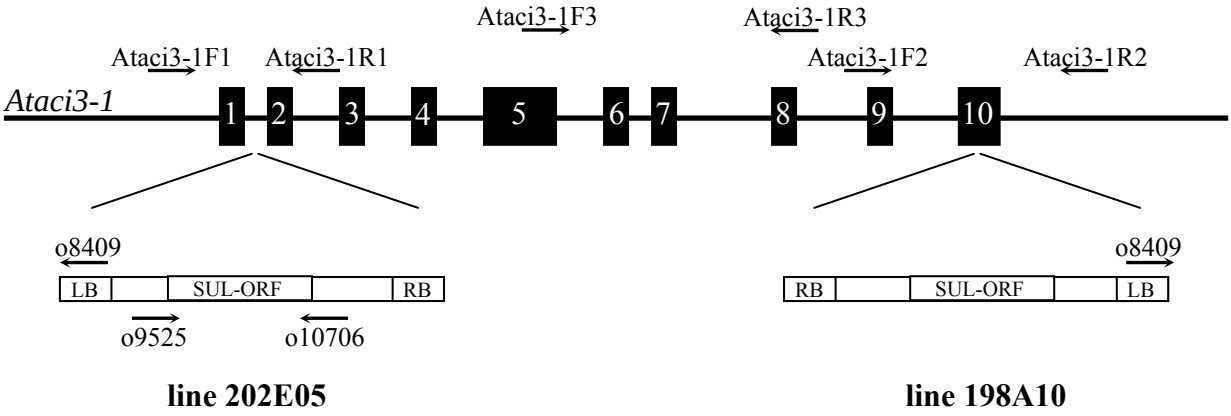

Figure 33: T-DNA insertion loci in the first intron (line 202E05) or in the tenth exon (line 198A10) of *Ataci3-1*. Exons are represented out of scale as numbered black bars. Arrows indicate approximate position and orientation of oligonucleotides used for analysis of the T-DNA insertion lines by PCR. Presence of a T-DNA insertion was tested by PCR, using primers Ataci3-1F1 and o8409 in line 202E05 or primers Ataci3-1R2 and o8409 in line 198A10. Amplification by PCR of the genomic DNA corresponding to the wild-type allele with primers Ataci3-1F1 and Ataci3-1R1 in line 202E05 or with primers Ataci3-1F2 and Ataci3-1R2 in line 198A10 was possible only when no T-DNA was inserted. A PCR fragment amplified with primers o9525 and o10706 from the SUL-ORF (Sulfadiazine resistance gene) carried by the T-DNA was used as a probe to determine number of insertion loci in both mutant lines through Southern blot analysis. Ataci3-1F3 and Ataci3-1R3 are additional primers used to monitor *Ataci3-1* transcript by RT-PCR in both insertion lines.

Plants homozygous for the T-DNA insertion in *Ataci3-1* were identified by PCR. In line 202E05, PCR using primers Ataci3-1F1 and Ataci3-1R1 which anneal to genomic regions flanking the insertion locus of the T-DNA produced a fragment of 588 bp that identified the wild-type allele. In case of an insertion, these primers annealed too far from each other to allow amplification of the genomic DNA by PCR. When no amplification product was obtained, amplification with primers Ataci3-1F1 and o8409 confirmed the presence of a T-DNA insertion. The same procedure was performed in line 198A10 with primers Ataci3-1F2 and Ataci3-1R2 5' to identify the wild-type allele, and Ataci3-1R2 and o8409 to identify the T-DNA insertion. In line 202E05, plant number 12 from generation T2 (subsequently called T2-12) was identified as homozygous for the T-DNA insertion in the first intron of *Ataci3-1*. In line 198A10, plant number 28 from generation T2 (T2-28) was homozygous for the T-DNA insertion in the tenth exon of *Ataci3-1*.

To show if T-DNA insertions in *Ataci3-1* effectively silenced the gene, RT-PCR was performed using RNA isolated from the progeny of plants T2-12 and T2-28. In situ localisation of GUS activity previously showed that *Ataci3-1* was expressed in seedlings 2 days after germination. Hence, RNA was extracted from seedlings of wild-type and mutant lines 202E05 and 198A10 grown for 2 days on MS-agarose medium. One µg RNA extracted from each line was reverse transcribed using the gene-specific oligonucleotide Ataci3-1R3. Oligonucleotide Ataci3-1R3 annealed on *Ataci3-1* transcript at the transition between exon 8

and exon 9. The primers Ataci3-1R3 and Ataci3-1F3 allowed amplification by PCR of a 334 bp piece of cDNA comprising part of the coding sequence found between exons 5 and 9. Amplification products were detected in wild-type Arabidopsis, as well as in both mutant lines (Figure 34). Since RT-PCR is not a quantitative method to determine mRNA levels, it was not possible to quantify the degree of silencing of *Ataci3-1*, and it was concluded that neither insertion of a T-DNA in the first intron nor in the last exon of *Ataci3-1* led to a full inactivation of the gene.

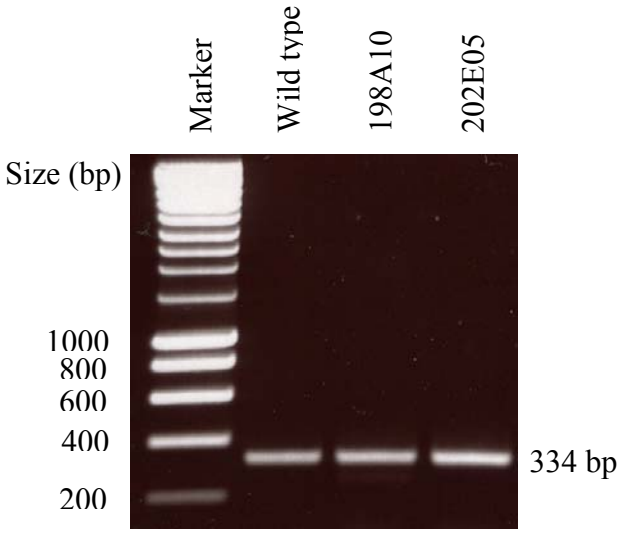

Figure 34: DNA gel electrophoresis of RT-PCR products obtained with the primers Ataci3-1F3 and Ataci3-1R3. Lane 1, Smart Ladder DNA molecular weight marker (Eurogentec, Seraing, Belgium). The sizes of fragments under 1000 bp are written on the left side of each band. Lane 2, RT-PCR product from wild-type Arabidopsis. Lane 3, RT-PCR product from line 198A10, T2-28. Lane 4, RT-PCR product from line 202E05, T2-12. The size of the RT-PCR product is indicated on the right of the picture. Nucleic acid were separated on a 1× TAE, 1% (w/v) agarose gel containing 5 µg/mL EtBr, and visualised under UV light.

Despite the fact that line 202E05 harboured an insertion in the first intron of *Ataci3-1*, RT-PCR allowed amplification of a part of *Ataci3-1* transcript overlapping exons 5 to 9. It seemed that *Ataci3-1* was not silenced in line 202E05. Moreover, Southern blot analysis in line 202E05 using a T-DNA-specific probe amplified by PCR with primers o9525 and o10706 on genomic DNA extracted from the plant T2-12, line 202E05 (Figure 33) revealed that T-DNAs were inserted at multiple loci (data not shown). Multiple T-DNA insertions combined with ineffective silencing of *Ataci3-1* prevented any attempt of phenotypic characterisation of line 202E05.

The same portion of *Ataci3-1* cDNA was amplified in line 198A10, indicating that insertion of a T-DNA in the last exon of *Ataci3-1* did not silence the gene either. It is however possible that insertion led to a transcript truncated at the 3'-end. Hybridisation patterns of a T-DNA-specific probe with genomic DNA from line 198A10 digested with EcoRI or with SalI showed a unique insertion locus (data not shown). Further characterisation of this line will be performed after assessing to what extent *Ataci3-1* transcript might be truncated.

3.2.4.2.5. Characterisation of Arabidopsis plants overexpressing *Ataci3-1*.

The *Ataci3-1* cDNA was cloned in sense orientation behind the 35S CaMV promoter, into the vector pB2WG7. This vector carried the bacterial bialaphos resistance (bar) gene, encoding the enzyme phosphinothricin acetyl transferase that inactivates the herbicide glufosinate ammonium (BASTA). Following *Agrobacterium*-mediated Arabidopsis transformation, selection of Arabidopsis transformants was performed by spraying 5 day-old seedlings with a 100 µM BASTA solution (Weigel and Glazebrook, 2002). However, screening for BASTA resistant plants did not allow recovery of transgenic plants. A generally observed yield between 0.1 and several percent transformation of Arabidopsis by "floral dip" (Clough and Bent, 1998) is usually efficient enough to allow recovery of a few transgenic seedlings per plant infected with *Agrobacterium*. The results obtained through histochemical localisation of GUS activity showed that *Ataci3-1* was tightly regulated during development and expressed in growing tissues. It is conceivable that overexpression of *Ataci3-1* lead to embryos or seedlings with altered development resulting in premature death of transformed plants. To test this hypothesis, around 100 seedlings derived from *Agrobacterium*-infected plants were grown on filter paper imbibed with MS medium without imposing BASTA selection. Using 35S promoter-specific primers, PCR on genomic DNA extracted from a pool of 5 seedlings 5 days after germination, showed that at least one seedling carried a sequence corresponding to the 35S promoter (data not shown). From a wild-type genetic background, no PCR product was obtained using 35S promoter-specific primers, which demonstrated that T-DNA integration into the genome indeed occurred during transformation. Since mature Arabidopsis plants derived from Agrobacterium transformation did not contain the 35S promoter sequence, it was concluded that overexpression of *Ataci3-1* was detrimental during early stages of seedling development.

4. Discussion.

In partially submerged deepwater rice plants, ethylene is the primary signal that triggers elongation of the youngest internode. Through unknown signalling components, ethylene increases the level of bioactive GA and responsiveness of the tissue to GA. GA is ultimately responsible for induction of growth. Since physiological responses to ethylene are regulated at the transcriptional level, we hypothesised that ethylene induces expression of genes involved in ethylene to gibberellin signalling in deepwater rice. Identification of such genes was attempted by subtractive hybridisation of cDNA libraries constituted from excised stem sections incubated with the ethylene precursor ACC. Northern blot analysis of ACC-induced (*aci*) genes led to the identification of two genes, *aci7* and *aci3* which are regulated by ethylene *in planta*. Sequence comparison and domain searches provided a likely function for the protein encoded by *aci7* in the MTA recycling pathway that relates to ethylene biosynthesis. For OsACI3-1 a putative role in the ethylene to gibberellin signalling pathway was established and is discussed.

4.1. Time course of internodal growth induction by ACC.

ACC is the natural precursor of ethylene. It is produced from S-adenosylmethionine by ACC synthase in the first committed rate-limiting step of ethylene biosynthesis (Bleecker and Kende, 2000). In partially submerged deepwater rice plants, ACC synthase activity was shown to be upregulated in the intercalary meristem and in the elongation zone of growing internodes (Cohen and Kende, 1987). In order to induce ethylene synthesis without imposing hypoxic conditions and to overcome the rate-limiting step of ACC synthesis, stem sections containing the growth-responsive internode were treated with ACC under normoxic conditions.

In excised stem sections, ACC induced internodal growth in a dose-dependent manner with a maximum response at 10 mM, which suggested that 10 mM ACC provided excised stem sections with ethylene concentrations optimal for induction of internodal growth. This result is in accordance with previous observations from Métraux and Kende (1983) who showed that inhibition of growth of submerged plants treated with the ACC biosynthesis inhibitor aminoethoxyvinylglycine could be fully reversed by application of ACC at a saturating concentration of 10 mM. However, it is also possible that the apparent saturation of the growth response at 10 mM ACC was the result of limiting ACC oxidase activity or ACC

uptake. The lag-phase for ACC-induced growth in excised deepwater rice stem sections was between 120 and 180 minutes. GA_3 was shown to trigger cell elongation in the intercalary meristem after a lag-phase of 40 minutes (Sauter and Kende, 1992). This means that ACC-induced increase in endogenous gibberellin likely was accomplished after 80 to 140 minutes following ACC treatment. Sauter and Kende (1992) attributed the lag time for GA-induced internodal growth to perception of gibberellin and to downstream signalling events leading to growth, while transport of the hormone to its site of action was estimated to contribute for approximately 10 minutes of the lag time. Moreover, ethylene accumulation was shown to precede increased GA by 120 minutes in internodes of submerged deepwater rice plants (Hoffmann-Benning and Kende, 1992). From these results, endogenous ethylene was expected to increase 20 minutes after onset of ACC treatment and the kinetics of ethylene to gibberellin signalling in internodes of ACC-treated stem sections were estimated as shown in Figure 35. Measurement of ethylene emission and quantification of the bioactive gibberellins synthesised in ACC-treated stem sections would however be needed to verify our assumptions. Isolation through subtractive hybridisation of genes induced after 40 minutes or 90 minutes of treatment with 10 mM ACC was aimed at identifying ethylene-responsive genes involved in the ethylene to gibberellin signalling pathway (Figure 35).

Figure 35: Deduced kinetics of hormonal changes induced by incubation of excised deepwater rice stem sections in 10 mM ACC. ACC, aminocyclopropane-1-carboxylic acid; ABA, abscisic acid; GA, gibberellin; ↑, increase in concentration; ↓, decrease in concentration.

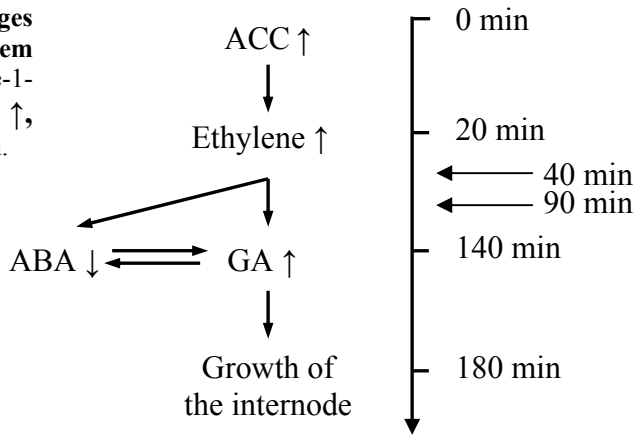

4.2. Isolation of ACC-induced genes through subtractive hybridisation.

As adapted from Wang and Brown (1991) and Buchanan-Wollaston and Ainsworth (1997), subtractive hybridisation was designed to enrich cDNA libraries in cDNA species corresponding to genes induced by treatment of stem sections with 10 mM ACC. However, with the experimental set-up that required excision of stem sections, isolation of genes induced by signals other than ACC, such as wounding and mechanical stimuli, could not be

circumvented. In fact, 7 out of 11 cDNAs (*aci1*, *aci2*, *aci3*, *aci6*, *aci7*, *aci9* and *aci11*) represented genes whose transcripts showed elevated levels after 40 minutes or after 90 minutes of incubation, regardless of the presence or absence of ACC. In order to avoid gene induction inherent to the excision of stem sections, treatment of intact plants with ethylene gas would be ideal.

Except for *aci2* which encodes a chloroplastic isoform of ascorbate peroxidase that is involved in detoxification of reactive oxygen species (Smirnoff, 1996), no obvious link was established between genes induced similarly in control and in ACC-treated stem sections with stress-related pathways. On the other hand, among the three *aci* genes whose transcript levels diminished to the same degree in control and in ACC-treated stem section, a*ci5* encoded a plastidic isoform of phosphoglucomutase that is linked to glycolysis and aci10 encoded an aconitate hydratase which is involved in the citric acid cycle. Decreased expression of these two genes after 90 minutes possibly indicated a decline in aerobic respiration after excision of stem sections. Sequence analysis of *aci* genes that were not specifically regulated by ACC did not point to a function in signalling. Characterisation of these genes was therefore not pursued, and emphasis was put on *aci7* and *aci3* which were induced specifically by ACC.

4.3. *Aci7* encodes an ethylene-regulated dioxygenase of the MTA recycling pathway.

As predicted through sequence comparisons, a*ci7*, or *Osard1* putatively encodes an acireductone dioxygenase involved in the Yang or MTA cycle. MTA is a cytotoxic by-product of ethylene biosynthesis that is detoxified through the MTA cycle. In addition, this metabolic route recycles the methylthio moiety of MTA to methionine which can re-enter the ethylene biosynthesis pathway (Miyazaki and Yang, 1987). Preliminary results obtained from enzyme activity assays showed that, like the ARD/ARD′ enzyme of *Klebsiella oxytoca* (Dai *et al*., 2001), OsARD1 when complexed with Ni^{2+} catalyses the off-pathway formation of CO and formate (Thomas Pochapsky, personal communication), indicating that OsARD1 functions in the MTA cycle.

In submerged deepwater rice plants, Lorbiecke (1998) showed that *Osard1* expression was induced in the intercalary meristem and in the elongation zone between 1 and 2 hours after onset of submergence. Transient expression was highest after 2 hours of submergence. Both spatial and temporal regulation of *Osard1* expression in submerged plants correlated with enhanced ethylene synthesis. In addition, through ethephon treatment of stem sections

pre-incubated with cycloheximide, *Osard1* was shown to be an early ethylene-induced gene (Lorbiecke, 1998). Upregulation of *Osard1* during submergence was thought to support high rates of ethylene biosynthesis through activation of the MTA cycle. Expression of *Osard1* therefore constitutes a molecular marker to detect the appearance of ethylene under physiologically-relevant concentrations.

Identification of *Osard1* in the L40-0 subtractive library and strong induction of *Osard1* expression in stem sections after 90 minutes of treatment with 10 mM ACC strongly supported the estimated kinetics of ethylene synthesis and signalling in ACC-treated stem sections (Figure 35) as well as our choice for isolating ethylene-responsive genes after 40 and 90 minutes of incubation with ACC. Upregulation of *Osard1* in ACC-treated stem sections suggested further that ethylene derived from exogenously-applied ACC triggered *de novo* ethylene biosynthesis through a positive feedback loop. It was previously reported that ethylene activates its own synthesis through transcriptional activation of ACC synthase and ACC oxidase during tomato fruit ripening (Nakatsuka *et al*., 1997) or through induction of expression of ACC oxidase during pea seed germination (Petruzzelli *et al*., 2000). In addition, Kushad et. al (1985) showed that increased activity of 5'-methylthioribose kinase, another enzyme of the MTA recycling pathway, correlated with the burst of ethylene production associated with tomato ripening. Ethylene biosynthesis in deepwater rice might depend on the MTA recycling pathway, which is activated by ethylene at the transcriptional level through induction of *Osard1* expression.

4.4. *Osaci3-1* is induced by ethylene.

Submergence-induced ethylene synthesis was previously shown to be highest in the 1-cm basal portion of the growth responsive internode comprising the intercalary meristem and part of the elongation zone (Cohen and Kende, 1987). In this tissue, ethylene levels increased as early as 1 hour after submergence. Since ethylene treatment of intact plants induced *Osaci3-1* expression in the 1-cm basal portion of the internode within 1 hour, induction of *Osaci3-1* expression after 2 hours of submergence likely occurred in response to increased endogenous ethylene. Additionally, in ACC-treated stem sections accumulation of *Osaci3-1* transcripts was observed after 90 minutes of treatment, suggesting that ACC is converted to ethylene and that the ethylene signal is perceived and transduced to the nucleus of cells from the IM and the EZ in less than half an hour. This is consistent with the kinetics of ethylene synthesis estimated for ACC-treated stem sections.

Identification of a functional homologue of ETHYLENE-INSENSITIVE 2 (Jun *et al*., 2004) and of an ethylene responsive element binding protein (EREBP) transcription factor in rice (Shen and Wang, 2004) indicated that components of the ethylene signalling pathway that were originally discovered in other plant species were conserved in rice. Therefore, genomic sequences corresponding to the putative promoter region of *Osaci3-1* which was located on chromosome 3 were systematically scanned for known ethylene cis-activating elements such as the GCC box present in the promoter of ethylene-responsive genes in diverse plant species (Ohme-Takagi and Shinshi, 1995). Although no such elements were found (data not shown), regulation of *Osaci3-1* expression through known components of the ethylene signalling pathway cannot be ruled out.

Up-regulation of *Osaci3-1* in the intercalary meristem and in the elongation zone within 2 hours of submergence (Figure 24) preceded the previously observed four-fold increase in bioactive gibberellin GA_1 measured 3 hours after submergence in the same tissues (Hoffmann-Benning and Kende, 1992). Furthermore, *Osaci3-1* was neither upregulated nor downregulated by GA_3-treatment of stem sections, suggesting that gibberellin does not influence *Osaci3-1* expression. Since it is induced by ethylene prior to activation of gibberellin synthesis, *Osaci3-1* constitutes a good candidate gene for the signalling pathway between ethylene and gibberellin in deepwater rice.

4.5. *Osaci3-1* and *Ataci3-1* are both expressed in young and growing tissues.

In the youngest internode of deepwater rice, *Osaci3-1* was expressed at higher levels in the intercalary meristem and in the elongation zone in comparison with the differentiation zone. *Osaci3-1* transcripts were also detected in the apical meristem. On the other hand *Osaci3-1* was expressed at much lower levels in older tissues of the stem. Through histochemical localisation of GUS activity in Arabidopsis shoots, *Ataci3-1* was shown to be expressed as well in young growing tissues. Expansion of Arabidopsis cotyledons is mainly dependent on cell elongation (Tsukaya *et al*., 1994). *Ataci3-1* expression was strongest in cotyledons of two day-old seedlings and decreased with the course of cotyledon expansion. In that *Ataci3-1* was predominantly expressed in immature shoot organs, its expression patterns resembled that of *AtGRF* genes which code for transcription factors involved in cotyledon and leaf growth (Kim *et al*., 2003). Arabidopsis plants overexpressing AtGRF1 and AtGRF2 displayed larger leaves and cotyledons due to an increased cell size. It can therefore be hypothesised that expression

of *Ataci3-1* accompanies cell expansion. It was previously shown that in a GA-insensitive (*gai*) mutant background, growth of leaf blades and petioles was reduced as a consequence of limited cell expansion (Tsukaya *et al*., 2002). On the other hand, application of gibberellin is know to increase the size of shoot organs by activating cell elongation and cell division. In leaves of 7 day-old Arabidopsis seedlings grown without hormone, *Ataci3-1* expression was restricted to petioles while at the same age, seedlings grown with 10 µM GA_3 displayed larger petioles and leaf blades as well as an *Ataci3-1* expression distributed homogeneously throughout the leaf. It appeared from these results that upregulation of *Ataci3-1* was concomitant with gibberellin-promoted cell expansion.

Gibberellin is partly responsible for differential growth of the hypocotyl during apical hook formation in etiolated Arabidopsis seedlings treated with ethylene (Vriezen *et al*., 2004). Differential *Ataci3-1* expression on the upper side of the hypocotyl hook in etiolated seedlings grown in the presence of ACC colocalised with an increased growth rate at this side of the hook. The Arabidopsis ethylene-responsive gene *HOOKLESS1* affects distribution of auxin or response to auxin in the hypocotyl which is required for the establishment of hypocotyl curvature through differential cell growth (Lehman *et al*., 1996). It is unclear if ethylene, gibberellin or auxin ultimately regulates *Ataci3-1* expression in the hook. Pharmacological experiments using inhibitors of ethylene sensing, auxin transport or gibberellin biosynthesis should help to better understand hormonal regulation of *Ataci3-1*.

In primary roots *Ataci3-1* was expressed exclusively in the endodermis. Among the genes known to be involved in radial root patterning, *Scarecrow* (*Scr*) is specifically expressed in the endodermis and is required for determination of this tissue. Unlike *Scr* transcripts that are distributed all along the root (Di Laurenzio *et al*., 1996), *Ataci3-1* was expressed only in the endodermis of zones where lateral roots are initiated, focusing a possible role of *Ataci3-1* on lateral root formation. Before lateral root tips acquire meristematic activity, cell division is restricted to pericycle founder cells (Casimiro *et al*., 2001). Since its expression is contained to the endodermis, *Ataci3-1* is likely not involved in activation of cell division. Seedlings grown for 10 days with the auxin analogue NAA showed enhanced *Ataci3-1* expression at branching points of lateral roots. A time course study of lateral root formation in seedlings grown with NAA will assess whether or not auxin induced *Ataci3-1* expression prior to lateral root initiation. It was recently reported that auxin regulates primary root growth by modulating the response to gibberellin (Fu and Harberd, 2003). In 7 day-old seedlings grown in the presence of 10 µM GA_3, *Ataci3-1* expression was increased along almost all of the root. Ongoing experiments where roots are treated with the GA

biosynthesis inhibitor paclobutrazol will allow to verify if *Ataci3-1* expression in roots indeed depends on GA or relates to GA-regulated growth and may help dissect interactions between auxin and GA in regulating *Ataci3-1*.

Sequence analysis of the 1.2 kb *Ataci3-1* promoter fragment that was used to drive expression of beta-glucuronidase did not reveal cis-activating elements known from gibberellin signalling. Rather an auxin-responsive element (Liu *et al*., 1994) identical to the consensus sequence 5'-TGTCTC-3' was identified 1062 bp upstream of the ATG (data not shown). Based on the observation that the *le* mutant from *Pisum sativum* which carries a non-functional GA3ox1 gene had reduced levels of IAA (Law and Davies, 1990), Ross *et al*. (2000) hypothesised that auxin and GA positively regulate each others synthesis. Auxin is also involved in apical hook formation (Lehman *et al*., 1996). In light of these results, it is possible that long-term treatment with auxin influenced synthesis rates of gibberellin, or conversely, activation of *Ataci3-1* expression in GA-treated seedlings was mediated by auxin signalling components. Analysis of *Ataci3-1* expression in auxin or gibberellin biosynthetic or signalling mutants is an approach that is envisaged to decipher hormonal regulation of *Ataci3-1* expression. Additionally, short-term effects of hormone treatments on *Ataci3*-1 promoter activity will be monitored by *in vitro* GUS activity assays and will be completed by *Ataci3-1* expression analysis through Northern-blot or real-time quantitative PCR.

4.6. *Osaci3-1* and *Ataci3-1* are regulated by ethylene in a different manner.

In terrestrial plants, ethylene generally acts as a repressor of growth (Bleecker and Kende, 2000). In contrast several wetland species display a positive growth-response after application of ethylene. In rice as well as in the dicotyledonous *Rumex palustris*, ethylene modifies endogenous gibberellin content and responsiveness, and the resulting accelerated growth accounts for the flooding avoidance mechanism (Kende *et al*., 1998; Voesenek *et al*., 2003). Treatment of intact deepwater rice plants with 1 ppm ethylene resulted in induction of *Osaci3-1* expression in the youngest internode within 1 hour. In contrast in Arabidopsis, overall expression of *Ataci3-1* was diminished in seedlings grown for 7 days with 10 µM ACC, which suggested that ethylene negatively regulates *Ataci3-1* expression. Local expression of *Ataci3-1* in zones of exaggerated curvature of leaf blades from ACC-treated seedlings grown in the light and on the upper side of the apical hook in ACC-treated etiolated seedlings positively correlated with differential growth processes. *Ataci3-1* and *Osaci3-1* are thus thought to be functional homologues involved in growth regulation. Opposite regulation

of these genes by ethylene in Arabidopsis and in rice may be explained by divergent adaptations of these species in their physiological response to ethylene.

4.7. Nucleo-cytoplasmic partitioning of AtACI3-1.

Phylogenetic analysis of OsACI3-1-related proteins revealed a core-group comprising OsACI3-1, AtACI3-1 and AtACI3-2 that displays sequence homology with MIP1, a MADS-box interacting protein from *Antirrhinum majus*. MIP1 is thought to play a role in transcriptional regulation of MADS-box target genes (Causier *et al*., 2003).

AtACI3-1 was predicted to be nuclear-localised which supported the idea of functional homology with MIP1. In a transient assay, AtACI3-1-GFP fusion protein was localised in both cytoplasm and nucleus of epidermal onion cells. Since the size of the fusion protein exceeded the size exclusion limit of nuclear pores (Raikhel, 1992), the presence of AtACI3-1-GFP in nuclei indicated that active transport of the fusion protein rather than passive diffusion had to take place.

Nucleo-cytoplasmic partitioning controls the steady-state level of transcription factors within the nucleus, and alterations in the rate of either nuclear import or nuclear export favours accumulation of the protein in one cellular compartment, thereby determining its activity as a transcription factor (Merkle, 2001). REPRESSOR OF SHOOT GROWTH (RSG) is a bZip transcription factor involved in GA signalling, which is distributed in both cytoplasm and nucleus despite the fact that it contains an NLS. The dual localisation of RSG results from a balance between nuclear targeting through NLS and nuclear export through binding with 14-3-3 proteins (Igarashi *et al*., 2001). In 14-3-3-interacting proteins, the consensus binding site for 14-3-3 proteins is RSXpS, where pS represents a phosphoserine residue (Sehnke *et al*., 2002). The N-terminal sequence HxRSKS conserved in AtACI3-1, AtACI3-2 and OsACI3-1 corresponds to the definition of a 14-3-3 binding domain. It can therefore be hypothesised that the apparent dual cytoplasmic and nuclear localisation of AtACI3-1-GFP fusion protein resulted from an equilibrium between nuclear import triggered by an NLS and nuclear export possibly mediated by a 14-3-3 protein. In this regard the predicted function of AtACI3-1 as a transcription factor is supported by the experimental data. The question of whether nuclear export through binding to 14-3-3 proteins is responsible for the presence of AtACI3-1-GFP in the cytoplasm still needs to be assessed.

4.8. Differential splicing of *Osaci3-1* pre-messenger: a mechanism to determine subcellular localisation?

Analysis of a collection of 28.000 full-length cDNAs from rice revealed that approximately 12% of these were alternatively spliced (Kikuchi *et al*., 2003). Compelling evidence supplied by individual and combined efforts show that alternative splicing in plants is a common mechanism that considerably increases versatility of the proteome by modulating enzyme activity or protein subcellular localisation (Kazan, 2003). A recent report indicated for instance that the subcellular localisation of protein serine/threonine phosphatase 5 from tomato was determined by alternative splicing (de la Fuente van Bentem *et al*., 2003).

Differential splicing of *Osaci3-1* pre-messenger at the 5'-end of exon 2 results in the addition of 12 amino acids to the N-terminus of OsACI3-1, of which 5 are conserved between OsACI3-1, AtACI3-1 and AtACI3-2. Within this stretch of 12 amino acids the conserved motif HxRSKS corresponds to a putative 14-3-3 binding domain (Sehnke *et al*., 2002). Assessment of the binding activity of OsACI3-1 with 14-3-3 proteins and its effect on the subcellular localisation of OsACI3-1 proteins resulting from the two splice forms of *Osaci3-1* pre-messenger remain to be determined. Nonetheless, finding two alternatively spliced forms of *Osaci3-1* transcript raised the question of how this process might be regulated. Is it solely dependent on endogenous factors or is it triggered in response to external stimuli? Kong *et al*. (2003) found differential accumulation of two splice forms of the alternative oxidase OsIM1 under salt stress, while both transcripts coexist at similar levels under normal conditions. Alternative splicing can thus be influenced by external signals. In the case of *Osaci3-1*, future experiments will be aimed at identifying the regulatory signal.

4.9. Functional analysis of *Ataci3-1* in Arabidopsis.

Both gene inactivation and gene overexpression were used as molecular genetic tools to evaluate the function of *Ataci3-1* in seedling development. Inactivation of gene function through T-DNA insertions is a tool commonly used to characterise genes of unknown function. However, insertional mutagenesis presents severe drawbacks. T-DNA integration often induces deletions or duplications (<500 bp) at the insertion site (Kumar and Fladung, 2002), and multiple T-DNA insertions have been shown to be the source of major chromosomal rearrangements (Nacry *et al*., 1998; Tax and Vernon, 2001). In addition, as it is the case in line 202E05 used in this work, multiple insertion loci are susceptible to inactivate

other gene functions. If, as it may be possible for multigenic families which members show functional overlap, no obvious phenotype is linked to the insertion in the gene of interest, analysis of T-DNA segregation followed with molecular markers in backcrossed populations may be tedious (Weigel and Glazebrook, 2002). T-DNA insertions that affect the 3'-end or the 3'-UTR of messengers can constitute silent mutations if the coding sequence and the resulting protein are not altered. An *Ataci3-1* transcript possibly truncated at the 3'-end was detected in line 198A10 in this study. The extent of the truncation and its possible effect on AtACI3-1 synthesis still need to be assessed. In addition, AtACI3-2 that shares 45% amino acid identity with AtACI3-1 may compensate for the loss of AtACI3-1 function. Therefore another approach based on RNA-interference is currently being performed in order to specifically suppress formation of both *Ataci3-1* and *Ataci3-2* gene products.

As a complementary approach to gene silencing, ectopic expression of *Ataci3-1* was used to investigate its function in Arabidopsis. However as mentioned earlier, no adult plants carrying the transformation vector were isolated, which led to the conclusion that overexpression of *Ataci3-1* was detrimental for seedling development. Since *Ataci3-1* was shown to be expressed at increased levels in the presence of gibberellin, inclusion of gibberellin or of a gibberellin biosynthesis inhibitor during screening of plants overexpressing *Ataci3-1* may help recover primary transformants. In addition it is envisaged to drive ectopic expression of *Ataci3-1* through a promoter inducible by the glucocorticoid analogue dexamethasone. Such a system was already successfully applied in Arabidopsis (Szymanski *et al*., 1998; Hay *et al*., 2003) where it allows tight control of the expression of the transgene. This may be useful when overexpression is for instance embryo-lethal.

4.10. OsACI3-1 and AtACI3-1 are homologous to a MADS-box interacting protein.

Studies on MADS-box proteins have long been restricted to flower development but compelling evidence suggests a central role for these transcription factors in root (Burgeff *et al*., 2002) and shoot development (Rosin *et al*., 2003). In rice, a dominant mutation abolishing DNA binding of OsMADS14 led to plants with increased internode length and number, which was the result of an upregulation of GA biosynthetic genes. This finding suggests that OsMADS14 normally represses expression of these genes and therefore acts as a repressor of internode elongation (Jeong *et al*., 2003). On the other hand, in Arabidopsis the MADS-box gene *SOC1* is induced by gibberellin and plays a central role in the integration of

vernalization and GA-dependent flowering pathways (Moon *et al*., 2003). An interplay between MADS-box genes responsive to gibberellin and MADS-box genes regulating gibberellin biosynthesis could theoretically confer fine tissue or developmental plasticity in the regulation of gibberellin synthesis. The finding that OsACI3-1 is homologous to the MADS-box interacting protein MIP1 pinpointed a possible role for OsACI3-1 in co-operating with MADS-box proteins to regulate gibberellin biosynthesis. De-repression of physiological responses to hormones has emerged as a regulatory mechanism commonly used in the plant kingdom (Harberd, 2003; Rogg and Bartel, 2001). With this in mind, we can speculate that OsACI3-1 interacts with MADS-box proteins of unknown nature to de-repress expression of GA biosynthetic genes.

In mammals, MEF2 is a MADS-box transcriptional regulator that is held in an inactive form by the class II histone deacetylase HDAC. Upon phosphorylation, HDAC is transported out of the nucleus via 14-3-3-dependent nuclear export, which relieves inhibition of MEF2 activity (Ellis *et al*., 2003). Following a similar scheme, we can speculate that alternative splicing of *Osaci3-1* pre-messenger regulates OsACI3-1 subcellular localisation through revealing a 14-3-3 protein-binding domain, which affects transcriptional regulation of GA biosynthetic genes through MADS-box proteins. The fact that *Osaci3-1* is upregulated by ethylene within 2 hours of submergence would seal in this scenario a link between ethylene and gibberellin signalling in deepwater rice.

5. Summary.

Flooding avoidance in deepwater rice is characterised by rapid growth of the youngest internode which allows the plant to keep part of its foliage above the surface of raising flood waters. The primary signal triggering internodal elongation is the phytohormone ethylene which accumulates as a result of increased ethylene biosynthesis and entrapment. Through unknown signalling components, ethylene increases the level of bioactive gibberellins (GA) and responsiveness of the tissue to GA. GA is the hormone ultimately responsible for induction of internodal growth by promoting cell division and cell elongation. Since physiological responses to ethylene are regulated at the transcriptional level, it was hypothesised that ethylene induces expression of genes involved in the signalling pathway between ethylene and gibberellin in deepwater rice. I report the identification of ACC-induced (*aci*) genes through subtractive hybridisation of cDNA libraries constituted from internodes incubated with the ethylene precursor ACC. Two *aci* genes, *aci7* and *Osaci3-1* were shown to be regulated by ethylene but not by GA *in planta*. Sequence comparison and domain searches provided a likely function for ACI7 in the MTA recycling pathway which is linked to ethylene biosynthesis. Expression of *Osaci3-1* was induced by ethylene prior to increase in GA content. Therefore *Osaci3-1* was designated a putative candidate gene for the ethylene to gibberellin signalling pathway. *Ataci3-1* is the closest homologue of *Osaci3-1* in *Arabidopsis thaliana*. Like *Osaci3-1*, expression of *Ataci3-1* correlated to elevated growth rates during vegetative growth. Unlike *Osaci3-1*, *Ataci3-1* was induced by gibberellin and inhibited by ethylene, which may illustrate differential adaptations of these two plant species in their physiological responses to ethylene, namely promotion of growth in rice and repression of growth in *Arabidopsis thaliana*. In addition, differential expression of *Ataci3-1* during apical hook formation and in roots prior to lateral root initiation evoked a possible regulation of *Ataci3-1* by auxin, a phytohormone required for these processes. Finally, the importance of a tight regulation of *Ataci3-1* was underlined by the observation that ectopic AtACI3-1 expression was detrimental at early stages of Arabidopsis seedling development. Sequence analysis of OsACI3-1 and AtACI3-1 revealed homology to MIP1, a MADS-box interacting protein from *Antirrhinum majus* likely involved in transcriptional regulation, which was in accordance with the subcellular localisation of AtACI3-1-GFP in both cytoplasmic and nuclear compartments. A recent report indicates that MADS-box transcription factors may participate in the regulation of GA biosynthetic genes in rice. Taken together, these results pinpoint a possible role for OsACI3-1 and AtACI3-1 in co-operating with MADS-box proteins to regulate GA biosynthesis.

5. Zusammenfassung.

Tiefwasserreis zeigt bei Überflutung schnelles Wachstum des jüngsten Internodiums. Dieses verstärkte Wachstum ermöglicht der Pflanze ihre Blätter über der Wasseroberfläche zu halten. Das primäre Signal, welches Wachstum des Internodiums auslöst, ist Ethylen. Der Ethylengehalt steigt aufgrund verstärkter Synthese und verringerter Diffusion an. Über unbekannte Signalwege erhöht Ethylen den Gehalt von bioaktivem Gibberellin (GA) and die Sensitivität des Gewebes gegenüber GA. GA aktiviert Zellteilung und Zellstreckung und ist damit für das Stängelwachstum verantwortlich. Physiologische Antworten auf Ethylen werden auf Transkriptionsebene reguliert. Vermutlich werden auch bei Tiefwasserreis Gene induziert, die im Signalweg zwischen Ethylen und Gibberellin eine Rolle spielen. In der vorliegenden Arbeit wurden ACC-induzierte (*aci*) Gene über substraktive Hybridisierung von cDNA Banken identifiziert. Die cDNAs wurden aus Internodien gewonnen, welche mit der Ethylenvorstufe ACC inkubiert wurden. Zwei der *aci*-Gene (*aci7* und *Osaci3-1*) werden *in planta* durch Ethylen aber nicht durch GA reguliert. Nach Sequenzvergleich und Domänenanalyse von ACI7 wurde eine Funktion des Proteins im MTA-Zyklus postuliert. Der MTA-Zyklus ist an die Ethylensynthese gekoppelt. Die Expression von *Osaci3-1* wird durch Ethylen induziert bevor es zur Erhöhung des GA-Gehalts kommt. Aus diesem Grund wurde *Osaci3-1* als putativer Kandidat für den Signalweg zwischen Ethylen und GA angesehen. *Ataci3-1* aus *Arabidopsis thaliana* ist das ähnlichste Homolog zu *Osaci3-1*. Genau wie bei *Osaci3-1* korreliert die Expression von *Ataci3-1* mit einer erhöhten Wachstumsrate. Anders als bei *Osaci3-1* wird *Ataci3-1* durch Gibberellin induziert und durch Ethylen inhibiert. Dieses könnte die unterschiedliche Anpassung der beiden Pflanzenarten auf die Ethylenantwort widerspiegeln, einerseits Förderung des Wachstums bei Reis und andererseits Hemmung des Wachstums bei *Arabidopsis thaliana*. *Ataci3-1* wird während der Entwicklung des Hypokotylhakens und bei der Initiierung von Lateralwurzeln differentiell exprimiert. Diese beiden Prozesse werden durch Auxin reguliert. Aus diesem Grund könnte *Ataci3-1* auch ein Auxin reguliertes Gen sein. Die Bedeutung der zeitlichen und räumlichen Regulation von *Ataci3-1* wird durch die Beobachtung unterstrichen, dass die Überexpression von AtACI3-1 lethal ist und zum Tod im frühen Keimlingsstadium führt. OsACI3-1 und AtACI3-1 sind zu MIP1 homolog, einem mit MADS-Box Transkriptionsfaktoren interagierenden Protein von *Antirrhinum majus*. MIP1 scheint dort an der transkriptionellen Regulation beteiligt zu sein. Diese Beobachtung passt zu der subzellulären Lokalisation von AtACI3-1-GFP im Cytoplasma und im Kern. Kürzlich wurde gezeigt, dass MADS-Box Transkriptionsfaktoren eine Rolle bei der Regulation der Gene der GA-Biosynthese in Reis spielen können. Zusammenfassend lässt sich daraus folgern, dass OsACI3-1 und AtACI3-1 zusammen mit MADS-Box Proteinen die GA-Biosynthese regulieren könnten.

6. References.

Achard, P., Vriezen, W.H., Van Der Straeten, D., Harberd, N.P. (2003). Ethylene regulates Arabidopsis development via the modulation of DELLA protein growth repressor function. *Plant Cell* **15**: 2816-2825.

Alonso, J.M. and Ecker, J.R. (2001). The ethylene pathway: a paradigm for plant hormone signaling and interaction. *Science's STKE* 70: RE1.

Azuma, T., Mihara, F., Uchida, N., Yasuda, T., Yamaguchi, T. (1990). Plant hormonal regulation of internodal elongation of floating rice stem sections. *Japan J. Trop. Agr.* **34**: 271-275.

Beeckman, T., Burssens, S., Inzé, D. (2001) The peri-*cell*-cycle in *Arabidopsis*. *J. Exp. Bot.* **52**: 403-411.

Birnboim, H.C. and Doly, J. (1979). A rapid alkaline extraction procedure for screening recombinant plasmid DNA. *Nucl. Acids Res.* **7**: 1513.

Bleecker, A.B. and Kende, H. (2000). Ethylene: a gaseous signal molecule in plants. *Annu. Rev. Cell Dev. Biol.* **16**: 1-18.

Buchanan-Wollaston, V. and Ainsworth, C. (1997). Leaf senescence in *Brassica napus*: cloning of senescence related genes by subtractive hybridisation. *Plant Mol. Biol.* **33**: 821-834.

Burgeff, C., Liljegren, S.J., Tapia-López, R., Yanofsky, M.F., Alvarez-Buylla, E.R. (2002). MADS-box gene expression in lateral primordia, meristems and differentiated tissues of *Arabidopsis thaliana* roots. *Planta* **214**: 365-372.

Casimiro, I., Marchant, A., Bhalerao, R.P., Beeckman, T., Dhooge, S., Swarup, R., Graham, N., Inzé, D., Sandberg, G., Casero, P.J., Bennett, M. (2001). Auxin transport promotes arabidopsis lateral root initiation. *Plant Cell* **13**: 843-852.

Causier, B., Cook, H., Davies, B. (2003). An *Antirrhinum* ternary complex factor specifically interacts with C-function and SEPALLATA-like MADS-box factors. *Plant Mol. Biol.* **52**: 1051-1062.

Chao, Q., Rothenberg, M., Solano, R., Roman, G., Terzaghi, W., Ecker, J.R. (1997). Activation of the ethylene gas response pathway in *Arabidopsis* by the nuclear protein ETHYLENE-INSENSITIVE3 and related proteins. *Cell* **89**: 1133-1144.

Cheng, C. and Shuman, S. (2000). Recombinogenic flap ligation pathway for intrinsic repair of Topoisomerase IB-induced double-strands breaks. *Mol. Cell. Biol.* **20**: 8059-8068.

Cho, H. and Kende, H. (1997a). Expansins in deepwater rice internodes. *Plant Physiol.* **113**: 1137-1143.

Cho, H. and Kende, H. (1997b). Expansins and internodal growth of deepwater rice. *Plant Physiol.* **113**: 1145-1151.

Clark, K.L., Larsen, P.B., Wang, X., Chang, C. (1998). Association of the *Arabidopsis* CTR1 Raf-like kinase with the ETR1 and ERS ethylene receptors. *Proc. Natl. Acad. Sci. USA* **95**: 5401-5406.

Clough, S.J. and Bent, A.F. (1998). Floral dip: a simplified method for *Agrobacterium*-mediated transformation of *Arabidopsis thaliana*. *Plant J.* **16**: 735-743.

Cohen, E. and Kende, H. (1987). *In vivo* 1-aminocyclopropane-1-carboxylate synthase activity in internodes of deepwater rice. *Plant Physiol.* **84**: 282-286.

Creutz, E., Tomsig, J.L., Snyder, S.L., Gautier, M.C., Skouris, F., Beisson, J., Cohen, J. (1998). The copines, a novel class of C2 domain-containing, calcium-dependent, phospholipid-binding proteins conserved from *Paramecium* to humans. *J. Biol. Chem.* **273**: 1393-1402.

Dai, Y., Wensink, D.C., Abeles, R.H. (1999). One protein, two enzymes. *J. Biol. Chem.* **274**: 1193-1195.

Dai, Y., Pochapsky, T.C., Abeles, R.H. (2001). Mechanistic studies of two dioxygenases in the methionine salvage pathway of *Klebsiella pneumoniae*. *Biochemistry* **40**: 6379-6387.

Davies, B., Egea-Cortines, M., de Andrade Silva, E., Saedler, H., Sommer, H. (1996). Multiple interactions amongst floral homeotic proteins. *EMBO J.* **15**: 4330-4343.

de la Fuente van Bentem, S., Vossen, J.H., Vermeer, J.E.M., de Vroomen, M.J., Gadella, T.W.J., Haring, Jr.M.A., Cornelissen, B.J.C. (2003). The subcellular localization of plant protein phosphatase 5 isoforms is determined by alternative splicing. *Plant Physiol.* **133**: 702-712.

Dennis, E.S., Dolferus, R., Ellis, M., Rahman, M., Wu, Y., Hoeren, F.U., Grover, A., Ismond, K.P., Good, A.G., Peacock, W.J. (2000). Molecular strategies for improving waterlogging tolerance in plants. *J. Exp. Bot.* **51**: 89-97.

Di Laurenzio, L., Wysocka-Diller, J., Malamy, J.E., Pysh, L., Helariutta, Y., Freshour, G., Hahn, M.G., Feldmann, K.A., Benfey, P.N. (1996). The *SCARECROW* gene regulates asymmetric cell division that is essential for generating the radial organization of the Arabidopsis root. *Cell* **86**: 423-433.

Dill, A., Jung, H.S., Sun, T.P. (2001). The DELLA motif is essential for gibberellin-induced degradation of RGA. *Proc. Natl. Acad. Sci. USA* **98**: 14162-14167.

Dunwell, J.M., Purvis, A., Khuri, S. (2004). Cupins: the most functionally diverse protein superfamily? *Phytochemistry* **65**: 7-17.

Ellis, J.J., Valencia, T.G., Zeng, H., Roberts, L.D., Deaton, R.A., Grant, S.R. (2003). CaM kinase IIdeltaC phosphorylation of 14-3-3beta in vascular smooth muscle cells: activation of class II HDAC repression. *Mol. Cell Biochem.* **242**: 153-61.

Fu, X., Richards, D.E., Ait-ali, T., Hynes, L.W., Ougham, H., Peng, J., Harberd, N.P. (2002). Gibberellin-mediated proteasome-dependent degradation of the barley DELLA protein SLN1 repressor. *Plant Cell* **14**: 3191-3200.

Fu, X. and Harberd, N.P. (2003). Auxin promotes Arabidopsis growth by modulating gibberellin response. *Nature* **421**: 740-743.

García-Maroto, F., Ortega, N., Lozano, R., Carmona, M.J. (2000). Characterization of the potato MADS-box gene *STMADS16* and expression analysis in tobacco transgenic plants. *Plant Mol. Biol.* **42**: 499-513.

Gomi, K. and Matsuoka, M. (2003). Gibberellin signalling pathway. *Curr. Opin. Plant Biol.* **6**: 489-93.

Guo, H. and Ecker, J.R. (2003). Plant responses to ethylene gas are mediated by SCF(EBF1/EBF2)-dependent proteolysis of EIN3 transcription factor. *Cell* **115**: 667-677.

Guo, H. and Ecker, J.R. (2004). The ethylene signaling pathway: new insights. *Curr. Opin. Plant Biol.* **7**: 40-49.

Guruprasad, K., Reddy, B.V.B., Pandit, M.W. (1990). Correlation between stability of a protein and its dipeptide composition: a novel approach for predicting in vivo stability of a protein from its primary sequence. *Prot. Engineering* **4**: 155-161.

Hall, T.A. (1999). BioEdit: a user-friendly biological sequence alignment editor and analysis program for Windows 95/98/NT. *Nucl. Acids Symp. Ser.* **41**: 95-98.

Hallén, S., Brändén, M., Dawson, P.A., Sachs, G. (1999). Membrane insertion scanning of the human ileal sodium/bile acid co-transporter. *Biochemistry* **38**: 11379-11388.

Harberd, N.P. (2003). Relieving DELLA restraint. *Science* **299**: 1853-1854.

Hay, A., Kaur, H., Phillips, A., Hedden, P., Hake, S., Tsiantis, M. (2002). The gibberellin pathway mediates KNOTTED1-type homeobox function in plants with different body plans. *Curr. Biol.* **12**: 1557–1565.

Hay, A., Jackson, D., Ori, N., Hake, S. (2003). Analysis of the competence to respond to KNOTTED1 activity in Arabidopsis leaves using a steroid induction system. *Plant Physiol.* **131**:1671-1680.

Hedden, P. and Kamiya, Y. (1997). Gibberellin biosynthesis: enzymes, genes and their regulation. *Annu. Rev. Plant Physiol. Plant Mol. Biol.* **48**: 431-460.

Hoffmann-Benning, S. and Kende, H. (1992). On the role of abscisic acid and gibberellin in the regulation of growth of rice. *Plant Physiol.* **99**: 1156-1161.

Hofmann, K. and Bucher, P. (1996). The UBA domain: a sequence motif present in multiple enzyme classes of the ubiquitination pathway. *Trends Biochem. Sci.* **21**: 172-173.

Hua, J., Grisafi, P., Cheng, S.H., Fink, G.R. (2001). Plant growth homeostasis is controlled by the *Arabidopsis BON1* and *BAP1* genes. *Genes Dev.* **15**: 2263-2272.

Igarashi, D., Ishida, S., Fukazawa, J., Takahashi, Y. (2001). 14-3-3 proteins regulate intracellular localization of the bZip transcriptional activator RSG. *Plant Cell* **13**: 2483-2497.

Inoue, H., Nojima, H., Okayama, H. (1990). High efficiency transformation of *Escherichia coli* with plasmids. *Gene* **96**: 23-28.

Jackson, M.B. (1985). Ethylene and responses of plants to soil waterlogging and submergence. *Annu. Rev. Plant Physiol.* **36**: 145-174.

Jackson, D., Veit, B., Hake, S. (1994). Expression of maize *KNOTTED-1* related homeobox genes in the shoot apical meristem predicts patterns of morphogenesis in the vegetative shoot. *Development* **120**: 405-413.

Jacobsen, S.E. and Olszewski, N.E. (1993). Mutations at the *SPINDLY* locus of Arabidopsis alter gibberellin signal transduction. *Plant Cell* **5**: 887-896.

Jacobsen, S.E., Binkowski, K.A., Olszewski, N.E. (1996). *SPINDLY*, a tetratricopeptide repeat protein involved in gibberellin signal transduction in Arabidopsis. *Proc. Natl. Acad. Sci. USA* **93**: 9292-9296.

Jeong, D.H., Lee, K., Jeon, J.S., An, G. (2003). Effect of overexpression of the truncated OsMADS14 on internode elongation in rice. 7th International Congress of Plant Molecular Biology, Barcelona, June 23-28 2003, S20-7.

Jun, S.H., Han, M.J., Lee, S., Seo, Y.S., Kim, W.T., An, G. (2004). OsEIN2 is a positive component in ethylene signaling in rice. *Plant Cell Physiol.* **45**: 281-289.

Kasahara, H., Hanada, A., Kuzuyama, T., Takagi, M., Kamiya, Y., Yamag, S. (2002). Contribution of the mevalonate and methylerythritol phosphate pathways to the biosynthesis of gibberellins in Arabidopsis. *J. Biol. Chem.* **277**: 45188-45194.

Kazan, K. (2003). Alternative splicing and proteome diversity in plants: the tip of the iceberg has just emerged. *Trends Plant Sci.* **8**: 468-471.

Kende, H., Van der Knaap, E., Cho, H.T. (1998). Deepwater rice: a model plant to study stem elongation. *Plant Physiol.* **118**: 1105-1110.

Kepinski, S. and Leyser, O. (2002). Ubiquitination and auxin signaling: a degrading story. *Plant Cell* S81-S95.

Kieber, J.J., Rothenberg, M., Roman, G., Feldmann, K.A., Ecker, J.R. (1993). *CTR1*, a negative regulator of the ethylene response pathway in Arabidopsis, encodes a member of the Raf family of protein kinases. *Cell* **72**: 427-441.

Kikuchi *et al*. (2003). Collection, mapping, and annotation of over 28,000 cDNA clones from *japonica* rice. *Science* **301**: 376-379.

Kim, J.H., Choi, D., Kende, H. (2003). The AtGRF family of putative transcription factors is involved in leaf and cotyledon growth in Arabidopsis. *Plant J.* **36**: 94-104.

Kinkema, M., Fan, W., Dong, X. (2000). Nuclear localization of NPR1 is required for activation of *PR* gene expression. *Plant Cell* **12**: 2339-2350.

Kiyosue, T. and Ryan, C.A. (1997). A novel gene of tomato preferentially expressed in fruit encodes a protein with Ca^{2+}-dependent lipid-binding domain. *Plant Mol. Biol.* **35**: 969-972.

Koncz, C. and Shell, J. (1986). The promoter of T_L-DNA gene 5 controls the tissue-specific expression of chimeric genes carried by a novel type of Agrobacterium binary vector. *Mol. Gen. Genet.* **204**: 383-396.

Kong, J., Gong, J.M., Zhang, Z.G., Zhang, J.S., Shen, S.Y. (2003). A new homologous gene OSIM from rice (*Oryza sativa* L.) with an alternative splicing mechanism under salt stress. *Theor. Appl. Genet.* **107**: 326-331.

Kumar, S. and Fladung, M. (2002). Transgene integration in aspen: structures of integration sites and mechanism of T-DNA integration. *Plant J.* **4**: 543-551.

Kushad, M.M., Richardson, D.G., Ferro, A.J. (1985). 5'-Methylthioadenosine nucleosidase and 5'-methylthioribose kinase activities and ethylene production during tomato fruit development and ripening. *Plant Physiol.* **79**: 525-529.

Kyte, J. and Doolittle, R.F. (1982). A simple method for displaying the hydropathic character of a protein. *J. Mol. Biol.* **157**: 105-132.

Landschulz, W.H., Johnson, P.F., McKnight, S.L. (1988). The leucine zipper: a hypothetical structure common to a new class of DNA binding proteins. *Science* **240**: 1759-1764.

Law, D.M. and Davies, P.J. (1990). Comparative indole-3-acetic-acid levels in the slender pea and other pea phenotypes. *Plant Physiol.* **93**: 1539-1543.

Lee, S.H. and Clark, J.B. (1997). High-yield method for isolation of λ DNA. *BioTechniques* **23**: 598-600.

Lee, Y. and Kende, H. (2001). Expression of β-expansins is correlated with internodal elongation in deepwater rice. *Plant Physiol.* **127**: 645-654.

Lehman, A., Black, R., Ecker, J.R. (1996). *HOOKLESS1*, an ethylene response gene, is required for differential cell elongation in the Arabidopsis hypocotyl. *Cell* **85**: 183-194.

Liu, Z.B., Ulmasov, T., Shi, X., Hagen, G., Guilfoyle T.J. (1994). Soybean GH3 promoter contains multiple auxin-inducible elements. *Plant Cell* **6**: 645-657.

Lorbiecke, R. (1998). Molekulare und physiologische Charakterisierung des Adventivwurzelwachstums bei Tiefwasserreis (*Oryza sativa* L.). PhD thesis, University of Hamburg, Germany.

Lorbiecke, R. and Sauter, M. (1998). Induction of cell growth and cell division in the intercalary meristem of submerged deepwater rice (*Oryza sativa* L.). *Planta* **204**: 140-145.

Lorbiecke, R. and Sauter, M. (1999). Adventitious root growth and cell-cycle induction in deepwater rice. *Plant Physiol.* **119**: 21-29.

McGinnis, K.M., Thomas, S.G., Soule, J.D., Strader, L.C., Zale, J.M., Sun. T.P., Steber, C.M. (2003). The *Arabidopsis SLEEPY1* gene encodes a putative F-box subunit of an SCF E3 ubiquitin ligase. *Plant Cell* **15**: 1120-1130.

McQueen-Mason, S.J. and Cosgrove, D.J. (1994). Disruption of hydrogen-bonding between plant-cell wall polymers by proteins that induce wall extension. *Proc. Natl. Acad. Sci. USA* **91**: 6574-6578.

Menegus, F., Cattaruzza, L., Mattana, M., Beffagna, N., Ragg, E. (1991). Response to anoxia in rice and wheat seedlings. Changes in the pH of intracellular compartments, glucose-6-phosphate level, and metabolic rate. *Plant Physiol.* **95**: 760-767.

Merkle, T. (2001). Nuclear import and export of proteins in plants: a tool for the regulation of signalling. *Planta* **213**: 499-517.

Métraux, J.P. and Kende, H. (1983). The role of ethylene in the growth response of submerged deep water rice. *Plant Physiol.* **72**: 441-446.

Métraux, J.P. and Kende, H. (1984). The cellular basis of the elongation response in submerged deep-water rice. *Planta* **160**: 73-77.

Miyazaki, J.H. and Yang, S.F. (1987). The methionine salvage pathway in relation to ethylene and polyamine synthesis. *Physiol. Plant.* **69**: 366-370.

Moon, J., Suh, S.S., Lee, H., Choi, K.R., Hong, C.B., Paek, N.C., Kim, S.G., Lee, I. (2003). The *SOC1* MADS-box gene integrates vernalization and gibberellin signals for flowering in Arabidopsis. *Plant J.* **35**: 613-623.

Murashige, T. and Skoog, F. (1962). A revised medium for rapid growth and bioassays with tobacco tissue cultures. *Physiol. Plant.* **15**: 473-497.

Nacry, P., Camilleri, C., Courtial, B., Caboche, M., Bouchez, D. (1998). Major chromosomal rearrangements induced by T-DNA transformation in Arabidopsis. *Genetics* **149**: 641-650.

Nakatsuka, A., Shiomi, S., Kubo, Y., Inaba, A. (1997). Expression and internal feedback regulation of ACC synthase and ACC oxidase genes in ripening tomato fruit. *Plant Cell Physiol.* **38**: 1103-1110.

Neuteboom, L.W., Kunimitsu, L.W., Webb, D., Christopher, D.A. (2002). Characterization and tissue-regulated expression of genes involved in pineapple (*Ananas comosus* L.) root development. *Plant Sci.* **163**: 1021-1035.

Nishimura, A., Tamaoki, M., Sato, Y., and Matsuoka, M. (1999). The expression of tobacco knotted1-type class 1 homeobox genes correspond to regions predicted by the cytohistological zonation model. *Plant J.* **18**: 337–347.

Ohme-Takagi, M. and Shinshi, H. (1995). Ethylene-inducible DNA binding proteins that interact with an ethylene-responsive element. *Plant Cell* **7**: 173-182.

Ouaked, F., Rozhon, W., Lecourieux, D., Hirt, H. (2003). A MAPK pathway mediates ethylene signaling in plants. *EMBO J.* **22**: 1282-1288.

Padgett, R.A., Grabowski, P.J., Konarska, M.M., Seiber, S., Sharp, P.A. (1986). Splicing of messenger RNA precursors. *Annu. Rev. Biochem.* **55**: 1119-1150.

Petruzzelli, L., Coraggio, I., Leubner-Metzger, G. (2000). Ethylene promotes ethylene biosynthesis during pea seed germination by positive feedback regulation of 1-aminocyclo-propane-1-caroxylic acid oxidase. *Planta* **211**: 144-149.

Periappuram, C., Steinhauer, L., Barton, D.L., Taylor, D.C., Chatson, B., Zou, J. (2000). The plastidic phosphoglucomutase from Arabidopsis. A reversible enzyme reaction with an important role in metabolic control. *Plant Physiol.* **122**: 1193-1199.

Pontig, C.P., Blake, D.J., Davies, K.E., Kendrick-Jones, J., Winder, S.J. (1996). ZZ and TAZ: new putative zinc fingers in dystrophin and other proteins. *Trends Biochem. Sci.* **21**: 11-13.

Potuschak, T., Lechner, E., Parmentier, Y., Yanagisawa, S., Grava, S., Koncz, C., Genschik, P. (2003). EIN3-dependent regulation of plant hormone signaling by two arabidopsis F box proteins: EBF1 and EBF2. *Cell* **115**: 679-689.

Puissant, C. and Houdeline, L.M. (1990). An improvement of the single-step method of RNA isolation by acid guanidium thiocyanate-phenol-chloroform extraction. *BioTechniques* **8**: 148-149.

Raikhel, N.V. (1992). Nuclear targeting in plants. *Plant Physiol.* **100**: 1627-1632.

Raskin, I. and Kende, H. (1984). Regulation of growth in stem sections of deep-water rice. *Planta* **160**: 66-72.

Reiser, L., Sanchez-Baracaldo, P., Hake, S. (2000). Knots in the family tree: evolutionary relationships and functions of knox homeobox genes. *Plant Mol. Biol.* **42**: 151-166.

Roberts, J.K.M., Callis, J., Jardetzky, O., Walbot, V., Freeling, M. (1984). Cytoplasmic acidosis as a determinant of flooding intolerance in plants. *Proc. Natl. Acad. Sci. USA* **81**: 6029-6033.

Roberts, J.K.M., Andrade, F.H., Anderson, I.C. (1985). Further evidence that cytoplasmic acidosis is a determinant of flooding intolerance in plants. Plant Physiol. **77**: 492-494.

Rogg, L.E. and Bartel, G. (2001). Auxin signaling: derepression through regulated proteolysis. *Dev. Cell* **1**: 595-604.

Rosin, F.M., Hart, J.K., Van Onckelen, H., Hannapel, D.J. (2003). Suppression of a vegetative MADS box gene of potato activates axillary meristem development. *Plant Physiol.* **131**: 1613-1622.

Ross, J.J., O'Neil, D.P., Smith, J.J., Kerckhoffs, L.H.J., Elliott, R.C. (2000). Evidence that auxin promotes gibberellin A(1) biosynthesis in pea. *Plant J.* **21**: 547-552.

Rouleau, M., Marsolais, F., Richard, M., Nicolle, L., Voigt, B., Adam, G., Varin, L. (1999). Inactivation of brassinosteroid biological activity by a salicylate-inducible steroid sulfotransferase from *Brassica napus*. *J. Biol. Chem.* **274**: 20925-20930.

Rzewuski, G. and Sauter, M. (2002). The novel rice (*Oryza sativa* L.) gene *OsSbf1* encodes a putative member of the Na^+/bile acid symporter family. *J. Exp. Bot.* **53**: 1991-1993.

Sakamoto, T., Kamiya, N., Ueguchi-Tanaka, M., Iwahori, S., Matsuoka, M. (2001). KNOX homeodomain protein directly suppresses the expression of a gibberellin biosynthetic gene in the tobacco shoot apical meristem. *Genes Dev.* **15**: 581-590.

Sambrook, F., Fritsch E.F., Maniatis, T. (1989). Molecular cloning: A laboratory manual, 2nd ed. Cold Spring Harbor Laboratory Press, New York.

Sami-Subbu, R., Choi, S.B., Wu, Y., Wang, C., Okita, T.W. (2001). Identification of a cytoskeleton-associated 120 kDa RNA-binding protein in developing rice seeds. *Plant Mol. Biol.* **46**: 79-88.

Sanger, F., Nickler, S., Coulson, A.R. (1977). DNA sequencing with chain-terminating inhibitors. *Proc. Natl. Acad. Sci. USA* **74**: 5463-5467.

Sasaki, A., Itoh, H., Gomi, K., Ueguchi-Tanaka, M., Ishiyama, K., Kobayashi, M., Jeong, D.H., An, G., Kitano, H., Ashikari, M., Matsuoka, M. (2003). Accumulation of phosphorylated repressor for gibberellin signaling in an F-box mutant. *Science* **299**: 1896-1898.

Sato, Y., Sentoku, N., Miura, Y., Hirochika, H., Kitano, H., Matsuoka, M. (1999). Loss-of-function mutations in the rice homeobox gene OSH15 affect the architecture of internodes resulting in dwarf plants. *EMBO J.* **18**: 992-1002.

Sauter, M. and Kende, H. (1992). Gibberellin-induced growth and regulation of the cell division cycle in deepwater rice. *Planta* **188**: 362-368.

Sauter, M., Seagull, R.W., Kende, H. (1993). Internodal elongation and orientation of cellulose microfibrills and microtubules in deepwater rice. *Planta* **190**: 354-362.

Sauter, M. (1997). Differential expression of a CAK (cdc2-activating kinase)-like protein kinase, cyclins and cdc2 genes from rice during the cell cycle and in response to gibberellins. *Plant J.* **11**: 181-190.

Scott A., Wyatt, S., Tsou, P.L., Robertson, D., Allen, N.S. (1999). Model system for plant cell biology: GFP imaging in living onion epidermal cells. *BioTechniques* **26**: 1128-1132.

Sehnke, P.C., DeLille, J.M., Ferl, R.J. (2002). Consummating signal transduction: The role of 14-3-3 proteins in the completion of signal-induced transitions in protein activity. *Plant Cell* S339-S354.

Setter, T.L., Ellis, M., Laureles, E.V., Ella, E.S., Senadhira, D., Mishra, S.B., Sarkarung, S., Datta, D. (1997). Physiology and genetics of submergence tolerance in rice. *Annals of Botany* **79** (Suppl. A): 67-77.

Shen, H. and Wang, Z.Y. (2004). Expressional analysis of an EREBP transcription factor gene *OsEBP-89* in Rice. *Acta Biochim. et Biophysica Sinica* **36**: 21-26.

Silverstone, A.L., Jung, H.S., Dill, A., Kawaide, H., Kamiya, Y., Sun, T.P. (2001). Repressing a repressor: gibberellin-induced rapid reduction of the RGA protein in *Arabidopsis*. *Plant Cell* **13**: 1555-1566.

Smirnoff, N. (1996). The function and metabolism of ascorbic acid in plants. *Annals of botany* **78**: 661-669.

Solano, R., Stepanova, A., Chao, Q., Ecker, J.R. (1998). Nuclear events in ethylene signaling: a transcriptional cascade mediated by ETHYLENE-INSENSITIVE3 and ETHYLENE-RESPONSE-FACTOR1. *Genes Dev.* **12**: 3703-3714.

Szymanski, D.B., Jilk, R.A., Pollock, S.M., Marks, M.D. (1998). Control of *GL2* expression in Arabidopsis leaves and trichomes. *Development* **125**: 1161-1171.

Talon, M., Koorneef, M., Zeevaart, J.A. (1990). Endogenous gibberellins in Arabidopsis thaliana and possible steps blocked in the biosynthetic pathways of the semidwarf *ga4* and *ga5* mutants. *Proc. Natl. Acad. Sci. USA* **87**: 7983-7987.

Tax, F.E., Vernon, D.M. (2001). T-DNA-associated duplication/translocations in Arabidopsis. Implications for mutant analysis and functional genomics. *Plant Physiol.* **126**: 1527-1538.

Theissen, G. and Saedler, H. (2001). Floral quartets. *Nature* **409**: 469-471.

Toojinda, T., Siangliw, M., Tragoonrung, S., Vanavichit, A. (2003). Molecular genetics of submergence tolerance in rice: QTL analysis of key traits. *Annals of Botany* **91**: 243-253.

Tomsig, J.L., Snyder, S.L., Creutz, C.E. (2003). Identification of targets for calcium signaling through the copine family of proteins. *J. Biol. Chem.* **278**: 10048-10054.

Tsukaya, H., Tsuge, T., Uchimiya, H. (1994). The cotyledon: a superior system for studies of leaf development. *Planta* **195**: 309-312.

Tsukaya, H., Kozuka, T., Kim, G.T. (2002). Genetic control of petiole length in Arabidopsis thaliana. *Plant Cell Physiol.* **43**: 1221-1228.

Van Der Straeten, D., Zhou, Z.Y., Prinsen, E., Van Onckelen, H.A., Van Montagu, M. (2001). A comparative molecular-physiological study of submergence response in lowland and deepwater rice. *Plant Physiol.* **125**: 955-968.

Van Volkenburgh, E. (1999). Leaf expansion – an integrating plant behaviour. *Plant Cell Env.* **22**: 1463-1473.

Voesenek, L.A.C.J., Benschop, J.J., Bou, J., Cox, M.C.H., Groeneveld, H.W., Millenaar, F.F., Vreeburg, R.A.M., Peeters, A.J.M. (2003). Interactions between plant hormones regulate submergence-induced shoot elongation in the flooding tolerant dicot *Rumex palustris*. *Annals of Botany* **91**: 205-213.

Vriezen, W.H., Achard, P., Harberd, N.P., Van Der Straeten, D. (2004). Ethylene-mediated enhancement of apical hook formation in etiolated *Arabidopsis thaliana* seedlings is gibberellin dependent. *Plant J.* **37**: 505-16.

Wada, K., Marumo, S., Ikekawa, N., Morisaki, M., Mori, K. (1981). Brassinolide and homobrassinolide promotion of lamina inclination of rice seedlings. *Plant Cell Physiol.* **22**: 323-325.

Wang, Z. and Brown, D.D. (1991). A gene expression screen. *Proc. Natl. Acad. Sci. USA* **88**: 11505-11509.

Weigel, D. and Glazebrook, J. (2002). Arabidopsis: A laboratory manual. Cold Spring Harbor Laboratory Press, New York.

Wilkinson, C.R., Seeger, M., Hartmann-Petersen, R., Stone, M., Wallace, M., Semple, C., Gordon, C. (2001). Proteins containing the UBA domain are able to bind to multi-ubiquitin chains. *Nat.Cell Biol.* **3**: 939-943.

Wong, M.H., Oelkers, P., Dawson, P.A. (1995). Identification of a mutation in the ileal sodium-dependent bile acid transporter gene that abolishes transport activity. *J. Biol. Chem.* **270**: 27228-27234.

Yamamuro, C., Ihara, Y., Wu, X., Noguchi, T., Fujioka, S., Takatsuto, S., Ashikari, M., Kitano, H., Matsuoka, M. (2000). Loss of function of a rice *brassinosteroid insensitive1* homolog prevents internode elongation and bending of the lamina joint. *Plant Cell* **12**: 1591-1605.

7. Appendix.

7.1. Nucleotide and predicted amino acid sequence of *aci1*.

Nucleotides and amino acids are numbered on the left and right sides. The accession number for the nucleotide sequence is AK121440. The nucleotide sequence contains an ORF encoding a protein of 344 amino acids. 5'-UTR and 3'-UTR are 213 nucleotides and 218 nucleotides long, respectively. Nucleotides written in bold represent the sequence of the short *aci1* cDNA initially identified through subtractive hybridisation.

```
1      GGT CGA CTC GTC GTG GCC GCC GGC AAC TCA CGC CCA CCG CGC GCG    45
46     CGC GCG AAT TAA TAC AAA CAC ATT AAC ACA CAC AGA GAG AGA AAA    90
91     TTG GCG CGC CTC GCG CTG TGC GCC TTC GAA TTT TGG AGG CGA CGC    135
136    GCG GGA GGA CGG AAT CGG CCG GGG ATT CGC TGC GTC GCC GCG CGA    180

181    GAG CGA GAG GAG GAG GAG GAG GAG GAA GCC GGG ATG GGG GTG TCG    225
1                                                  M   G   V   S     4

226    GAC AAC ACG GTG GGG CTT TCG CTG GCG GTG GCG TCC AGC GCC TTC    270
5       D   N   T   V   G   L   S   L   A   V   A   S   S   A   F     19

271    ATC GGC GCC AGC TTC ATC CTC AAG AAG ATC GGA CTC ATC CGC GCC    315
20      I   G   A   S   F   I   L   K   K   I   G   L   I   R   A     34

316    GGC AAG GGC GGC GTC CGC GCA GGT GGT GGA GGA TAC ACT TAT CTT    360
35      G   K   G   G   V   R   A   G   G   G   G   Y   T   Y   L     49

361    TTG GAA CCT CTA TGG TGG GCT GGA ATG ATG ACA ATG TTG CTT GGG    405
50      L   E   P   L   W   W   A   G   M   M   T   M   L   L   G     64

406    GAG ATA GCA AAC TTC GTT GCT TAT ACC TTT GCA CCA GCC GTA CTT    450
65      E   I   A   N   F   V   A   Y   T   F   A   P   A   V   L     79

451    GTG ACT CCC CTT GGG GCA CTA AGC ATA ATC GTA AGT TCA TTT TTA    495
80      V   T   P   L   G   A   L   S   I   I   V   S   S   F   L     94

496    GCA CAT TTC GTG CTG AAG GAA CGG CTT GAG AAG CTA GGT GTT CTT    540
95      A   H   F   V   L   K   E   R   L   E   K   L   G   V   L    109

541    GGT TGT GTA TCA TGC ATT GTC GGT TCA GTT ATT GTT GTT ATA CAT    585
110     G   C   V   S   C   I   V   G   S   V   I   V   V   I   H    124

586    GCT CCT CAA GAA CAT ATG CCT AAT TCT GTA GAG GAA ATC TGG AAC    630
125     A   P   Q   E   H   M   P   N   S   V   E   E   I   W   N    139

631    TTA GCC ATT CAA CCA GGA TTT CTA ACA TAT GCG GTA GCA ACC TTA    675
140     L   A   I   Q   P   G   F   L   T   Y   A   V   A   T   L    154

676    GTA GTC GTG GCA GCA CTA GTT CTC TTC TTT GAA CCT CGA TAT GGT    720
155     V   V   V   A   A   L   V   L   F   F   E   P   R   Y   G    169

721    CAG ACA AAT ATC ATG ATA TAT CTG GGC ATC TGC TCT TCT ATG GGA    765
170     Q   T   N   I   M   I   Y   L   G   I   C   S   S   M   G    184
```

```
766   TCA CTA ACA GTC GTT AGC ATC AAA GCC ATT GGT GTT GCT ATA AAG   810
185    S   L   T   V   V   S   I   K   A   I   G   V   A   I   K    199

811   CTT ACG CTG GAT GGA ATG AAC CAG GTT GCT TAT CCA CAC ACA TGG   855
200    L   T   L   D   G   M   N   Q   V   A   Y   P   H   T   W    214

856   CTT TTT GTT ATC ATT GCA ATC ATC TGT GTG GTT TCT CAG ATA AAT   900
215    L   F   V   I   I   A   I   I   C   V   V   S   Q   I   N    229

901   TAC CTC AAT AAG GCA CTG GAT ACC TTT GAT TTA GCT GTT GTT TCT   945
230    Y   L   N   K   A   L   D   T   F   D   L   A   V   V   S    244

946   CCA ATT TAT TAT GTA ATG TTT ACG ACT CTT ACA ATA GTG GCA AGT   990
245    P   I   Y   Y   V   M   F   T   T   L   T   I   V   A   S    259

991   GGA ATT ATG TTC AAG GAC TGG GCT GGT CAA AGC TTC AGT AGC ATT   1035
260    G   I   M   F   K   D   W   A   G   Q   S   F   S   S   I    274

1036  GCT TCT GAA TTT TGT GGT CTG ATA ACA ATT CTT ACC GGA ACA ATT   1080
275    A   S   E   F   C   G   L   I   T   I   L   T   G   T   I    289

1081  ATG TTA CAC ACA GCA AAG GAG GAA GAA ACA GGC AGT TCT GCA GCT   1125
290    M   L   H   T   A   K   E   E   E   T   G   S   S   A   A    304

1126  TTG CCA TGG CCT TTG GAT AGA GGG TCC ATA TCC TGG TGT ATC AGT   1170
305    L   P   W   P   L   D   R   G   S   I   S   W   C   I   S    319

1171  TTA GGG AGC GAC AAT CTA CTG AAG AAT GTC AAT GAG GAC TAC TTT   1215
320    L   G   S   D   N   L   L   K   N   V   N   E   D   Y   F    334

1216  GCA GCT CTG CAA AGT TCT CCT GCG CCA GTT TAA TTG TAC ATT TGG   1260
335    A   A   L   Q   S   S   P   A   P   V   *                    344

1261  AAG TAA TTT CCT TTT ACT TCC ATT GAC GAA GAA ACT TAT AGA GTG   1305
1306  ATG TAC AAA ATA TCA TGC AAA TTG CAC AGG AAC CTT AGC AGT GCC   1350
1351  AAC ATT CTG GCA GTT TTG TTG TAG AAG ATT TTA TCT GAC ATT CTT   1395
1396  TCA CTG TAC ATA AGG ACT TGT AAA ATT TGT GAA ACC ATT CTT GGA   1440
1441  ACC ACA CGA TGT TAG GAA ATT CTT                              1464
```

7.2. Nucleotide and predicted amino acid sequence of *aci2*.

Nucleotides and amino acids are numbered on the left and right sides. The accession number for the nucleotide sequence is AK099201. The nucleotide sequence contains an ORF encoding a protein of 309 amino acids. 5'-UTR and 3'-UTR are 61 nucleotides and 302 nucleotides long, respectively. Nucleotides written in bold represent the sequence of the 261 nt-long *aci2* cDNA initially isolated by subtractive hybridisation.

```
2     AGC GAA CCA CTC CCA AAA CGC CAC CAA AAC CCT CCT CTC CCC ACC   46

47    TCC GCC GCC GCC GAC ATG GCC GTC GTC CAC CGC CTC CTC CGC CGC   91
1                         M   A   V   V   H   R   L   L   R   R    10

92    GGC CTC TCC GCC GCC TCT CCC CTC CCC TCT CTT CAG GAG CTC GGG   136
11     G   L   S   A   A   S   P   L   P   S   L   Q   E   L   G    25


137   AGG CGT CCG GCG AGC TCG TCG GCG GCG GCG GCG GGG GAC GCG GCG   181
26     R   R   P   A   S   S   S   A   A   A   A   G   D   A   A    40
```

```
182   GCT GAG CTG CGG GGC GCG CGG GAG GAC GTC AAG CAG CTG CTC AAG   226
41     A   E   L   R   G   A   R   E   D   V   K   Q   L   L   K    55

227   TCC ACC TCC TGC CAT CCC ATC CTG GTT CGG TTA GGG TGG CAT GAT   271
56     S   T   S   C   H   P   I   L   V   R   L   G   W   H   D    70

272   GCT GGT ACT TAT GAC AAG AAC ATT ACT GAA TGG CCA AAG TGT GGT   316
71     A   G   T   Y   D   K   N   I   T   E   W   P   K   C   G    85

317   GGT GCC AAT GGT AGC TTG AGA TTC GAA ATT GAG TTA AAA CAT GCG   361
86     G   A   N   G   S   L   R   F   E   I   E   L   K   H   A   100

362   GCT AAT GCA GGT CTT GTG AAT GCT TTG AAG CTG ATC CAG CCC ATC   406
101    A   N   A   G   L   V   N   A   L   K   L   I   Q   P   I   115

407   AAA GAC AAG CAT GCA GGT GTC ACT TAT GCA GAT CTG TTT CAG CTC   451
116    K   D   K   H   A   G   V   T   Y   A   D   L   F   Q   L   130

452   GCC AGT GCT ACA GCC ATT GAG GAA GCC GGT GGC CCC AAG ATC CCC   496
131    A   S   A   T   A   I   E   E   A   G   G   P   K   I   P   145

497   ATG ATC TAT GGA AGG GTT GAT GTT GCT GCC CCT GAA CAA TGC CCG   541
146    M   I   Y   G   R   V   D   V   A   A   P   E   Q   C   P   160

542   CCA GAG GGG AGA CTT CCT GCT GCT GGC CCT CCT TCA CCT GCG GAA   586
161    P   E   G   R   L   P   A   A   G   P   P   S   P   A   E   175

587   CAT CTA CGA GAA GTA TTC TAT AGA ATG GGC CTG AGT GAC AAG GAA   631
176    H   L   R   E   V   F   Y   R   M   G   L   S   D   K   E   190

632   ATT GTT GCA TTG TCA GGA GCT CAT ACA CTT GGA CGA TCT AGA CCA   676
191    I   V   A   L   S   G   A   H   T   L   G   R   S   R   P   205

677   GAG CGC AGT GGA TGG GGC AAA CCA GAA ACT AAA TAC ACT AAA AAC   721
206    E   R   S   G   W   G   K   P   E   T   K   Y   T   K   N   220

722   GGA CCT GGT GCA CCT GGA GGG CAA TCT TGG ACA TCA CAG TGG CTG   766
221    G   P   G   A   P   G   G   Q   S   W   T   S   Q   W   L   235

767   AAG TTT GAT AAT AGC TAC TTC AAG GAC ATC AAA GAA CGC CGA GAT   811
236    K   F   D   N   S   Y   F   K   D   I   K   E   R   R   D   250

812   GAG GAC CTT CTA GTT CTG CCT ACT GAT GCT GTG CTC TTT GAG GAC   856
251    E   D   L   L   V   L   P   T   D   A   V   L   F   E   D   265

857   TCA TCA TTC AAG ATC TAT GCT GAA AAG TAC GCC GCA GAT CAG GAT   901
266    S   S   F   K   I   Y   A   E   K   Y   A   A   D   Q   D   280

902   GCA TTT TTT GAA GAC TAT GCT GAA GCT CAT GCC AAA CTG AGC AAT   946
281    A   F   F   E   D   Y   A   E   A   H   A   K   L   S   N   295

947   CTC GGA GCA AAG TTT GAT CCT CCA AAG GGT ATT TCA CTG GAA TAA   991
296    L   G   A   K   F   D   P   P   K   G   I   S   L   E   *   309

992   GTG GCG TCT GCT GCC GAT GAG CTG CAT TTT GGC GAA TGA ACA AGA  1036
1037  CGA TAC CCT GTT TCT TCT TGC TAC TAT AGA GCA TAT TAT GGT TTT  1081
1082  ATT ACC GAT CCA GAA ATT TAA TCC ATT GAT CGG CAA ATG TGA TGT  1126
1127  TGG TGT TTT GTA TTG AGT TGT GCT CTC CAT TAG AAA TAA AAA TAG  1171
1172  CGG TGG CCA TTT TCG TTT CCA GGA CCA AAC ATT TTG GCA CAT TAC  1216
1217  AAT ACA ATG TTT TAG ATG ATG TCT GCA TTG AGC TCT TAC ACA GGA  1261
1262  TGA TCA AAA TAT ATG ACA TAA TTT ATT ACT                      1291
```

7.3. Nucleotide and predicted amino acid sequence of *aci3.*

Nucleotides and amino acids are numbered on the left and right sides. A full-length cDNA of *aci3* isolated from a rice λgt11 cDNA library had a 5'-UTR 28 bp longer than that of the cDNA published in the database under the accession number AK108855, which starts at position 1. Nucleotides written in bold font represent the sequence of the short *aci3* cDNA isolated by subtractive hybridisation.

```
-28                          G AAT CTC AGA GGT GCA GTG CAG GCT TGC
1     AGC GGA GTT GTT CAC TTG TAG GCT CCT TCC TTA ACC TGC TCA ATG   45
46    TAT CAT AGC CGC TCC AAG AGA TAG GAT CAG TTC TTG GCT AAT GCC   90

91    TAA TGA TCT TGA CGA ATT TGC ATC GGC AGC GAC TCT GTT AGA ATG   135
1                                                           M     1

136   CTC AGA ATG GAT GGC ACG GAT TTG TCT TCC CCA AGG TGC AAT GTT   180
2      L   R   M   D   G   T   D   L   S   S   P   R   C   N   V    16

181   CAG CAT CTA CAG AAT GCC GAA GAA CTG AAG GAT CAG AAT AGC ACC   225
17     Q   H   L   Q   N   A   E   E   L   K   D   Q   N   S   T    31

226   AAT AAG AGG CTG CCC CGG ACT ACA GAG CTC CCA TGC TCT TTG ATA   270
32     N   K   R   L   P   R   T   T   E   L   P   C   S   L   I    46

271   CAA GAG GTC CAA CAC CTT GAG AAG CGA CTA AAT GAT CAA TTT GCT   315
47     Q   E   V   Q   H   L   E   K   R   L   N   D   Q   F   A    61

316   ATG CGG CGT GCT TTG GAG AAA GCA TTA GGT TAT AAG CCT TGT GCC   360
62     M   R   R   A   L   E   K   A   L   G   Y   K   P   C   A    76

361   ATT CAT TCA TCC AAT GAG AGC TGC ATT CCA AAG CCT ACT GAG GAA   405
77     I   H   S   S   N   E   S   C   I   P   K   P   T   E   E    91

406   CTA ATA AAG GAG ATT GCT GTG CTG GAG CTA GAG GTC ATA TGC TTG   450
92     L   I   K   E   I   A   V   L   E   L   E   V   I   C   L   106

451   GAG CAA CAT CTC CTA GCA CTC TAC CGG AAG GCC TTT GAT CAA CAA   495
107    E   Q   H   L   L   A   L   Y   R   K   A   F   D   Q   Q   121

496   ATT TGC AGC GTG TCT TCT TCC TGT GAC ATG GAA ATC AAC AAG CAG   540
122    I   C   S   V   S   S   S   C   D   M   E   I   N   K   Q   136

541   TCA GCA AGG TCA TTC TCA GGT ATA CTC ACA GGA TCT TCA GAA CTG   585
137    S   A   R   S   F   S   G   I   L   T   G   S   S   E   L   151

586   GAT TTC TCA ACC CCA AGG AAA CAC CAA CTC CTG CAG TCC AGT GGC   630
152    D   F   S   T   P   R   K   H   Q   L   L   Q   S   S   G   166

631   ATG GTC ATG GCA CGC AAG TCT ACA CCG ACA ACT CTC ACT AGC GAA   675
167    M   V   M   A   R   K   S   T   P   T   T   L   T   S   E   181

676   ACC AGA ACT TCA CAT TAC AAT GAC AAG ACT GGT ATC GGA CGC AGC   720
182    T   R   T   S   H   Y   N   D   K   T   G   I   G   R   S   196

721   CAT TCC TCG CTC CTG CAG CGT TCC ATT TGT TCA GCC AGA GTA TCT   765
197    H   S   S   L   L   Q   R   S   I   C   S   A   R   V   S   211
```

```
766   CCT TCA GCA AAC AAT CTT GCT AGG GCT CTC AAA CCA TGC CAT ACT   810
212    P   S   A   N   N   L   A   R   A   L   K   P   C   H   T   226

811   TTG CCT CTA TCC TTT GTC GAG GAG GGC AAG TGC ATG GAT CCT GGT   855
227    L   P   L   S   F   V   E   E   G   K   C   M   D   P   G   241

856   ATT GTG AGC CTG GCG GAT ATC CTA GGG ACC AGG ATA GCA GAT CAT   900
242    I   V   S   L   A   D   I   L   G   T   R   I   A   D   H   256

901   GTT CCT CAA ACA CCG AAC AAA ATA ACT GAG GAC ATG ATC AAA TGC   945
257    V   P   Q   T   P   N   K   I   T   E   D   M   I   K   C   271

946   ATT GCT TCG ATA TAC ATA AGG ATT AGG GAC TTC AAT GCC GTG CAA   990
272    I   A   S   I   Y   I   R   I   R   D   F   N   A   V   Q   286

991   CAT CCC TTC TTC CCC TCA CCA TGC TCA TCA TTT TCA TCA GCG AGC   1035
287    H   P   F   F   P   S   P   C   S   S   F   S   S   A   S   301

1036  GGG CTC TCT TCC AAA TAC ACT GGG GAT ATA TGG AGC CCA AGA TGT   1080
302    G   L   S   S   K   Y   T   G   D   I   W   S   P   R   C   316

1081  AGG AAA GAG GGC TAT ATT GAG GCC TGG CAA GAC GAT GCG TCA GGA   1125
317    R   K   E   G   Y   I   E   A   W   Q   D   D   A   S   G   331

1126  ACT GGC GAA TCA AGA TAC TTC AGT CAA CAA TAT GAT TCT GTG ATT   1170
332    T   G   E   S   R   Y   F   S   Q   Q   Y   D   S   V   I   346

1171  GAG GTG TCT GCT CTT TGC AAG GGG GCC CAG AGG TCT GCT GAT GTT   1215
347    E   V   S   A   L   C   K   G   A   Q   R   S   A   D   V   361

1216  AAA GAC ATG CTA CAC AAA TAC AAG TCT CTT GTA CAG CTG CTA GAA   1260
362    K   D   M   L   H   K   Y   K   S   L   V   Q   L   L   E   376

1261  AGT GCT GAT CTC AAC GGA ATG AAA AAT GAA GAA AAA ATT GCT TTC   1305
377    S   A   D   L   N   G   M   K   N   E   E   K   I   A   F   391

1306  TGG ATC AAT GTG CAC AAT GCC ATG ATG ATG CAT GCC CAT ATA GAA   1350
392    W   I   N   V   H   N   A   M   M   M   H   A   H   I   E   406

1351  TAC GGG ATT CCG CAA AGT AAC AGC AAG AGA ATA TTG CTT ACT AAG   1395
407    Y   G   I   P   Q   S   N   S   K   R   I   L   L   T   K   421

1396  TTA TCT TAC CTC ATC AGT GGC CAG AGA GTA AAC CCG GAG TTG ATA   1440
422    L   S   Y   L   I   S   G   Q   R   V   N   P   E   L   I   436

1441  GAG TAC CAT ATC CTA TGC TGC CGA GTG CAC TCT CCT ACA CAG TGG   1485
437    E   Y   H   I   L   C   C   R   V   H   S   P   T   Q   W   451

1486  CTG AGA CTA CTC CTG TAC CCG AAA TGG AAG TCC AAG GAG AAG GAA   1530
452    L   R   L   L   L   Y   P   K   W   K   S   K   E   K   E   466

1531  GAC CTG CAG GGG TTC GCC GTC GAC AGG CCG GAG CCG CTG GTG CAC   1575
467    D   L   Q   G   F   A   V   D   R   P   E   P   L   V   H   481

1576  TTC GCG CTG TCG TCG GGG AGC CAC TCC GAC CCG GTG GTG CGG TTG   1620
482    F   A   L   S   S   G   S   H   S   D   P   V   V   R   L   496

1621  TAC CGG CCG GAG CGC CTC CTC CAG CAG CTG GAG GCG GCG AGG GAC   1665
497    Y   R   P   E   R   L   L   Q   Q   L   E   A   A   R   D   511

1666  GAG TTC GTC CGC GCC AAC GTC GGC GTC CGC GGG GGG CGG CGC GGG   1710
512    E   F   V   R   A   N   V   G   V   R   G   G   R   R   G   526
```

```
1711  CGC GGG CGC CGG GTG CTC CTC CTC CTC CCG AAG CTC CTC GAG CCG   1755
527    R   G   R   R   V   L   L   L   L   P   K   L   L   E   P    541

1756  TAC TCG AGG GAC GCC GGC CTC GGT GCG CAC GAC CTC CTC CGC GCG   1800
542    Y   S   R   D   A   G   L   G   A   H   D   L   L   R   A    556

1801  GTG GAG TCC TGC CTC CCG GAG CCG CTC CGG CCG GCG GCG CAG CAG   1845
557    V   E   S   C   L   P   E   P   L   R   P   A   A   Q   Q    571

1846  GCG GCG CGG TCG CGC GGC GGC GGC GGC GGC GTC GAG TGG AGG CCC   1890
572    A   A   R   S   R   G   G   G   G   G   V   E   W   R   P    586

1891  CAC AAC CCG GCC TTC CGC TAC CTG CTC GCG CGG GAG CTC GTG GGC   1935
587    H   N   P   A   F   R   Y   L   L   A   R   E   L   V   G    601

1936  CCA CCC GCG CCA ACG GCC CAC CTA TCC TCC ACG TAA AGT TTC ACG   1980
602    P   P   A   P   T   A   H   L   S   S   T   *               612

1981  GCC CAA TGT ACA GAG CCT TGT AAA GTT GAT ATT TTG GGC CCG GCC   2025
2026  CAA CAA ACT TGG AAA GTT AGT TAT CTG GGC CTG AAA AGA GGC CGT   2070
2071  GGC TTT TGG CCC ATG TTT GTG GAA CGT TCT ACC TGC TTG GTC TCT   2115
2116  CGG ATG GCA CGA ACG GAC GAC GAT TTC CGT CTT GGT GGA CAA GAA   2160
2161  AGA AAG TGG AAC GTT TTT GAC TTG GAT TCT TAA ACC CGC CAA TGG   2205
2206  TTT TCC ACG CGC CCA CGT TAT TGA GGG GTG TTT AGA TCT CAC ATC   2250
2251  AAA TAT TAT ATA GGT TAT CGC AGG GTG TTC AGA CAC TAA TAT AAA   2295
2296  AAA CTA ACT ACA GTA TCT GTC AGT AAA CCG CAA GAC GGA TTT ATT   2340
2341  AAG CCT AAT TAA TCT ATC ATT AGC GTA TAT TTA CTG TAG CAA TAC   2385
2386  ATT GTC AAA TCA TGG AGC AAT CAG GTT                          2412
```

7.4. Nucleotide and predicted amino acid sequence of *aci4.*

Nucleotides and amino acids are numbered on the left and right sides. The accession number for the nucleotide sequence is AK060230. The nucleotide sequence contains an ORF encoding a protein of 515 amino acids. 5'-UTR and 3'-UTR are 140 nucleotides and 282 nucleotides long, respectively. Nucleotides written in bold font represent the 238 nt-long *aci4* cDNA initially identified through subtractive hybridisation.

```
3     CCC TCC CCC TCG TCT CCT CCG CTG CGA AGC CGC AGA TCT CGA GCT   47
48    GCC ATT CGA TTG ATG AGG TAA GGG GGG TGC CGG CGC GAG AAG CGA   92
93    GGT TGG CTG GCC GGC GGA GGG CGG GCT GTC GGT CGC GGG TGC GCC   137

138   AGG ATG GGG CTG ATC TCG GGG ATG GTG ATG GGG ATG GTG GTC GGC   182
1          M   G   L   I   S   G   M   V   M   G   M   V   V   G    14

183   GTC GCG CTT ATG GCC GGG TGG AGC CGT GTG ATG CAG CGG CGC AGC   227
15     V   A   L   M   A   G   W   S   R   V   M   Q   R   R   S    29

228   AGG AAG CGC ATC GCT AAG GCT GCG GAT ATC AAG GTC CTT GGG TCT   272
30     R   K   R   I   A   K   A   A   D   I   K   V   L   G   S    44

273   CTC GGT AGG GAC GAT CTC AAG AAG CTG TGC GGC GAC AAT TTC CCC   317
45     L   G   R   D   D   L   K   K   L   C   G   D   N   F   P    59

318   GAG TGG ATA TCC TTC CCG CAG TAT GAG CAG GTG AAA TGG CTG AAC   362
60     E   W   I   S   F   P   Q   Y   E   Q   V   K   W   L   N    74
```

```
363   AAG CAT CTC AGC AAA CTC TGG CCT TTC GTT GAT CAA GCT GCC ACT   407
75     K   H   L   S   K   L   W   P   F   V   D   Q   A   A   T    89

408   GCA GTA GTC AAG GAA TCT GTT GAG CCA CTG CTA GAT GAT TAT CGA   452
90     A   V   V   K   E   S   V   E   P   L   L   D   D   Y   R   104

453   CCT CCA GGA ATA AAA TCT CTG AAG TTC AGC AAA TTC TCT CTT GGA   497
105    P   P   G   I   K   S   L   K   F   S   K   F   S   L   G   119

498   ACT GTT TCA CCA AAG ATA GAA GGT ATT CGC ATT CAA AAT ATT CAG   542
120    T   V   S   P   K   I   E   G   I   R   I   Q   N   I   Q   134

543   CCA GGC CAA ATC ATA ATG GAT ATA GAT CTT CGT TGG GGT GGT GAT   587
135    P   G   Q   I   I   M   D   I   D   L   R   W   G   G   D   149

588   CCA AGC ATA ATC CTT GCT GTT GAT GCT GTT GTT GCA TCA CTT CCT   632
150    P   S   I   I   L   A   V   D   A   V   V   A   S   L   P   164

633   ATT CAG CTC AAA GAT CTT CAA GTC TAC ACC ATT GTC CGT GTT GTA   677
165    I   Q   L   K   D   L   Q   V   Y   T   I   V   R   V   V   179

678   TTT CAA CTA TCA GAG GAG ATC CCT TGC ATC TCT GCT GTT GTT GTT   722
180    F   Q   L   S   E   E   I   P   C   I   S   A   V   V   V   194

723   GCT CTT CTT GCA GAG CCA GAG CCG AAA ATA CAA TAC ACT TTG AAG   767
195    A   L   L   A   E   P   E   P   K   I   Q   Y   T   L   K   209

768   GCT ATT GGA GGA AGT CTG ACC GCT GTT CCA GGA CTC TCC GAC ATG   812
210    A   I   G   G   S   L   T   A   V   P   G   L   S   D   M   224

813   ATT GAT GAC ACT GTC AAT TCA ATT GTT TCT GAC ATG CTC AAG TGG   857
225    I   D   D   T   V   N   S   I   V   S   D   M   L   K   W   239

858   CCA CAC AGG CTT GTT GTT CCA CTT GGT GTC AAT GTT GAT ACA AGT   902
240    P   H   R   L   V   V   P   L   G   V   N   V   D   T   S   254

903   GAG CTG GAG CTT AAA CCT CAG GGA AGA CTT ACT GTT ACT GTA GTA   947
255    E   L   E   L   K   P   Q   G   R   L   T   V   T   V   V   269

948   AAA GCA ACT TCA TTG AAG AAT AAG GAG TTG ATT GGT AAA TCA GAT   992
270    K   A   T   S   L   K   N   K   E   L   I   G   K   S   D   284

993   CCA TAT GTG ATA CTA TAT GTG CGT CCA ATG TTC AAG GTC AAA ACA  1037
285    P   Y   V   I   L   Y   V   R   P   M   F   K   V   K   T   299

1038  AAA GTC ATA GAT GAT AAC CTA AAT CCT GAA TGG AAT GAA ACA TTC  1082
300    K   V   I   D   D   N   L   N   P   E   W   N   E   T   F   314

1083  CCT CTG ATT GTT GAA GAC AAA GAA ACC CAG TCT GTC ATT TTT GAG  1127
315    P   L   I   V   E   D   K   E   T   Q   S   V   I   F   E   329

1128  GTA TAT GAT GAA GAC AGA CTT CAG CAA GAC AAA AAG CTT GGT GTA  1172
330    V   Y   D   E   D   R   L   Q   Q   D   K   K   L   G   V   344

1173  GCT AAA CTA GCA GTG AAC AGT CTT CAA CCT GAG GCT ACC AGT GAA  1217
345    A   K   L   A   V   N   S   L   Q   P   E   A   T   S   E   359

1218  ATC ACT TTG AAA CTT CAG CAA TCA CTA GAT TCT CTT AAA ATT AAG  1262
360    I   T   L   K   L   Q   Q   S   L   D   S   L   K   I   K   374

1263  GAC ACC AAG GAT AGA GGA ACA TTA CAT CTT CAG GTC ACA TAT CAC  1307
375    D   T   K   D   R   G   T   L   H   L   Q   V   T   Y   H   389
```

```
1308  CCA TTT TCA AAG GAA GAA CAG ATG GAA GCC CTA GAG TCT GAA AAG   1352
390    P   F   S   K   E   E   Q   M   E   A   L   E   S   E   K    404

1353  AGA GCT ATC GAG GAG AGA AAG CGA CTC AAG GAG GCT GGG GTT ATT   1397
405    R   A   I   E   E   R   K   R   L   K   E   A   G   V   I    419

1398  GGT AGT ACA ATG GAT GCT CTT GGT GGT GCT GCT TCA CTA GTT GGT   1442
420    G   S   T   M   D   A   L   G   G   A   A   S   L   V   G    434

1443  TCT GGT GTT GGA CTT GTG GGC ACT GGC ATT GTC GGC GGG GTT GGA   1487
435    S   G   V   G   L   V   G   T   G   I   V   G   G   V   G    449

1488  CTT GTT GGA TCA GGA ATT GGT GCT GGT GTT GGG CTT GTT GGT TCG   1532
450    L   V   G   S   G   I   G   A   G   V   G   L   V   G   S    464

1533  GGT GTT GGG CTT GTT GGT TCG GGT ATT GGC GCT GTC GGC AGC GGC   1577
465    G   V   G   L   V   G   S   G   I   G   A   V   G   S   G    479

1578  CTC GGT AAA GCT GGG AAA TTC ATG GGC AAG ACT GTG GCC GGG CCT   1622
480    L   G   K   A   G   K   F   M   G   K   T   V   A   G   P    494

1623  TTC AGT ATG TCC CGG AAG AAC GGT AGC AGC TCA ACT GCT CCC CAG   1667
495    F   S   M   S   R   K   N   G   S   S   S   T   A   P   Q    509

1668  GCT GAA CAA CCT TCT GCG TGA CTT GAT GTA CAG TGA TTG CAA TGG   1712
510    A   E   Q   P   S   A   *                                   515

1713  ACA TCG CAT GTT CAG TTG CGT GTT AAT TCT GTT TGA TAT AAA CTT   1757
1758  GTG ATA CCT AGA ATT ATA GGG TTG CAT ACC ATG CAT TTC AGT GTT   1802
1803  CTG GCA CCG TCG GTG TCA ATT ATA TGA CCA TCT GTT GCT TTT TTT   1847
1848  TCT TCG TTC TGT TTT TAC CTG AAG ATA AAT AGC AAG ATT AAA CTG   1892
1893  TAA ATT GGC AAG CTA GAC ATA TCC AGA TCC TTT CTG GAC AAT GCA   1937
1938  ATG GTA TTG AAA TTT GTC GTT ATT AAA AAA                      1967
```

7.5. Nucleotide and predicted amino acid sequence of *aci5.*

Nucleotides and amino acids are numbered on the left and right sides. The accession number for the nucleotide sequence is AK064893. The nucleotide sequence contains an ORF encoding a protein of 609 amino acids. 5'-UTR and 3'-UTR are 117 nucleotides and 186 nucleotides long, respectively. Nucleotides written in bold represent the 338 nt-long *aci5* cDNA initially isolated by subtractive hybridisation.

```
1     TGG CGG TGC AAG CGC AAC ACC ACC TCA CCT CAC TCC CCT TCT CAC   45
46    CTC TTC TCC CCT TCT CCA CCT CCT CTT CTC TCC GCG TGG CGG TGG   90

91    CAT TGC CGG CCG CCG CAT CGT CTC GGG ATG GCC TCG CAC GCG CTC   135
1                                       M   A   S   H   A   L    6

136   CGC CTC CAC CCG CTG CTC TTC TCC GCC GCC GCC GCG CGC CCG GCT   180
7      R   L   H   P   L   L   F   S   A   A   A   A   R   P   A    21

181   CCG CTC GCG GCG CGG CCC GGT GGT GGT GCC CGC CGG GTC CAC CGC   225
22     P   L   A   A   R   P   G   G   G   A   R   R   V   H   R    36

226   CGC CAC TCT CTC GCC GTC GTC CGG TGC TCC TCC TCC GCC GCC CAG   270
37     R   H   S   L   A   V   V   R   C   S   S   S   A   A   Q    51
```

```
271   GCG CTC AAG ATC AAG TCG ATT CCG ACC AAG CCC GTT GAG GGG CAG   315
52     A   L   K   I   K   S   I   P   T   K   P   V   E   G   Q    66

316   AAG ACC GGG ACC AGT GGG TTG AGG AAG AAG GTG AAA GTG TTC CAG   360
67     K   T   G   T   S   G   L   R   K   K   V   K   V   F   Q    81

361   CAG GAG AAT TAC CTC GCT AAT TGG ATT CAG GCT CTG TTC AAT TCA   405
82     Q   E   N   Y   L   A   N   W   I   Q   A   L   F   N   S    96

406   TTG CCC CCG GAG GAT TAT GTT GGT GGA ACC CTT GTG CTT GGT GGT   450
97     L   P   P   E   D   Y   V   G   G   T   L   V   L   G   G   111

451   GAT GGC CGA TAC TTT AAC AAG GAT GCT GCT CAG ATT ATC ACT AAA   495
112    D   G   R   Y   F   N   K   D   A   A   Q   I   I   T   K   126

496   ATT GCA GCT GGG AAT GGT GTT GGG AAG ATC CTA GTT GGC AGG AAC   540
127    I   A   A   G   N   G   V   G   K   I   L   V   G   R   N   141

541   GGT CTG CTG TCA ACG CCT GCT GTA TCT GCA GTA ATT CGT AAA AGA   585
142    G   L   L   S   T   P   A   V   S   A   V   I   R   K   R   156

586   CAA GCC AAT GGT GGC TTC ATC ATG AGT GCA AGC CAT AAT CCA GGT   630
157    Q   A   N   G   G   F   I   M   S   A   S   H   N   P   G   171

631   GGG CCA GAT AAT GAT TGG GGT ATC AAG TTC AAC TAT AGC AGT GGG   675
172    G   P   D   N   D   W   G   I   K   F   N   Y   S   S   G   186

676   CAG CCA GCA CCA GAG ACA ATT ACC GAC CAA ATA TAT GGA AAC ACA   720
187    Q   P   A   P   E   T   I   T   D   Q   I   Y   G   N   T   201

721   CTT TCG ATT TCT GAA ATA AAA ACG GCA GAT ATT CCT GAT GTT GAT   765
202    L   S   I   S   E   I   K   T   A   D   I   P   D   V   D   216

766   TTG TCC TCT CTA GGA GTT GTA AGC TAT GGT GAT TTC ACC GTT GAA   810
217    L   S   S   L   G   V   V   S   Y   G   D   F   T   V   E   231

811   GTG ATA GAC CCT GTC TTG GAC TAC CTT GAG CTA ATG GAG AAT GTG   855
232    V   I   D   P   V   L   D   Y   L   E   L   M   E   N   V   246

856   TTT GAC TTC CAA CTT ATC AAG GGC TTG TTG TCT CGG CCA GAT TTC   900
247    F   D   F   Q   L   I   K   G   L   L   S   R   P   D   F   261

901   AGG TTT GTA TTT GAT GCC ATG CAT GCT GTG ACT GGT GCA TAT GCG   945
262    R   F   V   F   D   A   M   H   A   V   T   G   A   Y   A   276

946   GAT CCT ATT TTT GTT GAG AAA CTT GGA GCT GAT CCG GAC TAT ATA   990
277    D   P   I   F   V   E   K   L   G   A   D   P   D   Y   I   291

991   TTA AAT GGT GTT CCA CTT GAA GAT TTT GGC AAT GGT CAC CCT GAT  1035
292    L   N   G   V   P   L   E   D   F   G   N   G   H   P   D   306

1036  CCT AAT TTA ACT TAT GCC AAA GAG CTT GTG TTT ACC ATG TTT GGA  1080
307    P   N   L   T   Y   A   K   E   L   V   F   T   M   F   G   321

1081  AGC GGA GCA CCT GAC TTT GGT GCA GCA AGT GAT GGT GAT GGT GAT  1125
322    S   G   A   P   D   F   G   A   A   S   D   G   D   G   D   336

1126  CGA AAC ATG ATT CTT GGA AGA AGG TTC TTT GTT ACA CCA TCA GAC  1170
337    R   N   M   I   L   G   R   R   F   F   V   T   P   S   D   351

1171  TCT GTT GCA ATA ATT GCA GCG AAT GCA CAG GCA GCA ATT CCT TAT  1215
352    S   V   A   I   I   A   A   N   A   Q   A   A   I   P   Y   366
```

```
1216  TTC CAA TCT GGT CCA AAA GGT CTT GCT AGA TCA ATG CCA ACG AGT   1260
367    F   Q   S   G   P   K   G   L   A   R   S   M   P   T   S    381

1261  GGT GCT CTT GAT CGT GTA GCT GAT AAA TTG AAT GTT CCG TTC TTT   1305
382    G   A   L   D   R   V   A   D   K   L   N   V   P   F   F    396

1306  GAG GTA CCA ACA GGA TGG AAA TTT TTT GGA AAC CTA ATG GAT GCA   1350
397    E   V   P   T   G   W   K   F   F   G   N   L   M   D   A    411

1351  GGT AAA TTG TCT ATA TGT GGA GAG GAA AGT TTT GGG ACA GGA TCT   1395
412    G   K   L   S   I   C   G   E   E   S   F   G   T   G   S    426

1396  GAT CAC ATC AGG GAG AAG GAT GGC ATA TGG GCT GTT CTA GCT TGG   1440
427    D   H   I   R   E   K   D   G   I   W   A   V   L   A   W    441

1441  CTG TCC ATA CTT GCA CAC CGG AAC AAG GAT AAG AAG GCC GGG GAG   1485
442    L   S   I   L   A   H   R   N   K   D   K   K   A   G   E    456

1486  AGA TTA GTG TCA GTG GAA GAT GTA GCT AGG GAA CAC TGG GCA ACC   1530
457    R   L   V   S   V   E   D   V   A   R   E   H   W   A   T    471

1531  TAT GGA AGG AAT TTC TTC TCC AGA TAT GAT TAT GAG GAG TGT GAA   1575
472    Y   G   R   N   F   F   S   R   Y   D   Y   E   E   C   E    486

1576  TCT GAG AGT GCA AAT AAG ATG ATG GAG CAT CTT AGA GAT GTG ATC   1620
487    S   E   S   A   N   K   M   M   E   H   L   R   D   V   I    501

1621  GCA AAA AGC AAG CCT GGA GAG AAA TAT GGA AAC TAT ACC CTT CAG   1665
502    A   K   S   K   P   G   E   K   Y   G   N   Y   T   L   Q    516

1666  TTT GCC GAT GAT TTC AGT TAC ACT GAT CCG GTG GAT GGT AGC ACT   1710
517    F   A   D   D   F   S   Y   T   D   P   V   D   G   S   T    531

1711  GTA TCT AAA CAA GGG CTT CGA TTT GTA TTC ACC GAT GGA TCT AGG   1755
532    V   S   K   Q   G   L   R   F   V   F   T   D   G   S   R    546

1756  ATT ATC TTC CGC CTT TCG GGA ACC GGA TCT GCT GGA GCA ACA ATC   1800
547    I   I   F   R   L   S   G   T   G   S   A   G   A   T   I    561

1801  CGT ATA TAC ATT GAG CAA TTC GAG TCT GAT GCC TCA AAG CAT GAT   1845
562    R   I   Y   I   E   Q   F   E   S   D   A   S   K   H   D    576

1846  CTG GAT GCA CAA ATA GCT TTG AAG CCT TTA ATA GAC CTA GCT CTA   1890
577    L   D   A   Q   I   A   L   K   P   L   I   D   L   A   L    591

1891  TCT GTT TCA AAG TTG AAG GAC TTC ACT GGA AGA GAT AAG CCT ACT   1935
592    S   V   S   K   L   K   D   F   T   G   R   D   K   P   T    606

1936  GTC ATA ACA TAA ACA TAC CGG TGA CAT TAG CAA TGT TAC CAC CTG   1980
607    V   I   T   *                                               609

1981  TGT ATT CTT TTA TTT CTT TGT TTT TAT AGC CCC TTC CAA CCG ATG   2025
2026  AAC CAA TAA TGT AAT CTT AGG CCA AGT TTT GTA CTG AGT TGA TGG   2070
2071  CAA ACT GTA TCT TGG AGG TAC CTT TCA TTG AAC ATA GTA TGC AGG   2115
2116  AAT GAA TAA GCT TTT                                         2130
```

7.6. Nucleotide and predicted amino acid sequence of *aci6.*

Nucleotides and amino acids are numbered on the left and right sides. The accession number for the nucleotide sequence is AK104932. The nucleotide sequence contains an ORF encoding a protein of 408 amino acids that was termed OsSBF1. 5'-UTR and 3'-UTR are 87 nucleotides and 303 nucleotides long, respectively. Nucleotides written in bold represent the 388 nt-long *aci6* cDNA initially identified through subtractive hybridisation.

```
1     AAC TCC ACC AGC AGC AGT CAC GCA CGT CTC TCT CTC TCG CCC CGC   45

46    GTC CTC CAC ATG GCG GCG TCC ACC ACC TGC CCT GCT CGC TCC ATG   90
1                                                           M     1

91    GCG TCC GTC TCC CGA GCC CTC CGC CCG CGG CCG CAC GCC GCT ATC   135
2      A   S   V   S   R   A   L   R   P   R   P   H   A   A   I    16

136   GCC TCC GCC GCC GTC CGC ACG GCT GCT CGT CTC GGG GGC GGA TTG   180
17     A   S   A   A   V   R   T   A   A   R   L   G   G   G   L    31

181   GGG ATC GTT TGT TCG ATG CCA AGC TAT GGT AGG AAG GAG AAG GAA   225
32     G   I   V   C   S   M   P   S   Y   G   R   K   E   K   E    46

226   GAA TGG GGA TTG ACC ATT GCG TCC GCA CCG GCG ACC ACT GCT GCT   270
47     E   W   G   L   T   I   A   S   A   P   A   T   T   A   A    61

271   CCG GCT CTG AGA AGC TGT CAA CTA TTG TGC AAG GCT GAA GCT AGC   315
62     P   A   L   R   S   C   Q   L   L   C   K   A   E   A   S    76

316   ATA TCC AGT AAT CTG CCA GAG AGC ATT CCT AGT GAA GCA AAC CAG   360
77     I   S   S   N   L   P   E   S   I   P   S   E   A   N   Q    91

361   TAC GAG AAA ATA GTT GAG CTG CTT ACC ACT CTT TTC CCT GTC TGG   405
92     Y   E   K   I   V   E   L   L   T   T   L   F   P   V   W   106

406   GTC ATA TTA GGT ACC ATT ATT GGC ATC TAC AAG CCA TCG ATG GTT   450
107    V   I   L   G   T   I   I   G   I   Y   K   P   S   M   V   121

451   ACC TGG TTG GAG ACT GAT CTT TTC ACT GTG GGC CTA GGA TTC CTA   495
122    T   W   L   E   T   D   L   F   T   V   G   L   G   F   L   136

496   ATG CTA TCA ATG GGA CTA ACA TTG ACC TTC GAA GAT TTC AGG AGA   540
137    M   L   S   M   G   L   T   L   T   F   E   D   F   R   R   151

541   TGC ATG AGG AAT CCA TGG ACT GTG GGT GTG GGA TTT CTT GCG CAG   585
152    C   M   R   N   P   W   T   V   G   V   G   F   L   A   Q   166

586   TAT TTG ATC AAA CCT ATG CTG GGA TTT GCT ATT GCC ATG ACC TTG   630
167    Y   L   I   K   P   M   L   G   F   A   I   A   M   T   L   181

631   AAG TTA TCT GCT CCT CTT GCA ACT GGT CTT ATT TTA GTG TCA TGT   675
182    K   L   S   A   P   L   A   T   G   L   I   L   V   S   C   196

676   TGC CCT GGT GGA CAA GCA TCA AAT GTT GCT ACT TAT ATA TCC AAA   720
197    C   P   G   G   Q   A   S   N   V   A   T   Y   I   S   K   211

721   GGA AAT GTC GCA CTT TCA GTT CTT ATG ACA ACT TGT TCG ACT ATT   765
212    G   N   V   A   L   S   V   L   M   T   T   C   S   T   I   226
```

```
766   GGT GCT ATA GTG ATG ACA CCA CTC CTT ACT AAA CTC CTA GCT GGT   810
227    G   A   I   V   M   T   P   L   L   T   K   L   L   A   G    241

811   CAA CTG GTT CCT GTC GAT GCT GCA GGA TTG GCC ATC AGT ACT TTT   855
242    Q   L   V   P   V   D   A   A   G   L   A   I   S   T   F    256

856   CAG GTT GTT TTA CTG CCA ACT ATT GTC GGA GTC TTG GCG CAT GAG   900
257    Q   V   V   L   L   P   T   I   V   G   V   L   A   H   E    271

901   TAT TTT CCT AAG TTT ACT GAG CGC ATT ATA TCC ATA ACA CCA TTG   945
272    Y   F   P   K   F   T   E   R   I   I   S   I   T   P   L    286

946   ATT GGG GTT CTC CTC ACC ACT TTG CTT TGT GCT AGT CCT ATC GGA   990
287    I   G   V   L   L   T   T   L   L   C   A   S   P   I   G    301

991   CAA GTC TCA GAG GTG TTG AAA GCT CAA GGT GGT CAA CTT ATA ATT  1035
302    Q   V   S   E   V   L   K   A   Q   G   G   Q   L   I   I    316

1036  CCC GTT GCT CTG CTG CAT GTT GCT GCC TTT GCA CTT GGG TAT TGG  1080
317    P   V   A   L   L   H   V   A   A   F   A   L   G   Y   W    331

1081  TTA TCA AAA GTT TCC TCT TTT GGG GAA TCA ACT TCT AGG ACT ATC  1125
332    L   S   K   V   S   S   F   G   E   S   T   S   R   T   I    346

1126  TCT ATT GAA TGC GGG ATG CAG AGT TCT GCA CTT GGA TTT TTA CTT  1170
347    S   I   E   C   G   M   Q   S   S   A   L   G   F   L   L    361

1171  GCC CAA AAG CAC TTC ACG AAT CCA CTC GTA GCT GTT CCA TCT GCT  1215
362    A   Q   K   H   F   T   N   P   L   V   A   V   P   S   A    376

1216  GTC AGT GTT GTA TGC ATG GCG CTT GGA GGG AGT GCT CTT GCA GTT  1260
377    V   S   V   V   C   M   A   L   G   G   S   A   L   A   V    391

1261  TTT TGG AGG AAC AGA GGG CTT CCA GCA AAT GAC AAA GAC GAT TTC  1305
392    F   W   R   N   R   G   L   P   A   N   D   K   D   D   F    406

1306  AAG GAA TGA AAC ACC AAC ACC CTC CAG TTT CTA GTC ATT ACC TAG  1350
407    K   E   *                                                   408

1351  TGT TGT TTT TTA GTT CAG TGG AGT TAT CAC AGC ATT TTT CTT GTT  1395
1396  ACC CAT ATT TTA GCA AGT TGA TTA TCA GTA GGA CTT GCC TAC TTG  1440
1441  GTA GGT CTG TTG TAT TGC ACT CTT ATC TTC CAA ATA AGC TGC AGG  1485
1486  TGC TTC TCT GCA AAG CAC TCA ATT TAT AGT CCG TTG CCA AGT GAA  1530
1531  TGC ATT GTA ATA TTA TGC GCG GTG AGT AAA TAG ATT TCC AAG AAT  1575
1576  TGC TAT TCC AAT CTA TTG AAA GGT CAA TAA GCT TTG TAT          1614
```

7.7. Nucleotide and predicted amino acid sequence of *aci7*.

Nucleotides and amino acids are numbered on the left and right sides. The accession number for the nucleotide sequence is AF050200. The nucleotide sequence contains an ORF encoding a protein of 199 amino acids that was termed OsARD1. 5'-UTR and 3'-UTR are 69 nucleotides and 206 nucleotides long, respectively. Nucleotides written in bold represent the 192 nt-long *aci7* cDNA initially identified through subtractive hybridisation.

```
3      ACG AAC AAA AAA CAG AAT CCA TCG CCA TAA TCG AAG GTT CGC TCT   47

48     TGC TTC CAC CCC GCA ATC CAC ATG GAG AAC GAA TTC CAG GAT GGT   92
1                                  M   E   N   E   F   Q   D   G    8

93     AAG ACG GAG GTG ATA GAA GCA TGG TAC ATG GAT GAT AGC GAA GAG   137
9       K   T   E   V   I   E   A   W   Y   M   D   D   S   E   E    23

138    GAC CAG AGG CTT CCT CAT CAC CGC GAA CCC AAA GAA TTC ATT CCT   182
24      D   Q   R   L   P   H   H   R   E   P   K   E   F   I   P    38

183    GTT GAT AAG CTT ACA GAA CTA GGA GTA ATC AGC TGG CGC CTA AAT   227
39      V   D   K   L   T   E   L   G   V   I   S   W   R   L   N    53

228    CCT GAT AAC TGG GAG AAT TGC GAG AAC CTG AAG AGA ATC CGC GAA   272
54      P   D   N   W   E   N   C   E   N   L   K   R   I   R   E    68

273    GCC AGA GGT TAC TCT TAT GTG GAC ATT TGT GAT GTG TGC CCA GAG   317
69      A   R   G   Y   S   Y   V   D   I   C   D   V   C   P   E    83

318    AAG CTG CCA AAT TAT GAA ACT AAG ATC AAG AGT TTC TTT GAA GAA   362
84      K   L   P   N   Y   E   T   K   I   K   S   F   F   E   E    98

363    CAC CTG CAT ACC GAT GAA GAA ATA CGC TAT TGT CTT GAA GGG AGT   407
99      H   L   H   T   D   E   E   I   R   Y   C   L   E   G   S   113

408    GGA TAC TTT GAT GTG AGA GAC CAA AAT GAT CAG TGG ATT CGT ATA   452
114     G   Y   F   D   V   R   D   Q   N   D   Q   W   I   R   I   128

453    GCA CTG AAG AAA GGA GGC ATG ATT GTT CTG CCT GCA GGG ATG TAC   497
129     A   L   K   K   G   G   M   I   V   L   P   A   G   M   Y   143

498    CAC CGC TTT ACG TTG GAC ACC GAC AAC TAT ATC AAG GCA ATG CGA   542
144     H   R   F   T   L   D   T   D   N   Y   I   K   A   M   R   158

543    CTG TTT GTT GGC GAT CCT GTT TGG ACA CCC TAC AAC CGT CCC CAT   587
159     L   F   V   G   D   P   V   W   T   P   Y   N   R   P   H   173

588    GAC CAT CTT CCT GCA AGA AAG GAG TTT TTG GCT AAA CTT CTC AAG   632
174     D   H   L   P   A   R   K   E   F   L   A   K   L   L   K   188

633    TCA GAA GGT GAA AAT CAA GCA GTT GAA GGC TTC TGA GGG TTT TGT   677
189     S   E   G   E   N   Q   A   V   E   G   F   *               199

678    TGG GCT CCT GCA CTG CGG TTC TAT ATT CAA CCT GAA TAA GAT GTG   722
723    CTA TAG CAA TGT AAA TTT AGC ACA GTG GCT ATG GTC GCC ACT CAC   767
768    CAA CTT GAA GTG AAA GAT TTA ATG ATT TTT GTT AAT TCT TAT GTA   812
813    TCA ATC GGC ATA TAG CAT TTC CGA AAT GTG TTT TCA ATA AAC AGG   857
858    AGT CAT GAA GCT GAA                                         872
```

7.8. Nucleotide and predicted amino acid sequence of *aci8*.

Nucleotides and amino acids are numbered on the left and right sides. The accession number for the nucleotide sequence is AK099686. The nucleotide sequence contains an ORF encoding a protein of 845 amino acids that was termed OsACI8. 5'-UTR and 3'-UTR are 252 nucleotides and 323 nucleotides long, respectively. Nucleotides written in bold font represent the 437 nt-long *aci8* cDNA initially identified through subtractive hybridisation, which covers

178 nucleotides of the sequence encoding the C-terminus of the protein and 259 nucleotides of the 3'-untranslated region.

```
1      GGG CCG CAT CGC CAC CGC CAC TCT CTC CTC TCC TCC TCT CTC TCT   45
46     CTC TCT CGC ACC ACC GCT CTC TTC CGC CGC TGC GGC TCA CGG CTA   90
91     CGC AGC TCT CTT CCC CTC CTC CTC GGC TCC GCT CTC TTC GAT CGA   135
136    TCT AGG GTT TGG TCT TCT GTT GGG GGA TTG TTG TTG CTC TTC CGC   180
181    GCG ATC GAT CGA CGC CGC GTC CTG AGG GTT TGA GGG GTT TCC GCC   225

226    CTC CCG CCG CAC GCC CGC ACC CCC GCG ATG TCC GGC CGG AGC TCG   270
1                                          M   S   G   R   S   S    6

271    CCG ATG TAC GAG GGG CTC GCG TCG CGT CCC GAC GAG TGG GAC GTC   315
7       P   M   Y   E   G   L   A   S   R   P   D   E   W   D   V    21

316    GTC CTC AAG GTG AAG TAT GGT GAA ACT CTT AAG AGG TTC GGT GGG   360
22      V   L   K   V   K   Y   G   E   T   L   K   R   F   G   G    36

361    TAT GTG CAA GGA CCA CAA TTC AGC CTG AAC TTA TCC GCT CTC CGG   405
37      Y   V   Q   G   P   Q   F   S   L   N   L   S   A   L   R    51

406    TCC AAG ATT GCA TCT GCT TTT AAG TTT GGT TCG GAT GTC GAC TTC   450
52      S   K   I   A   S   A   F   K   F   G   S   D   V   D   F    66

451    ATT CTG ACT TAC ACT GAT GAG GAT GGG GAT ATT GTC ATG CTG GAT   495
67      I   L   T   Y   T   D   E   D   G   D   I   V   M   L   D    81

496    GAT GAT GAT GAT CTG CAT GAT GCT GCT ATT CAT CAG AAA CTG AAC   540
82      D   D   D   D   L   H   D   A   A   I   H   Q   K   L   N    96

541    CCC CTC AGG ATT AAT GTT CAG TTA AAC AAC AGC CAC ACT GCA GCA   585
97      P   L   R   I   N   V   Q   L   N   N   S   H   T   A   A   111

586    CCT CAG GCC AAA CAG CAG GAT TCA GAT AAT ATA CCT CTC AGG TCC   630
112     P   Q   A   K   Q   Q   D   S   D   N   I   P   L   R   S   126

631    ACC ACC ACT GAA GAC CCA CTA GCT CAT ATT AAA TCA GTT ATC GAT   675
127     T   T   T   E   D   P   L   A   H   I   K   S   V   I   D   141

676    GAG GTT TTG AAG CCG ATA TCT ATG AAG TCC ATC CAG GAG CCA GTT   720
142     E   V   L   K   P   I   S   M   K   S   I   Q   E   P   V   156

721    CCT GAG ACA CTT GCG AAG CTG TCC CAT GAA GTA CTT GAA GCC GCA   765
157     P   E   T   L   A   K   L   S   H   E   V   L   E   A   A   171

766    TCA CCA CAA TTA GCT GAG CTA ATA AAA CCT TTT GTT AAA CTG GTT   810
172     S   P   Q   L   A   E   L   I   K   P   F   V   K   L   V   186

811    ACA CCA AGC AAC AAC AAC CCA TCT AAT GGG CAT GCT GAT GGT TCC   855
187     T   P   S   N   N   N   P   S   N   G   H   A   D   G   S   201

856    TGC AGC TCC TCA ACT GGT TTG CCC CAA ACA CAG GTT GAT CCC AAA   900
202     C   S   S   S   T   G   L   P   Q   T   Q   V   D   P   K   216

901    ACT AAT GAC GAG CCC AAA ATA GAC ACA AGT TTG GGG TCG CAA CCC   945
317     T   N   D   E   P   K   I   D   T   S   L   G   S   Q   P   231

946    TTG GAC ACG CAG AAC TCC AAA TCA TCT GGT GCT AGA GGT CTT AAG   990
232     L   D   T   Q   N   S   K   S   S   G   A   R   G   L   K   246
```

```
991   ACT CTG TCA GTT GAG GCT CCT GCT ACA TCG GGT GTT AAA TCT TCT   1035
247    T   L   S   V   E   A   P   A   T   S   G   V   K   S   S    261

1036  CAA GGT CAA CAG GCA TCA TTA TAC CCT TCC ATT GAG GAG TTG CTG   1080
262    Q   G   Q   Q   A   S   L   Y   P   S   I   E   E   L   L    276

1081  TTC TCC CCC TTT TTA CCG AAC TCA GGT GAT GAC AAA TCT GCC AGC   1125
277    F   S   P   F   L   P   N   S   G   D   D   K   S   A   S    291

1126  AAG GGA ATT AGT GAT GCT CAA AGC AAG GGA AAA TCT GTT ATG ACC   1170
292    K   G   I   S   D   A   Q   S   K   G   K   S   V   M   T    306

1171  TCT GCT ACA CCA CCT ACC CCT CCT GCT GCT CCT GCT TTC CGT CCA   1215
307    S   A   T   P   P   T   P   P   A   A   P   A   F   R   P    321

1216  GCT CCT CCA ATT CCA TCT CTG AAT GAT TGG TCT CAG CCA CCA GCA   1260
322    A   P   P   I   P   S   L   N   D   W   S   Q   P   P   A    336

1261  CGT GGA TCG ACA TTT TAC CCA TCT ATT TGG CAG TCT GAA GCT GAT   1305
337    R   G   S   T   F   Y   P   S   I   W   Q   S   E   A   D    351

1306  CCA AAA GCC AAT AGT GAT TCC AGA TGG CGT GTT CCA TTG TGC AGA   1350
352    P   K   A   N   S   D   S   R   W   R   V   P   L   C   R    366

1351  GCT GGC CAT CCA TTC CAA CCC CAT GCT CCC CTG AGC CGT CCA CCC   1395
367    A   G   H   P   F   Q   P   H   A   P   L   S   R   P   P    381

1396  CCA CCA ATG CCT GCA CCA ATG AGC TAT GGA CCT TCT CCA CAT TTT   1440
382    P   P   M   P   A   P   M   S   Y   G   P   S   P   H   F    396

1441  CCT TAC CCT GGC CGC CTC TTG TCC TCT GGC CAT CTG CAT GGA GAC   1485
397    P   Y   P   G   R   L   L   S   S   G   H   L   H   G   D    411

1486  CTT GGT AAT AAC ATT GAG AAC TCA CCA GCA CGC ACA TTC CAT AGA   1530
412    L   G   N   N   I   E   N   S   P   A   R   T   F   H   R    426

1531  TGG ATT CAG TGT GAT GGT TGT GGA GTG CAA CCA ATT GTT GGG CCT   1575
427    W   I   Q   C   D   G   C   G   V   Q   P   I   V   G   P    441

1576  CGA TAC AAG TCT AAA ACA AAA GAA GAT TAT GAT TTG TGT GAT GCC   1620
442    R   Y   K   S   K   T   K   E   D   Y   D   L   C   D   A    456

1621  TGC TTT CAT CGC ATG GGC AAT GAG GTC GAG TAC ACC AGG ATT GAC   1665
457    C   F   H   R   M   G   N   E   V   E   Y   T   R   I   D    471

1666  AAG CCA CTC TTA CCC CAG AGA TTA CTG AGA GAC CCT ACA TTG TGT   1710
472    K   P   L   L   P   Q   R   L   L   R   D   P   T   L   C    486

1711  CGC AAG ATC CAT TCA CGG GCT GCG ATG AAG TCA AAG CGG GAG AAA   1755
487    R   K   I   H   S   R   A   A   M   K   S   K   R   E   K    501

1756  CTT GAA AGT CGC TTC ATT TTG GAT GTA ACT GTC CTG GAT GGA ACA   1800
502    L   E   S   R   F   I   L   D   V   T   V   L   D   G   T    516

1801  TTG ATG GCA CCT TCA ACT CCG TTT ACT AAG ATT TGG CGT ATG CAT   1845
517    L   M   A   P   S   T   P   F   T   K   I   W   R   M   H    531

1846  AAC AAT GGG TCT ATC ATG TGG CCC TTG GGC ACA CAG CTT ATA TGG   1890
532    N   N   G   S   I   M   W   P   L   G   T   Q   L   I   W    546

1891  GTT GGT GGC GAC CAG TTT GCA CTG CAG ACC TAT GTT CCA TTA GAG   1935
547    V   G   G   D   Q   F   A   L   Q   T   Y   V   P   L   E    561
```

```
1936  ATT CCA GTG GAC GGG TTT CCT GTT GAT CAG GAG ATT GAT GTT GCT   1980
562    I   P   V   D   G   F   P   V   D   Q   E   I   D   V   A    576

1981  GTT GAT TTT GTG GCA CCT GCA AGG CCT GGG AGG TAT ATA TCT TAC   2025
577    V   D   F   V   A   P   A   R   P   G   R   Y   I   S   Y    591

2026  TGG AGG TTA GCA TCA CCT TCT GGC CAG AAA TTT GGT CAG CGT GTT   2070
592    W   R   L   A   S   P   S   G   Q   K   F   G   Q   R   V    606

2071  TGG GTT CAC ATC CAG GTG GAG GAT CCT TCT TTT GTC AGT AAC AAC   2115
607    W   V   H   I   Q   V   E   D   P   S   F   V   S   N   N    621

2116  AGG ACT GCC GCT ATA AAC TTG AAT TTG CCC CCA GAA AGC AAT ATC   2160
622    R   T   A   A   I   N   L   N   L   P   P   E   S   N   I    636

2161  ACA AAC ACA AGT AAT TTG ATT GAT GTC AAT ATT GAG CCT GTG GAT   2205
637    T   N   T   S   N   L   I   D   V   N   I   E   P   V   D    651

2206  CAA GTC TTC AAC CAA CAT GTC AAT AGC ACA AAC AAG GAG TTA CTT   2250
652    Q   V   F   N   Q   H   V   N   S   T   N   K   E   L   L    666

2251  GAA CAT TTG ATA CAC CAC CAG ATT GAC GAG CCC AAG AAT CCT GAG   2295
667    E   H   L   I   H   H   Q   I   D   E   P   K   N   P   E    681

2296  CCT GCT CCA TTA CCT GTG CCC ATT GTT TCT TCC ACA ACA TCT CTT   2340
682    P   A   P   L   P   V   P   I   V   S   S   T   T   S   L    696

2341  CAC CCC ATC ATT GAT GTT GAT GTT CCC TCC AGT TCA ACT GCT GCT   2385
697    H   P   I   I   D   V   D   V   P   S   S   S   T   A   A    711

2386  GCT TTT GTG CCT GTC TTT GAT GAG CCT GCG CCT GAA CCT GCT GTG   2430
712    A   F   V   P   V   F   D   E   P   A   P   E   P   A   V    726

2431  ACT CCT GTG CCT CCA ACT GTT AAT GTG CCT GCT GGT AAT GCA CCT   2475
727    T   P   V   P   P   T   V   N   V   P   A   G   N   A   P    741

2476  GCG TCT GTT GGT GCA TCA TCA TCT GAT CAT CAT GGC ATT GAC AAT   2520
742    A   S   V   G   A   S   S   S   D   H   H   G   I   D   N    756

2521  CTC ACA GAA GAG AAA CTG CTG AAG GAA CTT GAG GAA ATG GGT TTT   2565
757    L   T   E   E   K   L   L   K   E   L   E   E   M   G   F    771

2566  AGG CAG GTC GAT CTG AAC AAG GAG ATA CTC AGG CAG AAC AAG TAC   2610
772    R   Q   V   D   L   N   K   E   I   L   R   Q   N   K   Y    786

2611  AAC CTG GAG CAG TCT GTC GAT GAT CTC TGT GGC GTC AGC GAA TGG   2655
787    N   L   E   Q   S   V   D   D   L   C   G   V   S   E   W    801

2656  GAC CCT CTC CTG GAG GAG TTG CAG GAA ATG GGC TTT GAG GAC ACT   2700
802    D   P   L   L   E   E   L   Q   E   M   G   F   E   D   T    816

2701  GAG ATA AAC AAG GAG ATG CTC GAG AAG AAC GGA GGA AGC ATC AAG   2745
817    E   I   N   K   E   M   L   E   K   N   G   G   S   I   K    831

2746  CGG GCT GTG ATG GAC CTC ATC GCT AGG GAG AAG AAA GAC CAG TGA   2790
832    R   A   V   M   D   L   I   A   R   E   K   K   D   Q   *    845

2791  AGA TCG TGT GCT CTT GAG CCA TCC CTA TCT ATA ACC TAA CTA TGT   2835
2836  GTG TAT ATG CGT AAA TAA TGT GAC GAG GTG TAA GGC TAG CGC CGG   2880
2881  CCG CCG GGG CTG CTG CTA CAG TCT CAG GGC CTG CTT GCT TAT GAA   2925
2926  CTG TGT GTG GTG TTG TGC GAC TGG TAT ATT TGT CGC GGA GAT ATG   2970
2971  TGT TAA GTG CGC GTG CGC GCC TCT TAA AAA GCG GTT ACC TTG CCA   3015
3016  GGT AAA CTG CGT GTA ATT ACT ATG GGC TTA GCT GCT CTA TGC CTC   3060
```

```
3061  TTA TCT ACT GCT GTG ACT GGA ACT TGA TGG ATT AAT AAG ATC TAT   3105
3106  GTT GCG                                                     3111
```

7.9. Nucleotide and predicted amino acid sequence of *aci9*.

Nucleotides and amino acids are numbered on the left and right sides. The accession number for the nucleotide sequence is AK120851. The nucleotide sequence contains an ORF encoding a protein of 585 amino acids. 5'-UTR and 3'-UTR are 249 nucleotides and 624 nucleotides long, respectively. Nucleotides written in bold correspond to the 380 nt-long *aci9* cDNA initially identified through subtractive hybridisation, which covers 154 nucleotides of the sequence encoding the C-terminus of the protein and 226 nucleotides of the 3'-untranslated region.

```
1     GGG CGG AAC AGG GAC AAA GCC GTA AAT TCC GCC CCG TTT CGC TGT   45
46    GCC GTG CCG TCC CTT CCC CTC CCG TGC GTC TCG GCC TCG CCT AGT   90
91    GTT TGA GGG GTC CAA AGT CTC CGT GTC GTC TCC ACG ACT CCA CTT   135
136   GCT CTC CTC TCG CTC TCG CTC TCC CTC TTC CTC CCA CCT CCA GAT   180
181   CGA TGC GTC GGC GGT AGA TCT CGC TCG CCT CCT CCC CCT CCT GCT   225
226   CGA CGG CGA GGA GAG CCA CTA GCC ATG GGG AAC TGC TGC TCC GAC   270
1                                    M   G   N   C   C   S   D    8

271   GAG ATG GGC GGC GGC GGC GGC CAC GCG GGC CGC CAC TCC GTC GGC   315
9      E   M   G   G   G   G   G   H   A   G   R   H   S   V   G    23

316   CCC GCG GCG GCC GCG GCT GCG GCG GCG GCG GAG GCC GCG TCC GCC   360
24     P   A   A   A   A   A   A   A   A   A   E   A   A   S   A    38

361   GCG GCC GAC CGC TTC CTC CGC TCC CGC GGC GCC GGC GCG TCC ACG   405
39     A   A   D   R   F   L   R   S   R   G   A   G   A   S   T    53

406   CAG GTC GAG TTA TCT CTC TCT GCA TCA AAT TTG GGC GAC CAA GAA   450
54     Q   V   E   L   S   L   S   A   S   N   L   G   D   Q   E    68

451   TTC TTT ACC AAG AGC AAT CCC ATG GTC ATT GTA TAT TCT AAA AGC   495
69     F   F   T   K   S   N   P   M   V   I   V   Y   S   K   S    83

496   AAA GAA GGA GCA CTT GAA GAA CTT GGG CGT ACT GAA GTA ATA TTG   540
84     K   E   G   A   L   E   E   L   G   R   T   E   V   I   L    98

541   AAT TCT TTG AAC CCA TCT TGG AAT GCA AGA ATC AAC GTG CAC TAC   585
99     N   S   L   N   P   S   W   N   A   R   I   N   V   H   Y   113

586   CAG TTT GAG GTT CTT CAA CCA ATT GTG TTT CAG GTA TAT GAC ATT   630
114    Q   F   E   V   L   Q   P   I   V   F   Q   V   Y   D   I   128

631   GAT CCA CAG TTT CAT GAT GTC AAT GAA AAG ATG CTT AAA CTG GAA   675
129    D   P   Q   F   H   D   V   N   E   K   M   L   K   L   E   143

676   GAG CAA CAA TTT CTT GGG GAG GCT GTC TGT CTT TTG TCT GAG GTT   720
144    E   Q   Q   F   L   G   E   A   V   C   L   L   S   E   V   158

721   ATC ACT AAA CAA AAC AGA CTG TTG ACT CTA AAG CTT GGC GTT TCC   765
159    I   T   K   Q   N   R   L   L   T   L   K   L   G   V   S   173
```

```
766   GAA CAT AAC CTA CCA AAT CCT AGT AAA TTT GGT GAA CTA AAT GTT   810
174    E   H   N   L   P   N   P   S   K   F   G   E   L   N   V   188

811   CAG GCA GAA GAA AGT GCT GGT TCA AAA GCA ATA ATG GAG ATG GTA   855
189    Q   A   E   E   S   A   G   S   K   A   I   M   E   M   V   203

856   TTC CGC TGT TCA GAT CTT GAA ATC AAG GAC CTT CTC TCA AAA AGT   900
204    F   R   C   S   D   L   E   I   K   D   L   L   S   K   S   218

901   GAT CCC TTT TTA CTA ATA TCT AGA ATA TCA GAG AGT GGA GTG CCT   945
219    D   P   F   L   L   I   S   R   I   S   E   S   G   V   P   233

946   GTT CCA ATT TGT AAG ACG GAA GTA AGG AAG AAC GAC CTC AAT CCC   990
234    V   P   I   C   K   T   E   V   R   K   N   D   L   N   P   248

991   AAG TGG AAG CCA GTG ATC TTG AAT CTC CAA CAG ATT GGA AGT AAG   1035
249    K   W   K   P   V   I   L   N   L   Q   Q   I   G   S   K   263

1036  GAG AAC CCT TTA ATC ATA GAG TGC TTC AAC TTC AGT AGC AAC GGC   1080
264    E   N   P   L   I   I   E   C   F   N   F   S   S   N   G   278

1081  AAA CAT GAC CTA ATA GGC AAG ATA GTA AAA TCG GTC GCA GAA TTG   1125
279    K   H   D   L   I   G   K   I   V   K   S   V   A   E   L   293

1126  GAA AAG ATG TAT CAT AGT CAG GAT GGT GAA AAT TTC TTT GTT CCT   1170
294    E   K   M   Y   H   S   Q   D   G   E   N   F   F   V   P   308

1171  GCC AGC ACT GCT CAT GAT AGT CAC AGT AAG GAG GTA CTA AAG AGT   1215
309    A   S   T   A   H   D   S   H   S   K   E   V   L   K   S   323

1216  CAA GTG TAT GTG GAG AAA TAT CTT GAG AAC AAC AGA CAG ACT TTT   1260
324    Q   V   Y   V   E   K   Y   L   E   N   N   R   Q   T   F   338

1261  CTA GAT TAT ATT TCT GCT GGG TGC CAA TTG AAT TTT ATG GTA GCC   1305
339    L   D   Y   I   S   A   G   C   Q   L   N   F   M   V   A   353

1306  GTA GAC TTC ACA GCT TCA AAT GGA AAT CCA CGG CTT CCA GAT TCC   1350
354    V   D   F   T   A   S   N   G   N   P   R   L   P   D   S   368

1351  TTG CAT TAT ATT GAT CCC ACT GGT CGG CCA AAT GCA TAT CAG AGA   1395
369    L   H   Y   I   D   P   T   G   R   P   N   A   Y   Q   R   383

1396  GCA ATA CTG GAA GTA GGA GAT GTA CTA CAG TAC TAT GAC CCA GCT   1440
384    A   I   L   E   V   G   D   V   L   Q   Y   Y   D   P   A   398

1441  AAG CGG TTT CCC TCA TGG GGC TTT GGT GCT AGA CCT ATT GAT GGT   1485
399    K   R   F   P   S   W   G   F   G   A   R   P   I   D   G   413

1486  CCT GTT TCC CAC TGT TTC AAC CTG AAT GGT AGC ACC TAT CAA CCT   1530
414    P   V   S   H   C   F   N   L   N   G   S   T   Y   Q   P   428

1531  GAG GTT GAG GGA ATA CAA GGG ATT ATG TCA GCT TAT ATC AGT GCG   1575
429    E   V   E   G   I   Q   G   I   M   S   A   Y   I   S   A   443

1576  CTT CGT AAT GTC TCA TTG GCT GGG CCC ACC CTA TTT GGT CCA GTA   1620
444    L   R   N   V   S   L   A   G   P   T   L   F   G   P   V   458

1621  GTT AGC ACT GCT ACG GCA ATA GCA AAC CAA TCA CTT GCC AAC AAC   1665
459    V   S   T   A   T   A   I   A   N   Q   S   L   A   N   N   473

1666  CAG CAG AAA TAC TTT GTT CTG TTA ATA GTC ACG GAT GGT GTG GTG   1710
474    Q   Q   K   Y   F   V   L   L   I   V   T   D   G   V   V   488
```

```
1711  ACT GAT TTC CAA GAG ACT ATC GAT GCA ATC ATA AAG GCA TCT GAT   1755
489    T   D   F   Q   E   T   I   D   A   I   I   K   A   S   D    503

1756  TTT CCT TTG TCC ATT CTT GTT GTT GGA GTT GGT GGA GCG GAC TTC   1800
504    F   P   L   S   I   L   V   V   G   V   G   G   A   D   F    518

1801  AAG GAA ATG GAG TTT CTA GAT CCA AAT AAA GGA GAG AGA CTA GAA   1845
519    K   E   M   E   F   L   D   P   N   K   G   E   R   L   E    533

1846  AGC TCA ACA GGA AGA GTG GCA TCA AGG GAT ATG ATA CAG TTC GCC   1890
534    S   S   T   G   R   V   A   S   R   D   M   I   Q   F   A    548

1891  CCA ATG AAG GAT GCC CAT GGC AGT GGG ATT TCG ACA GTT CAG TCA   1935
549    P   M   K   D   A   H   G   S   G   I   S   T   V   Q   S    563

1936  CTT CTT GCT GAA ATA CCA GGG CAG TTC ATG ACC TAC ATG AGA ACA   1980
564    L   L   A   E   I   P   G   Q   F   M   T   Y   M   R   T    578

1981  AGA GAA ATT CAA GCA ATC AGT TAA TAT ATG GTG CCG TCT ATT TGT   2025
579    R   E   I   Q   A   I   S   *                               585

2026  GAT TCT TAG TTG ATA GAA GAT GCA CAT TCT AAT GGT CTT GTT GGT   2070
2071  ATG GTT TTG GCT GTT GGG CCA CAT CAT CAT GCA AAT TTT AAA GCC   2115
2116  ATT GAT GTG TGA AAA GGT GGA AAG ATG GAT AGT CTG GAC ATG TTA   2160
2161  CAA GTA AGA AAT ATG GAT CTG CTG GAA ATT TGT AGC CAA GGT CTA   2205
2206  ATA TCA GTG GCG CAT TGT CCG TAC TTG TCT TGT TGC TAC TCA TGT   2250
2251  TGA CAA TGT GGT GCA GGG CAA TTG AAT TGA GGC ATG AAT TGC TTG   2295
2296  GCA CTG CAG ATT GGA AAC TGT TGT CTC TGA AGA AAC ATT TGA ATT   2340
2341  GTG TAT GAT TCG TGT AAA GGT CAA AGG TTC GTA GTT TCG AAC TTG   2385
2386  CTG CTC AAA TCA AGC GAG TGG TAG TTT TTT TTT CTT CTA TAT TCT   2430
2431  GGT TAT GGT GCT GAG TTT CCT CAG ATT AGC GGT TTC TAT CTG GGA   2475
2476  TTC GTC TTC TTC ATA CCT GCG TGT AAG ATC ATG TCT TGA AAT TAA   2520
2521  GGG TTG AAC CCC ATG TTG ACT CTT TGT GCG TAC CTG GTA AAA AAC   2565
2566  ATT TTT GTC AGT AAC TCT ACC ATG TTC TGG TGT TAT ATT GAT GTT   2610
2611  ACA TAT AGT TCT GTT                                         2625
```

7.10. Nucleotide and predicted amino acid sequence of *aci10*.

Nucleotides and amino acids are numbered on the left and right sides. The accession number for the nucleotide sequence is AK067183. A putative start codon represented in a box delimits an ORF encoding a protein of 575 amino acids. However, the limited 5'-UTR sequence does not allow to predict the translation start with high confidence. The 3'-UTR extends on 1475 nucleotides. Nucleotides written in bold correspond to the 214 nt-long sequence of the *aci10* cDNA initially identified through subtractive hybridisation.

```
1     CTC CTC CGC TTC GCA GAC CAG CCA GCC ATG CCT CCC CTC ACG AGC   45
1      L   L   R   F   A   D   Q   P   A   M   P   P   L   T   S    15

46    GCC CTC CTC TCC CGC TCC TCC TCT ACC CGC ATC CCC GCC GCG GCG   90
16     A   L   L   S   R   S   S   S   T   R   I   P   A   A   A    30

91    GCG GCG GCG GCG GCG ATC TCG AAT CCC GCG GGC GCC GCC GCG TCG   135
31     A   A   A   A   A   I   S   N   P   A   G   A   A   A   S    45
```

```
136   TCG TCG TCG CCG TCA CCG CCG CCT CCG AGC TCT CGC CCC AGG CCG   180
46     S   S   S   P   S   P   P   P   P   S   S   R   P   R   P    60

181   GCG TCC CCC TTC ACG TCC GGC CTC GCT GGC CGC ATC TTC GGC GGC   225
61     A   S   P   F   T   S   G   L   A   G   R   I   F   G   G    75

226   CGC CGC GCC GCC GCG CGC TCC TCG TCG TCC GCC GCG GCC GTC TTC   270
76     R   R   A   A   A   R   S   S   S   S   A   A   A   V   F    90

271   GAG CGG CGC TTC GCC TCG GCG GCG GCG AAG AAC TCG TAC GAT GAA   315
91     E   R   R   F   A   S   A   A   A   K   N   S   Y   D   E   105

316   ATC CTG ACG GGC CTC GCG AAG CCG GGA GGC GGA GCG GAG TTC GGG   360
106    I   L   T   G   L   A   K   P   G   G   G   A   E   F   G   120

361   AAA TAC TAC AGC CTG CCC GCG CTA TCC GAT CCG CGG ATC GAG CGA   405
121    K   Y   Y   S   L   P   A   L   S   D   P   R   I   E   R   135

406   CTC CCT TAC TCG ATA AGG ATT CTT CTC GAG TCG GCA ATC AGA AAC   450
136    L   P   Y   S   I   R   I   L   L   E   S   A   I   R   N   150

451   TGT GAT GAG TTC CAG GTC ACC GGG AAG GAC GTT GAG AAA ATC CTG   495
151    C   D   E   F   Q   V   T   G   K   D   V   E   K   I   L   165

496   GAC TGG GAG AAC AGC GCA CCA AAG CAA GTC GAA ATC CCA TTT AAG   540
166    D   W   E   N   S   A   P   K   Q   V   E   I   P   F   K   180

541   CCA GCC CGT GTC CTC CTC CAG GAT TTC ACT GGT GTT CCA GCA GTG   585
181    P   A   R   V   L   L   Q   D   F   T   G   V   P   A   V   195

586   GTT GAT CTT GCG TGC ATG AGG GAT GCT ATG AGC AAA CTT GGC AGT   630
196    V   D   L   A   C   M   R   D   A   M   S   K   L   G   S   210

631   GAC CCA AAC AAA ATT AAT CCT CTG GTA CCT GTA GAT CTT GTT ATT   675
211    D   P   N   K   I   N   P   L   V   P   V   D   L   V   I   225

676   GAT CAT TCA GTA CAA GTT GAT GTG GCA AGA TCA GAA AAT GCT GTT   720
226    D   H   S   V   Q   V   D   V   A   R   S   E   N   A   V   240

721   CAG GCA AAT ATG GAG CTA GAG TTC CAT CGT AAC AAG GAG AGG TTT   765
241    Q   A   N   M   E   L   E   F   H   R   N   K   E   R   F   255

766   GGA TTT TTG AAA TGG GGT TCA ACT GCT TTC CGT AAC ATG CTT GTT   810
256    G   F   L   K   W   G   S   T   A   F   R   N   M   L   V   270

811   GTT CCA CCT GGA TCT GGA ATT GTG CAT CAG GTT AAC CTT GAA TAT   855
271    V   P   P   G   S   G   I   V   H   Q   V   N   L   E   Y   285

856   CTG GCC AGA GTT GTG TTT AAC AAT GGT GGG ATC CTT TAC CCT GAT   900
286    L   A   R   V   V   F   N   N   G   G   I   L   Y   P   D   300

901   AGT GTT GTT GGA ACA GAC TCC CAC ACA ACT ATG ATA GAT GGT CTT   945
301    S   V   V   G   T   D   S   H   T   T   M   I   D   G   L   315

946   GGT GTT GCT GGA TGG GGA GTT GGT GGT ATA GAG GCA GAA GCT ACA   990
316    G   V   A   G   W   G   V   G   G   I   E   A   E   A   T   330

991   ATG CTT GGC CAG CCA ATG AGC ATG GTA TTG CCA GGA GTT GTG GGC  1035
331    M   L   G   Q   P   M   S   M   V   L   P   G   V   V   G   345

1036  TTC AAG TTA ACA GGG AAG CTG AGG AAC GGT GTT ACT GCT ACA GAT  1080
346    F   K   L   T   G   K   L   R   N   G   V   T   A   T   D   360
```

```
1081  TTG GTT CTA ACA GTA ACT CAA ATG CTT AGG AAA CAT GGC GTT GTC   1125
361    L   V   L   T   V   T   Q   M   L   R   K   H   G   V   V    375

1126  GGA AAA TTT GTT GAA TTT TAC GGG GGA GGC ATG AGT GAA TTA TCA   1170
376    G   K   F   V   E   F   Y   G   G   G   M   S   E   L   S    390

1171  CTG GCT GAT AGG GCT ACA ATT GCA AAC ATG TCA CCA GAA TAT GGT   1215
391    L   A   D   R   A   T   I   A   N   M   S   P   E   Y   G    405

1216  GCA ACT ATG GGT TTC TTC CCA GTT GAT GGA AAG ACA TTG GAC TAC   1260
406    A   T   M   G   F   F   P   V   D   G   K   T   L   D   Y    420

1261  TTG AAG CTA ACT GGC AGA AGT GAT GAC ACT GTG GCC ATG ATA GAG   1305
421    L   K   L   T   G   R   S   D   D   T   V   A   M   I   E    435

1306  TCT TAC CTG CGT GCC AAT AAG ATG TTC GTC GAC TAC AAC CAG CCT   1350
436    S   Y   L   R   A   N   K   M   F   V   D   Y   N   Q   P    450

1351  GAA GCT GAA AGA GTG TAC TCA TCT TAT CTG GAA CTT AAC TTG GAG   1395
451    E   A   E   R   V   Y   S   S   Y   L   E   L   N   L   E    465

1396  GAG GTA GAG CCA TGC TTG TCT GGA CCA AAA CGG CCT CAT GAC CGA   1440
466    E   V   E   P   C   L   S   G   P   K   R   P   H   D   R    480

1441  GTG ACT TTG AAG AAC ATG AAA TCA GAT TGG CTG TCT TGC TTG GAT   1485
481    V   T   L   K   N   M   K   S   D   W   L   S   C   L   D    495

1486  AAT GAT GTA GGC TTC AAG GGT TTT GCT GTC CCC AAA GAA TCA CAG   1530
496    N   D   V   G   F   K   G   F   A   V   P   K   E   S   Q    510

1531  GGT AAA GTT GCT GAG TTC TCT TTC CAT GGG ACA CCA GCA AAG CTA   1575
511    G   K   V   A   E   F   S   F   H   G   T   P   A   K   L    525

1576  AAG CAT GGT GAT GTT GTA ATT GCT GCT ATA ACC AGT TGC ACC AAC   1620
526    K   H   G   D   V   V   I   A   A   I   T   S   C   T   N    540

1621  ACA TCA AAT CCT AAT GTA ATG CTG GGA GCT GCT TTA GTT GCC AAA   1665
541    T   S   N   P   N   V   M   L   G   A   A   L   V   A   K    555

1666  AAG GCT TGT GAA TTA GGC CTT GAG GTC AAG CCA TGG ATT AAG ACA   1710
556    K   A   C   E   L   G   L   E   V   K   P   W   I   K   T    570

1711  AGT CTT GCA CCT GGT TCT GGA GTT GTG AAG AAG TAC ATG GAC TAG   1755
571    S   L   A   P   G   S   G   V   V   K   K   Y   M   D   *    585

1756  AGT GGT CTG CAG AAA TAT CTA GAC CAG CTT GGC TTC CAT ATT GTA   1800
1801  GGC TAT GGT TGC ACA ACC TGC ATA GGA AAT TCT GGA GAA CTT GAT   1845
1846  GAA ACA GTA TCT GCT GCA ATT TCT GAC AAC GAT ATT GTC GCT GCT   1890
1891  GCC GTG TTA TCT GGA AAC AGA AAT TTT GAA GGG CGT GTG CAC GCA   1935
1936  TTA ACC AGA GCA AAT TAT CTT GCC TCT CCT CCA TTG GTT GTG GCC   1980
1981  TAT GCC CTT GCT GGC ACG GTC AAT ATT GAT TTT GAG AAA GAA CCA   2025
2026  ATT GGC ATC TCG AAA GAT GGG AAG GAG GTT TAC TTC AGG GAC ATC   2070
2071  TGG CCT TCC ACT GAA GAG ATT GCT GAG GTT GTT AAA TCA AGT GTG   2115
2116  CTA CCT GAC ATG TTT AAG AGC ACA TAC GAG GCA ATA ACC AAA GGA   2160
2161  AAT CCT ATG TGG AAT GAG CTG TCT GTA TCA GCA AGC ACT CTC TAC   2205
2206  CCA TGG GAC CCG ACA TCT ACT TAC ATC CAT GAG CCT CCT TAT TTC   2250
2251  AAG GAT ATG ACA ATG TCC CCT CCT GGC CCA CGG CCT GTG AAG GGT   2295
2296  GCT TAC TGT CTC CTG AAC TTT GGT GAC AGT ATC ACA ACT GAT CAC   2340
2341  ATC TCA CCT GCC GGA AGT ATT CAC CCT GAC AGC CCT GCT GCT AGA   2385
2386  TAT CTG AAG GAG CGT GGT GTT GAA AGG AAG GAC TTC AAC TCA TAT   2430
2431  GGC AGT CGG CGA GGA AAT GAT GAG ATC ATG GCT AGG GGA ACT TTT   2475
2476  GCC AAC ATT CGC CTT GTG AAC AAG TTC TTG AAG GGT GAG GTT GGC   2520
2521  CCA AAA ACC ATC CAT ATT CCA TCA GGG GAG AAG CTC TCT GTT TTC   2565
```

```
2566  GAC GCT GCT ACG AAA TAC AAG AAT GAA GGA CAT GAC ACT ATT ATC   2610
2611  CTG GCT GGT GCT GAG TAC GGT AGT GGA AGC TCT CGG GAT TGG GCT   2655
2656  GCG AAG GGT CCA ATG CTA CAG GGA GTC AAG GCT GTG ATT GCT AAG   2700
2701  AGC TTT GAA AGG ATT CAC CGC AGC AAC CTT GCT GGT ATG GGT ATC   2745
2746  ATT CCT CTA TGC TTC AAG TCA GGG GAG GAC GCC GAC ACC CTT GGA   2790
2791  TTG ACT GGC CAT GAG CGT TTC ACG GTT CAC CTC CCG GCC AAT GTA   2835
2836  AGT GAG ATC AAG CCT GGG CAA GAT GTT ACT GTG ACG ACT GAT AAT   2880
2881  GGG AAG TCC TTC ACT TGC ACA CTT CGA TTT GAC ACT GAG GTG GAG   2925
2926  CTT GCA TAC TAC GAC AAT GGT GGC ATT TTA CCG TAT GTC ATC AGA   2970
2971  AAG ATC GCC GAG CAG TAG GAT GAA CGC TCA AGA AGA TTG CGA TGA   3015
3016  GGC GAA TCG TAA TTG TTG TAA ACA GCT TGA TTA GCG CAA CCC CAT   3060
3061  TTT TTA GGA ATA CCT TTC AAA TAA CCT TCT GAG ATA TCC GCG AAG   3105
3106  AAC TCA GAA ATT TTG TGA GCT ACT ACA CTT GCA GTT GTA CGC TGC   3150
3151  CAC GGG AAA TGC GGC GCT AAA TGA CGC TAT GTG AAC ATT AAC ATT   3195
3196  TTC ACT TAA ACA CAC GTT GCT AAT AAT TTT CCG                  3228
```

7.11. Nucleotide and predicted amino acid sequence of *aci11*.

Nucleotides and amino acids are numbered on the left and right sides. The accession number for the nucleotide sequence is AY320036. The nucleotide sequence without untranslated regions contains an ORF starting at position 1 encoding a protein of 986 amino acids. Nucleotides written in bold correspond to the 183 nt-long sequence of the *aci11* cDNA initially identified through subtractive hybridisation, which covers 22 nucleotides of the 5'-UTR and 160 nucleotides of the sequence encoding the N-terminus of the protein.

```
-22                                    T CTG AGG GTG TAG CTT ACT ATC

1     ATG GCG TCA GCC ACT GGA GCG TCT GGA TGG CTG AGG GGT AAG GTG   45
1      M   A   S   A   T   G   A   S   G   W   L   R   G   K   V   15

46    AAG GGT GTG ACT TCT GGG GAC TGT CTT CTC ATC ATG GGG AGC ACC   90
16     K   G   V   T   S   G   D   C   L   L   I   M   G   S   T   30

91    AAG GCG GAT GTC CCG CCG CCT GAG AAG TCG ATT ACT CTG TCA TAC   135
31     K   A   D   V   P   P   P   E   K   S   I   T   L   S   Y   45

136   CTC ATG GCC CCA AGG CTG GCT CGC CGT GGT GGA GTG GAT GAA CCA   180
46     L   M   A   P   R   L   A   R   R   G   G   V   D   E   P   60

181   TTT GCT TGG GAA AGC AGG GAG TTT CTA AGG AAA CTC TGC ATA GGA   225
61     F   A   W   E   S   R   E   F   L   R   K   L   C   I   G   75

226   AAG GAG GTC ACA TTC AGA GTG GAC TAC ACA GCT CCA AAT GTT GGA   270
76     K   E   V   T   F   R   V   D   Y   T   A   P   N   V   G   90

271   CGA GAA TTT GGT ACT GTT TAC CTC GGT GAC AAG AAT GTT GCC TAC   315
91     R   E   F   G   T   V   Y   L   G   D   K   N   V   A   Y   105

316   TCG ATA ATT GCT GCA GGA TGG GCA AGG GTA AAG GAG CAA GGC CCA   360
106    S   I   I   A   A   G   W   A   R   V   K   E   Q   G   P   120

361   AAG GGC GGT GAA CCG AGT CCA TAT CTT ACT GAG CTG CTA AGG TTG   405
121    K   G   G   E   P   S   P   Y   L   T   E   L   L   R   L   135
```

```
406   GAG GAA GTT GCT AAG CAG CAG GGT TTA GGT CGT TGG AGC AAG GAA   450
136    E   E   V   A   K   Q   Q   G   L   G   R   W   S   K   E   150

451   CCT GGT GCT GCT GAA GAA TCA ATA AGA GAT CTT CCA CCA TCA GCA   495
151    P   G   A   A   E   E   S   I   R   D   L   P   P   S   A   165

496   ATT GGT GAA GCT AGT GGT TTT GAT GCA AAG GGT TTT GCA GTT GCG   540
166    I   G   E   A   S   G   F   D   A   K   G   F   A   V   A   180

541   AAT AAA GGC AAG AGT CTG GAA GCC ATT GTT GAA CAA GTT CGT GAT   585
181    N   K   G   K   S   L   E   A   I   V   E   Q   V   R   D   195

586   GGC AGT ACA GTT CGT GTT TAC TTG CTC CCA AGT TTC CAA TTT GTT   630
196    G   S   T   V   R   V   Y   L   L   P   S   F   Q   F   V   210

631   CAG ATA TAT GTT GCT GGA GTT CAG TCT CCA TCC ATG GGG AGG CGC   675
211    Q   I   Y   V   A   G   V   Q   S   P   S   M   G   R   R   225

676   CCA CCG AAT CCT ACA GTG GTG GCT GCA GCA GAG AGT ACT GCT GAT   720
226    P   P   N   P   T   V   V   A   A   A   E   S   T   A   D   240

721   GGC GCT ACA AAC GGT GGA GAT TCT GAG GAA GCT CCA GCA CCA CTG   765
241    G   A   T   N   G   G   D   S   E   E   A   P   A   P   L   255

766   ACT ACA GCC CAA AGG CTT GCC GCA GCA GCG GTT TCT ACT GAA ATT   810
256    T   T   A   Q   R   L   A   A   A   A   V   S   T   E   I   270

811   CCA CCG GAC AGG TTT GGA ATA GAA GCT AAG CAC TTC ACA GAG ACA   855
271    P   P   D   R   F   G   I   E   A   K   H   F   T   E   T   285

856   CAC GTT CTC AAT AGA GAT GTG CGA ATT GTG GTG GAA GGC ACA GAT   900
286    H   V   L   N   R   D   V   R   I   V   V   E   G   T   D   300

901   AGT TTC AGC AAT ATA ATT GGC TCA GTG TAT TAC TCT GAT GGG GAT   945
301    S   F   S   N   I   I   G   S   V   Y   Y   S   D   G   D   315

946   ACA TTG AAG GAT CTG GCC CTT GAG CTT GTT GAA AAT GGT CTT GCC   990
316    T   L   K   D   L   A   L   E   L   V   E   N   G   L   A   330

991   AAG TAT GTT GAG TGG AGT GCC AAC ATG ATG GAC GTT GAT GCA AAA  1035
331    K   Y   V   E   W   S   A   N   M   M   D   V   D   A   K   345

1036  ATA AAG CTG AAG AAT GCT GAG CTT CAG GCT AAG AAG GAC CAG TTG  1080
346    I   K   L   K   N   A   E   L   Q   A   K   K   D   Q   L   360

1081  AGA ATT TGG ACA GGA TTT AAG CCA CCA GTG ACA AAC TCG AAG CCA  1125
361    R   I   W   T   G   F   K   P   P   V   T   N   S   K   P   375

1126  ATC CAC GAC CAG AAA TTC ACT GGA AAA GTT GTA GAG GTT GTG AGT  1170
376    I   H   D   Q   K   F   T   G   K   V   V   E   V   V   S   390

1171  GGG GAT TGC ATC ATT GTT GCT GAT GAC GCA GCT CCT TAC GGA AGT  1215
391    G   D   C   I   I   V   A   D   D   A   A   P   Y   G   S   405

1216  CCT TCT GCA GAA CGC CGG GTT AAT CTT TCA AGC ATT AGA GCT CCT  1260
406    P   S   A   E   R   R   V   N   L   S   S   I   R   A   P   420

1261  AAA ATG GGC AAC CCT CGT AGA GAT GAG AAG CCT GAT AAT TTT GCT  1305
421    K   M   G   N   P   R   R   D   E   K   P   D   N   F   A   435

1306  CGT GAA GCC AAG GAA TTC TTG CGC ACA AGG TTG ATT GGC AAG CAA  1350
436    R   E   A   K   E   F   L   R   T   R   L   I   G   K   Q   450
```

```
1351  GTG ACT GTT GAG ATG GAA TAC TCT AGA AGG ATC AGC ACT GTG GAT   1395
451    V   T   V   E   M   E   Y   S   R   R   I   S   T   V   D    465

1396  GGA CAG CCC ACA ACA AAC ACA GCT GAT GCC AGG GTT TTG GAT TAT   1440
466    G   Q   P   T   T   N   T   A   D   A   R   V   L   D   Y    480

1441  GGG TCG GTT TTT CTT GGT TCA CCT TCG CAG GCT GAT GGT GAT GAT   1485
481    G   S   V   F   L   G   S   P   S   Q   A   D   G   D   D    495

1486  GTT TCT TCC ATT CCA AGC TCA GGC AAC CAA CCT GGT ATC AAT ATT   1530
496    V   S   S   I   P   S   S   G   N   Q   P   G   I   N   I    510

1531  GCT GAA ACT CTG CTC TCA AGG GGC TTT GCT AAA ACA TCT AAA CAT   1575
511    A   E   T   L   L   S   R   G   F   A   K   T   S   K   H    525

1576  CGG GAC TAC GAA AAA AGG TCA CAC TAT TTT GAC CTG CTG TTG GCG   1620
526    R   D   Y   E   K   R   S   H   Y   F   D   L   L   L   A    540

1621  GCT GAA TCA CGA GCT GAG AAA GCA AAG AAA GGA GTT CAT TCT GCA   1665
541    A   E   S   R   A   E   K   A   K   K   G   V   H   S   A    555

1666  AAA AAA TCA CCT GTC ATG CAC ATA ACA GAC TTG ACA ACG GTT TCA   1710
556    K   K   S   P   V   M   H   I   T   D   L   T   T   V   S    570

1711  GCA AAG AAG GCC AGA GAC TTC CTT CCT TTC TTA CAG CGG AAC AGA   1755
571    A   K   K   A   R   D   F   L   P   F   L   Q   R   N   R    585

1756  AGA CAT TCC GCA ATT GTT GAA TAT GTC TTC AGT GGC CAC CGT TTC   1800
586    R   H   S   A   I   V   E   Y   V   F   S   G   H   R   F    600

1801  AAA CTA ACA ATT CCT AAG GAG ACT TGC AGC ATT GCC TTC TCT TTC   1845
601    K   L   T   I   P   K   E   T   C   S   I   A   F   S   F    615

1846  TCT GGT GTT AGA TGC CCT GGT AAA GAT GAG CCC TAC TCG AAC GAA   1890
616    S   G   V   R   C   P   G   K   D   E   P   Y   S   N   E    630

1891  GCT ATT GCT TTG ATG AGG AGG AGA ATT CTA CAG CGA GAT GTG GAG   1935
631    A   I   A   L   M   R   R   R   I   L   Q   R   D   V   E    645

1936  ATA GAG GTT GAA GCA GTT GAT AGA ACT GGG ACA TTC TTA GGT TCC   1980
646    I   E   V   E   A   V   D   R   T   G   T   F   L   G   S    660

1981  TTA TGG GAG TCC AAA ACC AAC ATG GCT TCT GTT CTT CTG GAG GCT   2025
661    L   W   E   S   K   T   N   M   A   S   V   L   L   E   A    675

2026  GGT CTG GCC AAG CTT AGT TCA TTT GGC TTG GAT AGG ATT CCG GAT   2070
676    G   L   A   K   L   S   S   F   G   L   D   R   I   P   D    690

2071  GCA AAT GTT CTA ATG AGG GCT GAA CAG TCT GCA AAG CAG CAG AAA   2115
691    A   N   V   L   M   R   A   E   Q   S   A   K   Q   Q   K    705

2116  CTC AAG ATC TGG GAG AAT TAT GTA GAG GGT GAA GAA GTT TCC AAT   2160
706    L   K   I   W   E   N   Y   V   E   G   E   E   V   S   N    720

2161  GGA TCT GCA TCT GAA TCC AAA CAA AAG GAA ATT CTC AAG GTT GTT   2205
721    G   S   A   S   E   S   K   Q   K   E   I   L   K   V   V    735

2206  GTA ACT GAA GTC CTT GGT GGT GGA AAG TTC TAT GTC CAA ACA GTT   2250
736    V   T   E   V   L   G   G   G   K   F   Y   V   Q   T   V    750

2251  GGT GAC CAT AGA GTG GCT TCC ATT CAA CAA CAG CTT GCA TCT TTA   2295
751    G   D   H   R   V   A   S   I   Q   Q   Q   L   A   S   L    765
```

```
2296  AAA CTT AAA GAT GCA CCT GTT ATT GGT GCT TTT AAT CCT GTG AAG   2340
766    K   L   K   D   A   P   V   I   G   A   F   N   P   V   K    780

2341  GGG GAA ATA GTT CTT GCT CAG TTT AGT GCT GAC AAC TCC TGG AAT   2385
781    G   E   I   V   L   A   Q   F   S   A   D   N   S   W   N    795

2386  AGA GCA ATG ATT GTG AAT GGA CCT CGA GGA GCT GTA TCA TCT CAA   2430
796    R   A   M   I   V   N   G   P   R   G   A   V   S   S   Q    810

2431  GAC GAC AAG TTT GAA GTA TTC TAC ATT GAC TAT GGC AAC CAA GAA   2475
811    D   D   K   F   E   V   F   Y   I   D   Y   G   N   Q   E    825

2476  GTC GTT CCT TAC AGT CGC ATA CGG CCT GCT GAC CCA TCA ATT TCC   2520
826    V   V   P   Y   S   R   I   R   P   A   D   P   S   I   S    840

2521  TCT TCG CCT GCT CTT GCT CAG TTG TGC AGC CTT GCC TTC ATA AAA   2565
841    S   S   P   A   L   A   Q   L   C   S   L   A   F   I   K    855

2566  GTG CCC AAC CTA GAA GAT GAT TTT GGC CAT GAA GCA GCA GTC TAT   2610
856    V   P   N   L   E   D   D   F   G   H   E   A   A   V   Y    870

2611  CTG AAT GAT TGC TTG CTC AAC AGC CAA AAA CAA TAC AGG GCA ATG   2655
871    L   N   D   C   L   L   N   S   Q   K   Q   Y   R   A   M    885

2656  ATT GAA GAG CGT GAT ACT TCT GGT GGA AAG TCC AAG GGA CAA GGC   2700
886    I   E   E   R   D   T   S   G   G   K   S   K   G   Q   G    900

2701  ACT GGA ACT ATT CTG ATT GTT ACA CTG GTT GAC GCA GAG ACA GAA   2745
901    T   G   T   I   L   I   V   T   L   V   D   A   E   T   E    915

2746  ACC AGC ATC AAT GCT ACC ATG CTT GAG GAA GGG CTT GCT CGG CTT   2790
916    T   S   I   N   A   T   M   L   E   E   G   L   A   R   L    930

2791  GAA AGA AGC AAG AGA TGG GAT ACT AGG GAG AGA AAG GCT GCT CTC   2835
931    E   R   S   K   R   W   D   T   R   E   R   K   A   A   L    945

2836  CAG AAT CTG GAA CAG TTC CAG GAG AAA GCA AAG AAG GAA AGG CTG   2880
946    Q   N   L   E   Q   F   Q   E   K   A   K   K   E   R   L    960

2881  CAG ATC TGG CAG TAT GGT GAT GTT GAA TCT GAC GAG GAA GAG CAA   2925
961    Q   I   W   Q   Y   G   D   V   E   S   D   E   E   E   Q    975

2926  GCT CCA GCG GCT AGG AGA ACT GGA GGG CGT CGG TAG               2961
976    A   P   A   A   R   R   T   G   G   R   R   *               986
```

7.12. Abbreviations.

nt	nucleotides	cm	centimetre
bp	base pair	µm	micrometre
kb	kilo base pair	nm	nanometre
kD	kilodalton	s	second
		min	minute
g	gram	rpm	rotations per minute
mg	milligram	v	volume
µg	microgram	w	weight
L	litre	Ci	Curie
µL	microlitre	OD	optic density
M	molar		
mM	millimolar	pfu	plaque forming unit
µM	micromolar	ORF	open reading frame
N	normal	UTR	untranslated region
ppm	part per million	UV	ultra-violet
m	metre		

ABA	abscisic acid
ACC	1-aminocyclopropane-1-carboxylic acid
ATP	adenosine 5'-triphosphate
BASTA	glufosinate ammonium
CSPD	disodium 3-(4-metho xyspiro {1,2-dioxetane-3,2-(5-chloro)tricyclo [3.3.1.13,7]decan}-4-yl)phenyl phosphate
CTAB	cetyltrimethylammonium bromide
dNTPs	2'-deoxynucleotides 5'-triphosphate
dUTP	2'-deoxyuridine 5'-triphosphate
EDTA	ethylendiamine-tetraacetic acid
EtBr	ethidium bromide
FAA	formaldehyde-acetic acid
GA	gibberellic acid
GUS	β-D-Glucuronidase
HE	HEPES, EDTA
HEPES	N-2-Hydroxyehtylpiperazine-N'-2-ethanesulfonic acid
LB	Luria-Bertani
MOPS	3-[N-morpholino]propane-sulfonic acid
MTA	methythioadenosine
NAA	α-naphtalene acetic acid
NAD^+	nicotinamide adenine dinucleotide, oxydised
PEG_{8000}	polyethylene glycol, molecular weight 8.000
SDS	sodium dodecyl sulfate
SM	sodium-magnesium
SSC	sodium chloride-sodium citrate
TAE	tris-acetate-EDTA
TBE	tris-borate-EDTA
TE	tris-EDTA
Tris	trihydroxymethylamino methan
X-Gluc	5-bromo-4-chloro-3-indolyl β-D-glucuronide
YEP	yeast extract, peptone

Acknowledgements.

I would like to heartily express my gratitude to Prof. Dr. Margret Sauter, who supervised my work during these almost four years of PhD thesis. Her vivacity and her enthusiasm for my project were constant, and the constructive discussions we had considerably enriched my work. I'm also thankful to her for helping me adapt to the German way of life and of work.

Dr. Tanja Marwedel (University of Bonn) guided my first steps in Prof. Sauter's laboratory. I therefore would like to acknowledge her and to wish her the best at the beginning of her career.

Sára Beszteri, I Thank you for your support (or for supporting me).

I thank Dr. Bianka Steffens for her late (but not too late) contribution.

I'm grateful to Dipl. Biol. Isabell Kilbienski and Susanne Braun for providing helpful advice and comments on ballistic transformation and to Dr. Maria Mulisch and Dr. Christine Desel (University of Kiel) for teaching me the use of confocal and photonic microscopy.

I am also in debt with Dr. Manfred Gahrtz (University of Hamburg) for a bunch of good advice concerning *Arabidopsis thaliana*.

I would like to express my sympathy to the members of the INTEGA (INTeractions between Ethylene and Gibberellic Acid) research network for the interesting discussions on my project during our frequent meetings. Special thanks go to Prof. Dr. Dominique Van der Straeten (University of Gent, Belgium) and Dr. Wim Vriezen (University of Nijmegen, The Netherlands) for their warmth support during my short stay in Gent, and to Dr. Andy Phillips (Rothamsted Research Institute, Harperden, United Kingdom) who nicely accepted to comment on the present manuscript.

Finally, I would like to acknowledge support from the European Union through the INTEGA research network HPRN-CT-2000-00090.

Curriculum vitae

Name **Rzewuski**
First name Guillaume
Date of Birth 2nd July 1977
Nationality French
Address Paul-Fuss-Strasse 25
D-24118 Kiel

University Degrees (University of Clermont-Ferrand, France)

1997 DEUG of Biology (first degree of undergraduate studies)

1998 Licence of Cell Biology, Plant and Animal Physiology (Bachelor degree)

1999 Maîtrise of Cell Biology, Plant Physiology (Master degree)

2000 Diplôme d'Etudes Approfondies of Molecular Physiology and Genetics

Training Periods

1999 3 weeks integrated in the Maîtrise course.
Subject: Study of the inhibition of the chymotrypsic activity of 26S proteasome isolated from sunflower protoplasts.

1999 3 months (June-August) in the Proteomics group at the Agricultural Biotechnology Laboratory of DuPont de Nemours, Newark, Delaware (U.S.A.).
Subject: Characterisation of proteins involved in a fungal disease of rice using the Yeast Two-Hybrid System.

2000 6 months of Masters training at the PIAF (Integrated Physiology of Fruit Trees) laboratory, Clermont-Ferrand University, France.
Subject: Biochemical and expression study of sugar metabolism key-enzymes in xylem parenchyma of Walnut Tree during dormancy in relation with branching.

Since 2000 PhD student under the supervision of Prof. Dr. Margret Sauter (2000-2003 at the University of Hamburg, 2003-2004 at the University of Kiel).
Subject: Molecular interactions between ethylene and gibberellic acid pathways in plants.